DOT/FAA/AR-97/66

Office of Aviation Research
Washington, D.C. 20591

Snow and Ice Particle Sizes and Mass Concentrations at Altitudes Up to 9 km (30,000 ft)

Richard K. Jeck
Flight Safety Research Section
Federal Aviation Administration
William J. Hughes Technical Center
Atlantic City International Airport, NJ 08405

August 1998

Final Report

U.S. Department of Transportation
Federal Aviation Administration

NOTICE

Technical Report Documentation Page

1. Report No.	2. Government Accession No.	3. Recipient's Catalog No.
DOT/FAA/AR-97/66		

4. Title and Subtitle	5. Report Date
SNOW AND ICE PARTICLE SIZES AND MASS CONCENTRATIONS AT ALTITUDES UP TO 9 km (30,000 ft)	August 1998
	6. Performing Organization Code AAR-421
7. Author(s) Richard K. Jeck	8. Performing Organization Report No.
9. Performing Organization Name and Address Federal Aviation Administration William J. Hughes Technical Center Atlantic City International Airport, NJ 08405	10. Work Unit No. (TRAIS) 11. Contract or Grant No.
12. Sponsoring Agency Name and Address U.S. Department of Transportation Federal Aviation Administration Office of Aviation Research Washington, DC 20591	13. Type of Report and Period Covered Final Report 14. Sponsoring Agency Code

15. Supplementary Notes

16. Abstract

About 7600 nautical miles (nm) (14,000 km) of select ice particle measurements over the United States have been compiled into a single, computerized database for use in characterizing ice crystal and snowflake (generally termed ice particle) size distributions and mass concentrations at flight altitudes. Data are from 50 research flights by six agencies in eight flight research projects using Particle Measuring Systems' one-dimensional (1-D) and two-dimensional (2-D) particle sizing probes. Primary recorded variables are average particle size distributions in the range 0.1 to 10 mm from each of 1625 microphysically uniform cloud intervals or other convenient distances in wintertime clouds, snowstorms, cirrus, and other high-altitude clouds. The findings are that, generally, the largest particles and the greatest concentrations of total ice particle mass (TIPM) are confined to altitudes below 20,000 ft (6 km). There, particles of 10 mm in maximum dimension and TIPM's up to about 3 g/m^3 may be found. Above 20,000 ft, particles are smaller than 2 mm and TIPM's are less than 0.2 g/m^3 in the cirrus and the upper reaches of deep winter storm clouds that are found at these levels. Exceptions are thunderstorm anvil clouds where 10 mm particles and TIPM's of at least 1 g/m^3 can be found up to at least 30,000 ft (9 km). Anvil clouds and stratiform clouds associated with warm season mesoscale convective systems have provided some of the largest TIPM's, the greatest particle concentrations, and the largest particle sizes at high and mid altitudes, respectively. In contrast to supercooled cloud droplets where the largest liquid water (mass) concentrations are confined to short distances of 3 nm or less in convective clouds, the largest average TIPM's in glaciated clouds have been found in layer clouds over distances up to 30 nm. Based on these analyses, a summary table of ice/snow cloud characteristics is proposed for use as engineering specifications for aviation purposes.

17. Key Words	18. Distribution Statement
Aircraft icing, Cloud physics, Snow, Ice particles, Icing condition	This document is available to the public through the National Technical Information Service (NTIS), Springfield, Virginia 22161.

19. Security Classif. (of this report)	20. Security Classif. (of this page)	21. No. of Pages	22. Price
Unclassified	Unclassified	94	

Form DOT F1700.7 (8-72) Reproduction of completed page authorized

PREFACE

The author and the FAA are indebted to the various agencies listed herein which provided the original data and to the scientists associated with these agencies who assisted in assuring the quality of the data.

TABLE OF CONTENTS

LIST OF FIGURES

LIST OF TABLES

ABBREVIATIONS AND ACRONYMS

AFGL	Air Force Geophysics Laboratories
AGL	Above Ground Level
ASL	Above Sea Level
CCOPE	Cooperative Convective Precipitation Experiment
CIC	Colorado International Corporation
COSE	Colorado Orographic Seeding Experiment
CRREL	Cold Regions Research and Engineering Laboratory
EvATIPM	Event-Averaged Total Ice Particle Mass
FAA	Federal Aviation Administration
LSCS	Large Scale Cloud Systems
LWC	Liquid Water Content
MCS	Mesoscale Convective System
MIT	Massachusetts Institute of Technology
NCAR	National Center for Atmospheric Research
NEWS	New England Winter Storms
NOAA	National Oceanic and Atmospheric Administration
NRL	Naval Research Laboratory
O-K PRE-STORM	Oklahoma-Kansas Preliminary Regional Experiment for STORM-Central
PMS	Particle Measuring Systems (Inc.)
SCPP	Sierra Cooperative Pilot Project
STORM	STormscale Operational and Research Meteorology
TIPM	Total Ice Particle Mass
USAF	United States Air Force
1D-C	One-Dimensional Cloud Droplet Size Spectrometer
1D-P	One-Dimensional Precipitation Particle Size Spectrometer
2D-C	Two-Dimensional Cloud Droplet Imaging Probe
2D-P	Two-Dimensional Precipitation Particle Imaging Probe

EXECUTIVE SUMMARY

This report covers one phase of a continuing research project to improve the understanding and quantitative description of aircraft icing conditions in the atmosphere. The project is the first of its kind since the late 1940's when researchers from the U. S. Weather Bureau and the National Advisory Committee for Aeronautics (NACA) originally collected flight data on icing conditions aloft. Those early data form the basis for the icing-related, engineering design information currently contained in the Federal Aviation Regulation, Part 25 (FAR 25), Appendix C. The first two phases of the current research project have more than doubled the original amount of flight data and have led to improved descriptions of the icing atmosphere. These are intended to supplement or perhaps revise the existing design data in FAR 25, Appendix C.

The FAR 25 document also requires all-weather certified aircraft to be capable of flying through "falling and blowing snow", but to date no suitable engineering data on snow conditions aloft have been available. The third phase of the ongoing research project attempts to fill that void by providing a large database of select in-flight measurements of snow and ice crystal concentrations, sizes, and mass accumulations at flight altitudes. To this end, data from 50 research flights in a variety of wintertime and high-altitude clouds up to 30,000 ft (9 km) and temperatures down to -50°C have been collected from six different research groups. Some 7600 nautical miles of select quality data have been compiled into a single, computerized database for use in developing the desired information for aircraft engineering purposes.

This report summarizes these results and presents a number of graphical analyses to illustrate the observed characteristics of ice and snow particle populations primarily as a function of altitude and temperature.

The engineering significance of the results are that generally the *worst* ice particle and snow conditions are at altitudes below about 20,000 ft (6 km). Notable exceptions are thunderstorm anvil clouds where large particles and mass accumulations can be carried up to altitudes of 30,000 ft (9 km) or more. Below 20,000 ft (6 km), snowflakes as large as 10 mm and mass accumulations up to 3 grams per cubic meter of air (g/m^3) may be found in some storm systems. Above 20,000 ft, particle sizes are smaller than 2 mm and particle mass appears to be less than 0.2 g/m^3 in the cirrus clouds and the upper reaches of deep winter storms that are usually found at these levels. In the thunderstorm anvils, however, 10 mm particles and masses of 1 g/m^3 can be found.

As a result of these analyses, an altitude-graduated table of ice/snow cloud properties is proposed for defining the "falling…snow" requirement in FAR 23.1093, FAR 25.1093, FAR 27.1093, and FAR 29.1093.

INTRODUCTION

Flight through a heavy snowfall or other ice particle clouds is known to sometimes be a hazard to aircraft, especially as it can affect the engines. Some helicopters and light aircraft are known to have crashed or executed emergency landings due to engine failure after takeoff into snowstorms. It has been reported that some transport jets have had difficulty regaining full power after cruising through high-altitude cirrus or anvil clouds.

Although federal aviation regulations FAR 23.1093, FAR 25.1093, FAR 27.1093, and FAR 29.1093 [1] require all-weather aircraft to be capable of flight through "falling and blowing snow", no quantified specification of snow has been available for engineering purposes. That is, no information on snow or ice particle masses or sizes as a function of altitude or air temperature has been promulgated. To overcome this deficiency, a data compilation and analysis effort was undertaken as part of a larger project to improve the understanding and characterization (engineering specification) of icing conditions in the atmosphere. The results are expected to be applicable to various aviation-related concerns such as meteorological design specifications and improved forecasting of icing conditions.

The information required for aviation engineering purposes is the range and probable values of snow and ice particle sizes, masses, and numbers for altitudes from sea level up to at least 9 km (30,000 ft). No compilation of such data has been previously available. A considerable amount of knowledge has been gained over the past several decades, however, and the pertinent aspects are reviewed in the BACKGROUND section.

BACKGROUND

WHAT IS ALREADY KNOWN ABOUT SNOW AND ICE PARTICLES.

TYPES OF PARTICLES. Some general categorizations are given here to help simplify the understanding of the apparently complex picture of particle shapes and their occurrences, both of which depend on the ambient temperature, available moisture, and other environmental influences. Most of this information is condensed from chapter 7 of reference 2. The reader is also referred to the glossary for some of the basic definitions.

Basically, frozen particles occur either in the form of symmetrical crystals, in which case their shape is referred to as a "habit", or as irregular or amorphous particles resulting from riming and/or aggregation of symmetrical crystals.

The symmetrical crystals result exclusively from the condensation of ambient water vapor onto an ice particle nucleus or other "seed" (i.e., particle fragment). There are only three basic habits for ice crystals—needles, planar crystals, and hexagonal columns. The planar crystals exhibit the greatest number of variations, ranging from thin, hexagonal plates to the elaborate dendrites (branched crystals) popularly brought to mind at the mention of *snowflakes*. Very small crystals have simple habits such as plates and prisms; elaborate habits like dendrites are not found smaller than about 200 μm (0.2 mm) in diameter.

Certain crystals, including needles, stellars, and dendrites, form only at or near water saturation.[*] At temperatures less than 0°C, water saturation generally occurs only in the presence of supercooled water droplets. In this case, riming is also likely if the ice particles are larger than about 200 μm.

Simpler, more solid habits (plates and columns) grow below water saturation (RH<100%) but above ice saturation.[**]

The ambient temperature also determines which crystal habits will grow, as summarized in the table below.

Air Temperature (°C)	Predominant Crystal Type
0 to -4°C	Plates
-4 to -10°C	Columns (or maybe some needles)
-10 to -20°C	Plates, thick plates, stellars, dendrites
-20 to -40°C	Columns, plates, bullets

These relationships can be helpful in deducing the crystal types present during measurements in an ice cloud but only if the sampled portion of the cloud is uncontaminated by other types of particles falling in from above or being brought in on updrafts from below. Suitable cases would include shallow clouds where the temperatures are entirely within one of the four ranges shown in the table or near the tops of deeper but nonconvective clouds.

The various forms of irregular or amorphous particles are generally known as graupel, sleet, hail, or snowflakes. They are all formed by riming and/or aggregation, neither of which are very effective until the maximum dimension of a crystal exceeds 200 μm or more. That is, crystals smaller than 200 μm are usually simple, unrimed plates or columns.

Graupel particles (see glossary) are usually white and friable, but some are more like solid ice. They are found in convective clouds where sufficiently strong updrafts maintain the supercooled droplet supply that is required for growth by riming, against the depleting effects of the growth of precipitation. Graupel or other rimed particles are called hailstones if they are larger than about 5 mm.

Ice particles may also form from the freezing of supercooled droplets. Sleet is a common name for frozen raindrops.

---

* Water saturation refers to the ordinary 100% relative humidity (RH) condition where no more water vapor can be added to a given volume of space at the existing temperature. Any increase of water vapor will immediately condense out as liquid droplets, forming a cloud.

** Ice saturation refers to the condition (temperature or absolute humidity) at which ice particles will just begin to grow via condensation of the ambient water vapor. At temperatures farther below freezing (0°C), this can occur at relative humidities farther below 100%, and therefore ice particles can form and grow in humidities too low for water droplets to form.

The most important type of accretion is that of snow crystals to form snow flakes. Close examination of snowflakes reveals that they may consist of tens, hundreds, or even thousands of individual ice crystals, rather than of a single, large, elaborate but symmetrical crystal as is popularly imagined. In the mid latitudes, 50% or more of the snow is in the form of aggregates.

At altitudes above the freezing level a given cloud volume is usually either all supercooled droplets or all frozen particles. There is seldom a mixture of both, except temporarily, since the mixed condition is an unstable state. A parcel of supercooled droplets is rapidly depleted if any ice particles are present, because the ice particles readily draw upon the common supply of water vapor to feed their growth. The supercooled droplets begin to evaporate as soon as they see the air around them becoming drier. This preferential condensation of water vapor onto the ice particles causes them to grow rapidly at the expense of the supercooled droplets. The cloud becomes glaciated and may dissipate as the growing ice particles begin to fall out. This is commonly seen with shallow cirrus or altostratus clouds as the wispy precipitation trails develop below them. Evidence of glaciation in larger clouds, like towering cumulus, for example, is the conversion of parts of the cloud from billowy (cauliflower) shapes indicative of a water droplet cloud, to a featureless "cotton candy" appearance indicative of an ice particle cloud. Most clouds remain in the form of supercooled droplets until temperatures approach -20°C or so, unless frozen particles have been introduced from colder parts of the cloud or have fallen in as precipitation from a glaciated cloud above.

PARTICLE SIZE DISTRIBUTIONS. Ice particles may be found as small as 5 μm or so in length or diameter and snowflakes may be as large as 2 cm. A number of technical reports and papers published since the 1940's give data on measured snow or ice particle size distributions for one or more case studies at particular locations. The first measurements at ground level were reported in 1948 by Marshall and Palmer for raindrops [3], and in 1958 by Gunn and Marshall for snowflakes [4]. Douglas reported on the observed size spectra of hailstones in 1964 [5]. Early measurements of ice particle size distributions at flight altitudes were reported in 1971 by Simpson and Wiggert [6].

These measurements show that the size distributions are all generally exponential, i.e., of the form

$$n(D) = n_o \exp(-\lambda D),$$

where D is the particle diameter and n_o and λ are the intercept and slope parameters, respectively. Thus n(D)dD gives the number of particles in the size interval D to D + dD observed at a particular time and location. A number of subsequent studies have shown that n_o and λ are variable, depending on temperature, crystal type, and the stage of particle growth (deposition, aggregation, and breakup) [7], for example.

MAXIMUM PARTICLE SIZE. The maximum possible size of a precipitation particle depends on the type of particle (p. 28, reference 8). Snowflakes are usually smaller than 2 cm, although most snowflakes have diameters between 2 and 5 mm. Both rimed and unrimed particles (single ice crystals, graupel particles, and ice pellets) usually have maximum dimensions less than 5 mm.

This means that Particle Measuring Systems Inc.'s (PMS) one-dimensional precipitation particle size spectrometer (1D-P) and two-dimensional precipitation particle imaging probe (2D-P), probes that cover sizes up to 6 mm or more, will usually be adequate for obtaining complete size distributions.

The maximum dimensions mentioned above are mostly from observations at or near ground level where maximum growth has usually already taken place during the fall from high altitudes. At high altitudes, smaller maximum limits may apply due to temperature effects, a shortage of water vapor, or a lack of aggregation processes. For example, a number of studies of cirrus clouds has shown that the mean lengths of the ice particles were between 0.1 and 1.0 mm. For these cases a PMS 2D-C probe that covers up to at least 800 μm may be sufficient.

Temperature (Altitude) Dependence. Air temperature and crystal shape play dominant roles in aggregation, the process by which large snowflakes are formed. Observations have shown that the maximum dimensions of snowflakes are largest near 0°C, and that the probability of aggregation decreases with decreasing temperature (increasing altitude). The shape of the component crystals is important too. Aggregates of columns and needles tend to stay small while aggregates of dendritic crystals tend to become large. Dendrites form only in the temperature range of about -10 to -20°C and are therefore not found at cirrus levels unless they are transported there from lower levels, as in thunderstorm anvils [9]. Only column-like crystals form at temperatures less than -20°C, so that both crystal shape and lack of aggregation will limit the maximum particle size to relatively smaller values at temperatures below about -20°C.

MAXIMUM PARTICLE CONCENTRATIONS. All particle counting or sizing devices are sensitive to only a limited range of particle sizes, and the range is different from one type of device to another. Since small ice particles are generally much more abundant than large particles, devices responsive to the smaller sizes will register the greater number of counts. This means that any reported values of total particle concentration (no./liter) will be strongly influenced by the size range it represents and especially by the lower size threshold. In order to make meaningful comparisons of total particle concentrations, it is therefore necessary for all values to represent the same size range or at least have the same lower size limit. Although no formal agreement is followed in the scientific literature, the lower limit is often found to be around 100 μm or 150 μm for various practical reasons usually associated with the available probes. In this report 100 μm (0.1 mm) will therefore be adopted as the lower size limit to be considered when reporting total particle concentrations.

Temperature (Altitude) Dependence. Ice particles may be present in any cloud where the temperature is below 0°C, although it is known that the thinner the cloud (vertically) and the warmer (lowest temperature greater than -10°C) the less likely the presence of ice particles. Nevertheless, in a study of 162 clouds of various types with lowest temperatures ranging from -2 to -32°C, Hobbs and Rangno (figure 2 of reference 10) observed ice particle concentrations (>0.1 mm) up to 200 per liter for temperatures down to -30°C and up to 300 per liter at -32°C. The trend was to increasing ice particle concentrations with decreasing temperature down to -32°C. Heymsfield (figure 6 of reference 11) reports concentrations (>0.1 mm) up to about 120 per liter in a number of stratiform ice clouds. This peak value occurred at about -20°C, and the maximum values dropped rapidly to less than one per liter with decreasing temperature between -30 and -53°C, the lowest temperature in his data set. This apparent decrease in particle concentration at temperatures lower than -30°C is probably because at these temperatures most of the particles are smaller than 0.1 mm, the minimum size under consideration. Other researchers have reported concentrations occasionally and briefly reaching up to 330 per liter at -5°C [12], and nearly 400 per liter at -17°C [13]. Taken together, these results indicate that, except for occasional and momentary bursts to perhaps 300-400 per liter in some convective cells, maximum particle concentrations (>0.1 mm) are generally less than about 250/liter for temperatures down to about -30°C, and they decrease to only a few per liter at temperatures below that.

MAXIMUM TOTAL MASS. Often referred to as the ice water content (IWC), the total ice particle mass concentration (TIPM) is the sum weight of all ice particles in a unit volume of air. It is usually expressed in units of grams of ice substance per cubic meter of air, g/m^3, or the equivalent unit of milligrams per liter, mg/liter.

Reports of TIPM in the literature are rare compared to reports of particle sizes and concentrations. Heymsfield [11] obtained about a hundred measurements of TIPM in a variety of stratiform ice clouds. The maximum total masses observed in several 10°C temperature intervals are tabulated below.

Temperature (°C)	Maximum Observed Total Mass (g/m^3)
-10° to 0°	0.8
-20° to -10°	1.5
-30° to -20°	0.5
-40° to -30°	0.25
-50° to -40°	0.04
-60° to -50°	0.008

In convective clouds the total mass can be larger and indeed Heymsfield [9] finds values up to 1 g/m^3 in a thunderstorm anvil at about -37°C. Total ice particle masses up to 3.5 g/m^3 have been reported [14] in the center of Swiss thunderstorms at temperatures of about -9°C.

Values of TIPM aloft can also be estimated from precipitation rates observed at the ground. The relationship

$$R(\text{mm/hr}) = 5(\text{TIPM})^{1.16}$$

was originally established for aggregate snow by Sekhon and Srivastava [15] in 1970. Heymsfield [11] showed that the same equation also worked for ice particles measured aloft in synoptic scale cloud systems. Werner (page 36 of reference 16) used this equation along with data on extreme 24-hour snowfalls in the United States to deduce a value for the 99th percentile

TIPM of snow as a function of the (surface) temperature at the time of observation. His results are:

Temperature (°C)	99th Percentile Snow TIPM (g/m^3)
-9	1.6
-4	1.9
+1.5	2.1

Thus it may be anticipated that TIPM's aloft will not exceed these values, except occasionally, particularly in some thunderstorms.

INSTRUMENTATION.

All of the ice particle data compiled here were obtained from one or more of four laser-based probes manufactured by Particle Measuring Systems (PMS), Inc. [17]. These probes are designed for airborne sampling purposes and have been in popular use since their commercial introduction in the mid 1970's. The probes make use of a low-power, closed-path laser beam to illuminate individual cloud or precipitation particles passing through the exposed sensitive volume of the beam during flight.

One type of probe design, known as the one-dimensional (1D) probe, instantaneously determines the size of the passing particle by electronically counting the number of photodiodes that are momentarily covered by the particle's shadow. This miniature, linear array of detecting photodiodes is necessarily aligned perpendicular to the flight path. This results in a measurement of only the particle dimension that is perpendicular to the flight path. Typically, the particle is assigned to one of 15 size bins distributed evenly over a size range of about 50-300 μm for the cloud particle (1D-C) probe, or 0.3-4.5 mm for the precipitation particle (1D-P) probe. After every 15 seconds or so of flight along a path containing ice particles within the size range covered by the probe, a particle size distribution can be developed from the number of counts accumulated in each of the 15 size bins. In turn, the total mass (g/m^3) of the ice particle population can be computed from the measured size distribution. Specific methods for computing the total particle mass are described in a following section.

A second version of these probes incorporates additional fast electronics to record multiple, sequential measurements, or time slices, of the particle width as it traverses the beam at aircraft speeds. This permits a two-dimensional reconstruction of each shadow, thereby yielding information on the shape of the particle in addition to its size. These two-dimensional (2D) probes usually cover a larger range of particle sizes than their 1D counterparts. Typically, the 2D-C and 2D-P probes cover the ranges 50-800 μm and 0.2-6.4 mm, respectively. In some 2D-P models, the upper limit is near 9 or 10 mm. Typical particle images (shadowgrams) are illustrated in figure 1.

In the database, the probes from which the data were obtained for each measurement are indicated by the variable called PROBE_ID. The maximum particle size (in mm) that was measurable with the probe(s) is given by the variable MAXDIAM. The predominant particle habits, if known, are given by the variable XTALTYPE. The original particle size information has been stored in the form of a coarse size and mass distribution, as further explained below, but the individual shadowgrams are not kept as part of the database. Reference the appendix for a further explanation of the retained variables.

SOURCES OF DATA.

All of the data compiled here come from either published reports or from digital data tapes provided by several agencies (universities or government research organizations) whose instrumented aircraft have collected useful data in various types of ice clouds. The field research projects from which data were obtained are described briefly to familiarize the reader with them and to indicate the scope of the atmospheric conditions that are represented.

1. The Air Force Geophysics Laboratory (AFGL) Cirrus Project, as the name implies, was conducted to measure ice particle sizes and mass loads in cirriform clouds. The project employed a Lockheed MC-130E aircraft instrumented with PMS 1D-C and 1D-P probes for a small number of flights during the fall and winter months of 1977-1979. Selected portions of the data from seven flights, as tabulated in a series of technical reports [19-25], have been incorporated into the database. The flights were mostly over New Mexico and ranged in altitude from about 6 to 9.5 km (20,000 to 31,500 ft) above sea level (ASL). The cirrus clouds were mostly associated with jet streams and frontal systems.

2. The AFGL Large Scale Cloud Systems (LSCS) Project made use of the same probes and aircraft to study the microphysical changes in limited portions of extensive, cyclonic winter storms as they developed and moved from the central to eastern United States over a period of 3 to 4 days. Selected portions of the data from 7 days (two storm systems) during March 1978, have been used here. The data are from published tables [26-27]. One storm was followed from New Mexico to Delaware with ice particle data from 3 to 9 km (9500 to 29,500 ft). The second storm was followed from Oklahoma into Pennsylvania at altitudes from 1.4 to 7.4 km (4600 to 24,000 ft) in the northeast quadrant of the storm.

3. The Cooperative Convective Precipitation Experiment (CCOPE) was a major, summertime, weather modification research project cosponsored by the Department of the Interior (Bureau of Reclamation) and the National Center for Atmospheric Research (NCAR). The project involved six or more aircraft and an observing network in the vicinity of Miles City, Montana, during May to August 1981. Tabulated data [9] have been taken from the NCAR Sabreliner flight in the spreading anvil of an airmass thunderstorm on August 1, 1981. The flight ranged from 8 to 9.3 km (26,000 to 30,500 ft).

4. The Colorado Orographic Seeding Experiment (COSE) was a multiyear weather modification project in mountainous northwest Colorado. Tabulated data [28] from 2

aircraft on 2 winter days in 1979 have been used in the database. The flights were in local orographic or wide area cloud systems with snow. Flight altitudes ranged from 2.5 to 6.6 km (8000 to 21,500 ft) ASL.

5. The New England Winter Storms (NEWS) project was organized at the Massachusetts Institute of Technology to study precipitation bands and frontal systems in the Boston area. Radar, aircraft, and surface data were obtained in 20 storms during three winters from 1981-82 to 1983-84. During December 1982 and January 1983 the project employed NCAR's Beechcraft Queen Air aircraft with a PMS 1D-P probe to collect snow and particle size data aloft. Digital data tapes were obtained from NCAR and selected data from six of these flights have been incorporated into the database. Ice particle data were obtained from the surface up to 5.5 km (18,000 ft) in and below a variety of stratiform and glaciated layers, and in some snow bands.

6. The Oklahoma-Kansas Preliminary Regional Experiment for STORM-Central (O-K PRE-STORM) took place in May and June of 1985 [29]. It was one phase of a large, multiyear project called STormscale Operational and Research Meteorology (STORM), recently organized to study large storm systems in the United States [30]. O-K PRE-STORM investigated the structure and dynamics of mesoscale convective systems (MCS), those major summertime thunderstorm complexes which occur only east of the Rocky Mountains. Cloud cover imagery from weather satellites easily reveals the MCS's characteristic high-altitude cloud shield, showing up as very dark (cold) in the infrared imagery and often covering an area the size of Kansas or larger. Selected data from one flight near Wichita, Kansas in portions of an MCS on June 10, 1985, were obtained on digital tape [31]. The aircraft was one of the National Oceanic and Atmospheric Administration's (NOAA) research planes, a Lockheed P-3 with PMS 2D-C and 2D-P probes aboard. Ice particle data were obtained at altitudes from 4.0 to 5.2 km (13,000 to 17,000 ft) in the trailing stratiform, precipitating region of the extensive MCS.

7. The three "Snow Growth" flights were from the AFGL LSCS and icing research flights of February and March of 1980. They were so named because of their special emphasis on studying the evolution of particle growth in snow producing clouds. The three took place in winter cyclonic storms—two off the coast of Washington state and one off the coast of New Hampshire. The slow, descending-spiral flight paths were at the approximate fall speed of snow, about 1 m/s, which allowed the growth of snow particles to be monitored as they descended and went through stages of growth by vapor deposition, aggregation, and eventual breakup. Data for three spiral descents are available in condensed form [7] and have been included in the database. Altitudes range from 6.9 to 2.3 km (22,700 to 7600 ft).

8. The largest, single source of data has been the Sierra Cooperative Pilot Project (SCPP) in central California. This was a multiyear, wintertime weather modification exercise over the windward slopes of the Sierra Nevada mountains [32]. The University of Wyoming's Beechcraft King Air, the primary cloud physics research aircraft for the project, flew a number of missions each winter from 1978 through 1984. Digital magnetic tapes of the

data from onboard PMS 2D-C, 2D-P, and other probes were obtained from the data archives maintained by the Bureau of Reclamation, the principal sponsor of the project. Data from 28 selected flights over 5 years (the 1978-79 to 1983-84 winter seasons) have been processed into the database. All major cloud and weather systems typical of the region are represented. These include banded, widespread, and orographically induced or enhanced clouds associated with major frontal passages and low-pressure centers. Flight altitudes ranged from 1.2 to 6.7 km (4,000 to 22,000 ft).

Table 1 lists the individual projects and the amount of data (in terms of flight miles) contributed by each of them to the database. Most of the projects were selected from a group surveyed earlier [18] to determine the availability of existing data suitable for use in building a snow and ice particle database.

TABLE 1. CONTRIBUTORS TO THE SNOW AND ICE PARTICLE DATABASE

Project	Agency	Data Miles (nm)	Events
AFGL Cirrus:77	USAF/AFGL (C-130)	100	20
AFGL Cirrus:78	USAF/AFGL (C-130)	585	113
AFGL Cirrus:79	USAF/AFGL (C-130)	105	5
AFGL LSCS:1978	USAF/AFGL (C-130)	238	38
CCOPE:1981	NCAR (Sabreliner)	99	23
COSE-II:1979	CIC (Learjet)	43	10
	NCAR (QueenAir)	48	19
NEWS:1982-83	NCAR (QueenAir)	1596	265
O-KPRE-STORM:1985	NOAA (P-3)	90	7
Snow Growth:80	MIT/AFGL (C-130)	520	52
SCPP:1978-79	U. Wyoming (King Air)	688	137
SCPP:1979-80	U. Wyoming (King Air)	703	169
SCPP:1981-82	U. Wyoming (King Air)	1268	279
SCPP:1982-83	U. Wyoming (King Air)	722	207
SCPP:1983-84	U. Wyoming (King Air)	826	281
For Entire Database		7631	1625

RESULTS

BIASES IN THE DATA.

CLOUD TYPES. Since ice particle clouds are mainly a wintertime and high-altitude phenomenon, the emphasis in this Database has been on data from these two regimes. It is there that aircraft are exposed to more vertically and/or horizontally extensive ice clouds compared to the warm seasons. Thus, winter clouds of all types, especially snowstorms, have been sought in addition to cirrus. The result has been that 66% of the data are from layer clouds (St, Sc, Ns, Ci, As, Ac) and only 34% are from strictly convective clouds (Cu, Cg, Cb, Or). Some of the layer clouds have included embedded convective cells, however. Nearly all of the convective clouds happened to be present during winter season research flights associated with the Sierra

Cooperative Pilot Project (SCPP) over the windward (western) foothills and slopes of the Sierra Nevada mountain range in central California. These clouds are representative of wintertime conditions there, but it is only one geographic location and it is characterized by orographic influences and maritime air masses.

Thunderstorms and other typical warm season clouds have been given low priority and are therefore poorly represented in the database. The two notable representatives of warm season clouds, though, are a thunderstorm anvil and the trailing stratiform region of a mesoscale convective system (MCS) [29]. Interestingly, both of these cases have provided some of the greatest particle concentrations (no./liter), particle sizes, and particle masses (g/m^3) of any clouds in the database.

For purposes of analyses, the data are often divided into layer and convective types. Choosing the proper category is sometimes difficult or arbitrary. For example, the thunderstorm anvil has been classified here as a convective cloud to stress its origins, although the shape and motions of the anvil may be more stratiform. On the other hand, the trailing stratiform region of the MCS was categorized as a layer cloud although it, too, is associated with a definitely convective system. Orographically induced or enhanced clouds are also classified as convective clouds because of their forced upward motion.

ALTITUDE AND TEMPERATURE REPRESENTATION. The representativeness of the data can be seen quantitatively in tables 2 and 3. These tables illustrate, percentage-wise and in terms of measurement miles, how well the various altitude and temperature intervals have been sampled. Table 3 shows that about half of the data were obtained in the 10°C temperature interval between -2.5 and -12.5°C. The -10°C level is a favorite one in cloud seeding studies and the large amount of data at this level reflects the emphasis of many of the flights. Table 2 shows that these occurred in the 5,000 ft (1.5 km) altitude interval between 7,500 ft (2.3 km) and 12,500 ft (3.8 km). About 20% of the measurements are spread evenly over the lower temperatures from -17.5 to -47.5°C corresponding to the higher altitudes of 17,500 to 32,500 ft (5.3 to 9.9 km). Fifteen percent of the data are from altitudes below 7,500 ft (2.3 km). No surface data are included.

TABLE 2. DISTRIBUTION OF OBSERVATIONS WITH ALTITUDE

Entries represent each 5,000 ft (1.5 km) altitude interval centered at the listed altitude.

Above Sea Level			
Altitude (ft)	Interval (km)	Data Miles (nm)	Percent of Total
0	0.0	145	2.0
5000	1.5	996	13.0
10000	3.0	3788	49.5
15000	4.6	1301	17.0
20000	6.1	495	6.5
25000	7.6	426	5.5
30000	9.1	480	6.5
		7630	100.0

TABLE 3. DISTRIBUTION OF OBSERVATIONS WITH TEMPERATURE
Entries represent each 5°C temperature interval centered at the listed temperature.

Temperature (°C)	Data Miles (nm)	Percent of Total
0	602	8.0
-5	1843	24.0
-10	2468	32.5
-15	1170	15.5
-20	396	5.0
-25	251	3.5
-30	323	4.0
-35	198	2.5
-40	186	2.5
-45	149	2.0
-50	42	0.5
	7630	100.0

TEMPERATURES AND ALTITUDES.

The temperatures and altitudes represented by the database are additionally illustrated by the scatterplot of datapoints in figure 2. Envelopes bounding the temperature-altitude combinations that are in use for supercooled stratiform and cumuliform clouds (figures 1 and 4 of reference 1) are shown for comparison.

Two derived curves and the standard atmosphere lapse rate [33] have also been drawn on figure 2. The curve labeled "Average Temperature" connects the average of all the temperatures recorded in each 1000-ft (0.3-km) altitude interval. Like similar curves in use for supercooled clouds (figure 4 of [34], and figure 1-16 of [35], it may be useful for selecting a most probable temperature at a given altitude when environmental values are needed for engineering design purposes. The curve (figure 2) labeled "Average Altitude" connects the average of all the altitudes at which each temperature was observed. It is seen to be a rough approximation to the standard lapse rate and may be used for assigning a representative altitude to any value of temperature for ice particle clouds. Note that the two curves Average Altitude and Average Temperature are different for this database where the data are truncated at 0°C.

ICE PARTICLE MASS.

COMPUTATION OF THE PARTICLE MASS. The computation of particle mass is perhaps the most important but least precise procedure in this report. There are several ways that particle mass can be computed from the recorded size spectra, but each method has its own deficiencies and uncertainties, as described below. The most commonly used methods are reviewed here.

Simple Particle Shapes. For particles of simple geometric shapes (i.e., spheres, cylinders, or disks), the mass of an individual particle can be computed from the simple formulas

$$m = (\pi/6)\rho D^3 \text{ or } m = (\pi/4)\rho D^2 L$$

for a sphere and cylinder or disk, respectively. Here, ρ is the density of ice and D is the diameter of a sphere, cylinder, or disk, and L is the length of a cylinder or the thickness of a disk.

Unfortunately, for nonspherical particles the PMS probes generally record neither D nor L, but some value in-between, depending on the orientation of the particle as it passes through the laser beam. In addition, the density ρ is highly variable, depending on the habit of individual crystals, the ambient temperature, and on the amount of riming. In any case, the method is limited to the relatively infrequent situations where simple shapes dominate. Dendrites, aggregates, and irregular particles are common shapes that require other methods for estimating their mass.

<u>Size-to-Mass Relationships</u>. A number of studies have discovered proportionalities between the measured mass, m, of various types of particles and their largest dimension, d_{max} [36, 11, and 37]. It has been found that plots of d_{max} versus m for most types of particles can be fit by equations of the form

$$m = A\,(d_{max})^B \tag{1}$$

where the values of A and B depend on the particular type of particle (e.g., columns, plates, conical graupel, aggregates of unrimed dendrites, etc.). These are simple equations and are therefore convenient for computing particle masses from measurements of maximum particle sizes. Figure 3 contains plots for a number of ice particle types from reference 36.

In principle, then, only a knowledge of the particle type and a measurement of its largest dimension is necessary. If the particle type is known, one may select the appropriate curve and very simply compute particle masses and sum them to get the total ice particle mass (TIPM), or "ice water" content, from the size distribution indicated by the available PMS probe. In practice, several problems arise. Firstly, the particle type may not be known unless a PMS 2D probe or some other imaging device was in use. Even then, several particle types may be present simultaneously, and the available data usually includes all particle types together. That is, separate size distributions for each particle type are usually not available. Secondly, the machine recorded particle sizes are generally not the maximum dimension of the particles, but the projection of the particle dimension that happens to be perpendicular to the laser beam at the time of measurement.

If the particles are randomly oriented in the air, then for the 1D probes anyway, a range of particle sizes from d_{max} to d_{min} will be recorded even if all the particles of a given type have exactly the same dimensions. The 2D probes allow the user to select the largest of two projections (one parallel and one perpendicular to the laser beam), but random particle orientations still result in apparent sizes smaller than d_{max} most of the time.

One helpful factor is the tendency for many precipitation sized particles to fall with a preferred orientation due to aerodynamic effects, depending on both their size and shape. For example, small (i.e., Reynolds number < 100) thin plates fall stably with the plate horizontal. Larger plates, though, begin to glide and/or tumble. Columns and needles tend to fall with their long axes horizontal. Some researchers have mounted their PMS probes with the laser beam pointing vertically to take advantage of these preferred orientations so that the longest particle dimension will be observed more often.

Bulk Density Method. This method makes use of observed radar reflectivities to "calibrate" the particle size distributions recorded in flight through the cloud volumes viewed by the radar [38]. The method assumes that the radar reflectivity factor, Z, can be computed from the recorded particle size distributions using the standard formula

$$Z = \rho \, \Sigma \, n \, D^6,$$

where n is the number of particles recorded in each of the 15 or so size channels in the PMS particle sizing probe, and D is the nominal particle size (diameter) associated with each size channel. The average density, ρ, for the precipitation particles is obtained by substituting into this equation the value of Z measured directly from the radar reflectivity. For spherical raindrops, $\rho = 1$ g/cm^3, and the values of D truly represent spherical diameters. For non-spherical ice particles or snowflakes, however, ρ is only an effective or apparent density, as the nominal diameters, D, are still used for simplicity and the actual shapes of the particles are not taken into account. This apparent density, sometimes termed the bulk density, is temperature dependent and has values in the range of 0.04 to 0.1 g/cm^3 at temperatures below -3°C (figure 23 in [38]). True ice densities are usually in the range of 0.3 to 0.9 g/cm^3 (tables 2-3 and 2-4 of [8]). In the melting layer (-3 to +1°C) the bulk density changes rapidly from 0.1 g/m^3 at -3°C to 1 g/cm^3 at +1°C. By using typical values of the bulk density, one can compute a value for the TIPM from the recorded particle size distribution with the equation

$$\text{TIPM(g/m}^3\text{)} = (\pi \, \rho/6) \, \Sigma \, n \, D^3,$$

where D is simply the nominal bin diameter.

SELECTION OF A METHOD. Methods 2 and 3 were both tried. A single method was sought which would serve satisfactorily as a universal method for all flights from all sources of data. The crucial factor was the ability of the method to give (1) computed TIPM's in reasonable agreement with those computed by the original authors (sources) of the various data sets and (2) realistic values of maximum, event-averaged, total ice particle mass (EvATIPM) for the dozen or so events which yielded the largest values of EvATIPM in the entire database.

This second criterion is somewhat subjective in that one has to decide what a realistic maximum value of EvATIPM is. In the BACKGROUND discussion of Maximum Total Mass, various pieces of evidence seemed to point to a value of about 2 g/m^3 as a realistic maximum EvATIPM to be expected at temperatures between 0 and -20°C. Occasionally, EvATIPM's as large as 3.5 g/m^3 may be found in unusual circumstances, such as in the center of a thunderstorm.

In trying out method 3, the bulk density method, it was found that computed EvATIPM's ranged up to 8 to 16 g/m^3 over several, separate, 3 nm intervals in the two flights with the largest EvATIPM's. These were flights by the University of Wyoming on March 27, 1979, and February 15, 1984, during the SCPP project in central California. Such large EvATIPM's are obviously unrealistic and, if retained, would call into question the credibility of all the computed particle masses. With this method there is little leeway in adjusting the equation or particle size spectrum to achieve smaller values of TIPM. For this reason, method 3 was discarded in favor of method 2.

With method 2, there are a number of size-to-mass curves to choose from, as shown in figure 3. This gives some flexibility in computing TIPM. The most satisfactory size-to-mass relationship for universal usage appears to be a combination of the curves labeled "rA" and "rC". The chosen curve is represented by the parameters A = 0.037 and B = 1.9 in equation 1, with m expressed in milligrams and d_{max} in millimeters. This is approximately the equation for both curves "rA" and "rC" in figure 3, and it very nearly represents some of the other nearby curves, such as "S" and "uA", as well. These curves are approximately colinear and together they represent most of the commonly observed particles (except for graupel) that are larger than about 1 mm. The chosen curve has been used here for particles of all sizes; that is, from 50 μm to 10 mm, taking the nominal bin diameters for d_{max}. In most cases the computed TIPM's compare favorably with those provided along with the original data. One notable exception is the mesoscale convective system (MCS) data, denoted by the plotting symbol "M" in some of the figures to follow. The MCS EvATIPM's computed here are all about 1 g/m^3 larger than the values obtained from radar reflectivity methods [56]. Otherwise, the maximum EvATIPM computed for any of the flights is about 2.5 g/m^3, in reasonable agreement with expectations. The range and distribution of the computed EvATIPM's can be seen in the scatterplots of EvATIPM vs. altitude or temperature, figures 4 to 11.

<u>ICE PARTICLE MASS VERSUS PARTICLE SIZE</u>. A second practical decision consisted of dividing the overall size range of 0-10 mm into several coarse, fixed subranges rather than trying to work with 15 size bins which will vary from probe to probe. Specifically, the chosen subranges are 50-100 μm, 100-300 μm, 300-1000 μm, 1-3 mm, 3-6 mm, and 6-10 mm. The reasoning is that for engineering assessments of the effects of ice and snow particles on aircraft engine inlets, etc., the important thing is how much mass is present in coarse-size ranges such as these. The finer scale distribution is of less importance. A small number of standard subranges is also helpful in keeping printouts of the database more readable. Both the recorded particle concentrations and the computed masses are sorted into these six size intervals, as indicated in table A-1 of appendix A.

Table 4 shows the percentage of the total mass that is contained in each of the size intervals in ice particle clouds. These values are averages for the entire database. The first three columns reveal that overall, the largest contribution to particle mass comes from the 1-3 mm size range irrespective of cloud type. Considerable contributions also come from the adjacent intervals of 0.3-1 mm and 3-6 mm. There is some dependence on altitude (temperature), however. Columns five and eight show that at altitudes above 20,000 ft (6 km) or temperatures less than -20°C, the greatest contributor to the total mass is the 0.3-1 mm size interval.

TABLE 4. PERCENTAGE DISTRIBUTION OF ICE PARTICLE MASS AMONG SIX SIZE INTERVALS

Size Interval	All Clouds	Convective Clouds	Layer Clouds	Altitude Range[a]			Temperature[b]	
				High	Mid	Low	Low	High
50-100 μm	0.2	0.2	0.2	1.5	0.2	0.02	1.2	0.2
100-300 μm	4.7	4.5	5.0	12.0	4.5	0.4	10.4	4.4
300-1000 μm	23.8	21.8	25.6	43.0	23.1	19.4	45.9	22.5
1-3 mm	41.4	41.0	41.7	36.8	41.4	48.0	36.4	41.6
3-6 mm	25.9	28.1	23.7	6.2	26.6	27.6	5.7	27.0
6-10 mm	4.0	4.4	3.7	0.5	4.2	4.7	0.4	4.2

a. Altitude (ASL) ranges are: High is above 20,000 ft (6 km), Mid is between 5,000 and 20,000 ft (1.5-6 km), Low is below 5,000 ft (1.5 km).

b. Temperature ranges are: High is from 0 to -20°C, Low is less than -20°C.

TOTAL ICE PARTICLE MASS VERSUS ALTITUDE. The ice particle mass that may be present at different flight altitudes is one of the primary interests in this newly assembled database. The event-averaged, total ice particle mass (EvATIPM) is obtained by summing the masses computed for each of the six coarse size intervals for the event. These intervals span the particle size range of 0.05 to 10 mm.

Figures 4a-4f show the distribution of EvATIPM with altitude for all the events in the Database. The largest values of computed EvATIPM are 2.5 to 3 g/m^3 and are from layer-type clouds below 20,000 ft (6 km) (figures 4e and 4f). These were from some nimbostratus clouds (frontal rainbands with embedded convection) during the SCPP project in central California (February 15, 1984) and from the trailing stratiform region of a mesoscale convective system over Kansas (June 10, 1985) [31,56]. As was mentioned earlier, the computed TIPM's shown here may be somewhat overestimated. TIPM's derived from radar reflectivity measurements at the time are about 1 g/m^3 smaller [56].

The apparent shortage of particle mass at altitudes below 3,000 ft (1 km) AGL is due mainly to a shortage of flight data there. Only 10% of all the data is from altitudes below 7,000 ft ASL, and measurements at ground level are also presently lacking in the database. Similarly, altitudes above 23,000 ft (7 km) ASL are represented by only 12% of the collected data. But there, the lack of EvATIPM's greater than 1 g/m^3 is more realistic due to the inherently restricted growth rates at the prevailing low temperatures, as reviewed in the BACKGROUND section of this report. In fact, as is the case here, EvATIPM's larger than about one-tenth of a gram per cubic meter appear to reach these heights only by being transported there from lower levels in thunderstorm anvils. In figure 4f, the large particle masses shown between about 25,000 ft and 31,000 ft (7.5 to 9.5 km) ASL are from the NCAR Sabreliner flights in the spreading anvil of a hail-producing, airmass thunderstorm over Montana (the CCOPE project, August 1, 1981; [9]).

Figure 4b shows the same data as in figure 4a, but the plotting symbols indicate the source of the data. Most of the EvATIPM's larger than 1 g/m^3 are from the University of Wyoming flights in the SCPP project. The rapid increase in maximum EvATIPM below 20,000 ft (6.1 km) is probably indicative of the onset of dendritic growth, riming, and aggregation at these altitudes and temperatures.

TOTAL ICE PARTICLE MASS VERSUS TEMPERATURE. Computed values of EvATIPM are plotted in figures 5a to 5e as a function of the in-cloud temperature at flight level. Examination of these figures suggests several general conclusions. The largest values of computed EvATIPM were found at temperatures between -15 and 0°C. At temperatures below about -25°C in layer clouds (figure 5e), the extreme EvATIPM's are less than 0.2 g/m^3. These colder clouds include cirrus types and upper levels of deep, cyclonic, winter storms. (Figure 5b shows that all of these layer cloud measurements at temperatures less than -25°C are from a single source—the AFGL C-130 flights [19-27]). The rapid increase in particle mass for temperatures greater than -25°C is probably indicative of the onset of dendritic growth, riming, and aggregation in this temperature range.

In convective clouds (figure 5d) the maximum computed EvATIPM's are about 1.5 to 2 g/m^3 and also occur at temperatures between -15 and 0°C. These extreme values are all from convective or orographically enhanced clouds near or over the windward slopes of the Sierra Nevada mountain range in California. The entries between -30 and -35°C are all from the one thunderstorm anvil sampled during the CCOPE project. The Database contains no measurements at temperatures less than -35°C in convective clouds.

To characterize the temperature dependence for engineering applications, one could conclude from figures 5a or 5b that for all cloud types together, extreme particle masses of 2.5 to 3 g/m^3 may be expected occasionally in the temperature range of 0 to -20°C. From -20 to -35°C, extreme values of ice particle mass can reach 1 g/m^3 in thunderstorm anvils. In cirrus and in the upper reaches of deep, wintertime, cyclonic storms, (i.e., at temperatures from -35 to -50°C), extreme values of particle mass will be less than about 0.2 g/m^3. Because thunderstorm anvils and portions of mesoscale convective systems can carry relatively large amounts of ice particle mass to high altitudes, extreme values may sometimes exceed 0.2 g/m^3 when these clouds penetrate into temperatures between -35 and -50°C. The dashed line in figure 5e is suggested as a tentative envelope bounding the apparent limit to total particle mass as a function of temperature aloft in layer clouds that are not associated with deep convective activity.

ICE PARTICLE CONCENTRATIONS.

CONCENTRATIONS VERSUS ALTITUDE. The numbers of ice particles (d_{max} > 100 m) that have been recorded per liter of air as a function of altitude are shown in figures 6a-6f. Several conclusions can be drawn from these figures. The greatest concentrations of ice particles at any altitude appear to be associated with either mesoscale convective systems (MCS) or thunderstorm anvils. Both are warm season phenomena and both are layer-type clouds associated with strongly convective systems. In general, the greatest concentrations may be expected at altitudes between 10,000 and 20,000 ft (3 to 6 km) ASL (figure 6f). Maximum concentrations there are about 200 particles per liter, except for the lone MCS case where concentrations between 200 and 400 per liter were found. Above 20,000 ft (6 km) ASL the maximum concentrations appear to be less than about 50/liter, except in thunderstorm anvils where concentrations up to about 100/liter have been observed. At these high altitudes and low temperatures, larger numbers of extremely small ice particles (d_{max} <100 µm) may occur, but these will account for a negligible amount of mass and are therefore not emphasized in this report.

CONCENTRATIONS VERSUS TEMPERATURE. Ice particle concentrations are plotted as a function of temperature in figures 7a-7e. The case for all cloud types together (figures 7a-7c) may be characterized by a gradual increase in maximum concentrations as temperatures increase from -50 to -10°C and then a decline as temperatures approach 0°C. The increase is probably due to the growth of increasing numbers of the extremely small particles into the size range d_{max} > 100 µm under consideration here. The decline between -10 and 0°C is presumably due to aggregation and the fallout of precipitation-sized particles in this temperature range. Peak concentrations are found at about -10°C for both convective (figure 7d) and layer clouds (figure 7e). At temperatures less than -20°C, layer clouds have less than about 40 particles per liter. Except for the anvil cloud, the database contains no measurements in convective clouds at temperatures less than -27°C. The available convective cloud data do show a much wider range of particle concentrations at temperatures from -20 to -35°C than is possible for layer clouds. As with particle mass, extremes in particle concentration appear to reside in MCS and anvil clouds.

ICE PARTICLE SIZE.

SIZE VERSUS ALTITUDE. The nonconforming nature of anvil clouds stands out most clearly in plots of maximum particle size versus altitude or temperature. Figures 8a-8d show the event-averaged maximum dimensions plotted according to altitude. The maximum particle dimension (MPD) is determined from the highest PMS probe channel to contain at least one particle per cubic meter in a given data record. The event-averaged MPD is the average value of the record-by-record MPD's over an entire event. Figures 8a and 8b identify the anvil data (plotting symbol, A) standing alone at altitudes well above the rest of the convective cloud data. Except for the large particles available in the anvil, there is otherwise an indication of a decrease in maximum particle size with altitude above 15,000 ft (4.5 km) ASL (or AGL) for both the convective (figure 8b) and layer clouds (figure 8c). It is also evident that the MCS trailing stratiform clouds (plotting symbol, M, in figures 8a and 8c) readily provide some of the largest particles in the Database. As in other altitude plots, the apparent absence of large (5-10 mm) particles below about 3000 ft (1 km) AGL is attributed to a shortage of measurements for those altitudes.

SIZE VERSUS TEMPERATURE. Figures 9a to 9c show maximum particle dimension (MPD) plotted against temperature. The trends resemble those seen in the plots of MPD versus altitude in that there is a trend to larger MPD's as temperatures increase from -50°C up to about -12°C. This is no doubt a result of increased growth by riming and aggregation at the higher temperatures, as well as the appearance of stellar and dendritic crystals at temperatures greater than about -20°C. As before, the anvil data stand alone in the range of -25 to -35°C and exhibit anomalously large particles in contrast to all other clouds at the same temperatures. The dashed line in figure 9c is suggested as a tentative envelope bounding the apparent limit to particle size as a function of temperature aloft in layer clouds not associated with deep convective activity.

HORIZONTAL EXTENT.

The horizontal extent of ice particle clouds is an important factor in assessing aircraft exposures in this environment just as it is with supercooled clouds. In this report, horizontal extents are equated to the distance flown on a more-or-less constant heading through sequential events until a particle-free interval of one nautical mile or more is reached. These groups of one or more events are termed an encounter.

The database at this writing is composed of 1625 individual events covering 7632 nautical miles. This gives an average of 4.7 nm per event. These events combine into 571 encounters with an average length of 13.4 nm, and the longest being 100 nm.

In most research flights the aircraft samples clouds in a local area rather than in a cross country type of flight plan. As a result, the indicated horizontal extents are usually not a measure of the actual extent of the cloud systems, which are often considerably larger. Rather, the compiled horizontal extents are more representative of arbitrarily limited passes through local portions of an available cloud system. Thus, the horizontal extents compiled from the database here should not be understood as necessarily typical of the cloud exposures that a cross-country flight may endure. Nevertheless, they are helpful for obtaining some idea of the exposures that are possible and for looking for any correlations of total ice particle mass with averaging distance.

AVERAGE ICE PARTICLE MASS VERSUS HORIZONTAL EXTENT. In supercooled clouds, the amount of liquid water content that is possible as an average over a pass is known to decrease with increasing horizontal extent of the pass. Figures 10a-10d have been prepared to look for any similar behavior in glaciated clouds. These figures do show a generally similar behavior in layer clouds. The larger total masses occur for encounters shorter than 20 nm or perhaps up to 30 nm in MCS stratiform clouds (figure 10c). For longer encounters, the average total mass is less than about 1 g/m^3 for all clouds. In contrast to supercooled clouds, where the largest values of liquid water contents (LWC's) are found in convective clouds, glaciated clouds appear to have their greatest particle masses in layer clouds. Also, in supercooled clouds the largest LWC's are confined to very short horizontal extents of less than about one nautical mile. In glaciated clouds the largest encounter-averaged total masses can be found over horizontal extents up to 30 nm.

HORIZONTAL EXTENT VERSUS ALTITUDE. Figures 11a-11c show the horizontal extents computed for each altitude (ASL). There appears to be no significant dependence on altitude—long encounters can be found at any altitude up to 30,000 ft (9 km). The longest encounter (100 nm) was during an AFGL flight in cirrostratus clouds associated with a subtropical jet stream at about 25,000 ft (7.5 km) ASL over Colorado. Other long encounters (70-90 nm) are tabulated below.

TABLE 5. THE LONGEST ENCOUNTERS IN THE DATABASE

Agency	Horizontal Ext. (nm)	Cloud Type	Circumstances	Altitude (ASL) Feet	(km)	Location	Events
USAF/AFGL	100	Cs	Subtropical jetstream	25,000	(7.5)	Colo.	20
USAF/AFGL	72	Cs	Short wave, 300 mb jetstream	29,000	(8.8)	N. Mex.	36
U. Wyoming	79	OrSt	Widespread overcast	7300	(2.3)	Calif.	13
U. Wyoming	69	OrSc	Widespread overcast	13,500	(4.1)	Calif.	10
NCAR/MIT	74	As	Widespread overcast	12,000	(3.7)	Mass.	2
NCAR/MIT	86	As	Snowfall below cloud	2700	(0.8)	Mass.	7

CIRRUS CLOUDS.

The observed particle characteristics of cirrus clouds are summarized as a separate topic here because of the possible interest in these clouds in relation to high-altitude flight. Cirrus clouds are understood to generally occur above about 20,000 ft (6 km) ASL and at temperatures less than about -20°C in temperate climates.

TOTAL ICE PARTICLE MASS. The 790 nm of cirrus cloud measurements contained in the database indicate that for altitudes above 20,000 ft (6 km) ASL or for temperatures less than -25°C, TIPM's are less than about 0.1 g/m^3. By way of comparison, these results are in good agreement with those of other airborne studies of cirrus clouds. From 20 hours of sampling in cirrus generating cells, Heymsfield and Knollenberg [39] found average TIPM's of 0.15 to 0.25 g/m^3. Another major study was conducted over the Soviet Union [40] during the years 1976-82. In 25 hours (about 6000 nm or about 11,000 km) of flight data in various types of cirrus, the largest TIPM observed by the Soviets was 0.3 to 0.4 g/m^3. They found that 95% of the TIPM's were less than 0.2 g/m^3, and 90% were less than 0.1 g/m^3. The mean and median values of TIPM were about 0.03 g/m^3. At temperatures less than -40°C, TIPM's were less than 0.01 g/m^3. Table 6 gives other reported maximum TIPM's for altitudes above 30,000 ft (9 km).

The cirrus measurements presently in the database appear to be adequately representative of mid-latitude cirrus at least and cirrus not immediately connected with strongly convective systems such as high-altitude anvils (or blowoff) from thunderstorms.

MAXIMUM PARTICLE SIZE. The Database indicates that the maximum particle dimension (MPD) in cirrus clouds above 20,000 ft (6 km) ASL is about 3 mm. The recent Soviet study [40] found a MPD of 4 mm in cirrus (unspecified altitude), but 95% of the MPD's were less than 2 mm and 90% were less than about 1.5 mm. Table 6 gives other reported MPD's at altitudes above 30,000 ft (9 km) ASL.

HIGH-ALTITUDE CIRRUS. In the present context, high-altitude cirrus refers to clouds above 30,000 ft (9 km) ASL or at temperatures less than about -50°C. The high-altitude cirrus, therefore, are clouds above the maximum altitudes currently available in the database. The only known references to airborne measurements in high-altitude, mid-latitude cirrus indicate that maximum particle dimensions are 2 mm or less and maximum TIPM's are 0.004 g/m^3 or less. Table 6 shows the pertinent details.

TABLE 6. SUMMARY OF HIGH-ALTITUDE, MID-LATITUDE CIRRUS MEASUREMENTS

Reference	Location	Altitude Range (At Sea Level)	Temperature Range (°C)	Maximum Particle Dimension	Maximum TIPM (g/m^3)
41	U.S.A.	36,000 ft (11 km)	-50 to -53	1.6 mm	0.004
41	U.S.A.	33,000 ft (10 km)	-55 to -60	1.0 mm	0.002

TROPICAL CIRRUS. As for the high-altitude cirrus, few references are available for particle size measurements in tropical cirrus. The data that are available give the following results. TIPM's of at least 0.4 g/m^3 appear to be possible in dense cirrus anvil outflows from active Cb cells [42], but otherwise, TIPM's are less than about 0.1 g/m^3. Data from the available references are summarized in table 7.

TABLE 7. SUMMARY OF TROPICAL CIRRUS MEASUREMENTS

Ref.	Location	Altitude Range (ASL)	Temperature Range (°C)	Maximum Particle Dimension	Maximum TIPM (g/m^3)	Cloud Type
42	Tropical Atlantic	26,000 to 43,000 ft (8-13 km)	< -55	0.5-1 mm	0.3-0.45	cirrus anvil
42	Tropical Atlantic	30,000 to 39,000 ft (9-12 km)	< -55	0.5-1 mm	0.1-0.15	not available
42	Tropical Atlantic	33,000 to 39,000 ft (10-12 km)	< -55	0.5 mm	0.05-0.07	tenuous layer
43	Not available	36,000 to 43,000 ft (11-13 km)	-40 to -58	0.6 mm	0.003	aging cb blowoff
44	Kwajalein	46,000 to 53,000 ft (14-16 km)	not available	0.15 mm	0.0001	tenuous layer
45	Marshall Island	53,000 ft (16.5 km)	-83	0.05 mm	0.0001	tenuous layer
46	Panama	52,000 ft (16 km)	-80	0.15 mm	0.003	aging anvil
46	Panama	52,000 ft (16 km)	-80	1 mm	0.03	cirrus anvil

THUNDERSTORM ANVILS.

As with cirrus clouds, the observed particle characteristics of anvil clouds are summarized as a separate topic because of their possible effects on high-altitude flight. They can contain large concentrations of ice particle mass and can cover large volumes of flight space at mid and high altitudes. Anvil clouds are understood here to be the upper level outflow from thunderstorms which have risen to the level of the tropopause. The strong temperature inversion at the tropopause generally prevents further vertical growth of the thunderstorm and, along with any upper level winds, forces the rising air (and cloud) to spread out horizontally. Anvil clouds may be deep and widespread and may therefore cover some of the high-altitude airways for hours.

MID-LATITUDE THUNDERSTORMS. The base of these anvil clouds is generally above 20,000 ft (6 km) ASL. Very few anvil clouds have been studied with particle sizing probes and most of those appear to be the eight reported by Heymsfield et al. [9, 39, and 47]. These cases demonstrate that anvils may contain large TIPM's compared to other cloud types (mostly cirrus) at the same altitudes. Only one anvil cloud [9] has been included in the database at this writing; it produced maximum TIPM's of about 1 g/m^3. No size distributions or particle concentrations were given in reference 47, but pass-averaged TIPM's were frequently up to 1 g/m^3 and occasionally up to about 3 g/m^3. Although the aircraft penetrations were typically conducted in quiescent regions removed from convective towers, significant updrafts, liquid water contents, and aircraft icing were occasionally encountered. The TIPM's greater than 1 g/m^3 occurred in regions containing updrafts of 4 m/sec or more.

TROPICAL THUNDERSTORMS. Anvil clouds are also a prominent feature of some strongly convective weather systems of subsynoptic size in both the continental and maritime tropics [48-51]. In these cases the anvil often refers to a thick layer of precipitating nimbostratus clouds extending from the 0°C level in the vicinity of 15,000 ft (4.5 km) to near the tropopause at 40,000-50,000 ft (12-15 km). These anvils are found extending far behind squall lines of convective towers (figure 12a), or as a merging outflow from nearby stationary towers (figure 12b). The anvil cloud usually forms several hours after deep convection first appears. It can become quite extensive with horizontal dimensions of the order of 100 to 300 km (50 to 150 nm) and may persist for up to 20 hours [48]. The precipitation from the anvil region is often widespread, uniform, long lasting, and has been estimated to account for as much as 40% of the total rainfall in the tropics.

Horizontally uniform precipitation like this in the mid-latitudes is usually associated with extratropical cyclones or frontal cloudiness and not with convective systems, except for the summertime, mesoscale convective systems (MCS). One of these mid-latitude MCS cases [31] has been included in the database and the large particle sizes, concentrations, and TIPM's associated with it have already been pointed out several times in this RESULTS section. This association of the widespread nimbostratus with convective clusters has often led to it being called a "mesoscale anvil", especially in the tropical setting.

Particle size measurements have been rare in these mesoscale anvils too, but the available evidence indicates that the ice particle characteristics are similar to mid-latitude anvils. The few high-altitude measurements have already been included in table 7 as cirrus anvil data. They show that 1 mm particles and TIPM's up to 0.03 g/m^3 can be found as high as 52,000 ft (16 km) ASL and -80°C in active tropical anvils [46]. In the absence of actual particle size measurements, radar reflectivity data has sometimes been used to estimate the TIPM in tropical anvils. Thus, TIPM's up to 0.9 g/m^3 were deduced for altitudes near 23,000 ft (7 km) in the stratiform region of one cloud cluster in the tropical Pacific [49]. In another case [48], values as high as 3 g/m^3 were estimated from radar data just above the melting layer in the vicinity of 15,000 ft (4.5 km) over the tropical Atlantic.

The most recent study [57] of thunderstorm anvils includes measurements from the Central Equatorial Pacific Experiment (CEPEX) of 1993. These include ice particle measurements up to 14 km (46,000 ft) and temperatures down to -60°C. Thus, these data extend to greater altitudes and to lower temperatures than in figures 4-11 of this report. The CEPEX data fill in some of the data-sparse areas in figures 4, 5, and 8, and they enlarge the envelopes of extreme values of TIPM at altitudes above 6 km (20,000 ft). Nevertheless, these new data do not seem to change any of the main conclusions of this report. Maximum reported TIPM in anvil clouds is about 2.5 g/m^3. Exact comparisons between the data in [57] and that in the present paper will require the measurements in [57] to be processed in the same way as in this report.

SNOW MEASUREMENTS NEAR GROUND LEVEL.

The database developed here contains no entries at the moment from any measurements near the surface. This deficiency can be remedied to some extent by examining available reports with information on recorded snowfall rates or actual TIPM measurements. One can then at least estimate the typical and likely maximum values of TIPM that may be expected near runway heights. One such estimation was given in the BACKGROUND section of this report where Werner (page 36 of reference 16) was quoted as estimating 99th percentile values of TIPM at about 2 g/m^3 for temperatures in the vicinity of -4 to +1°C. His estimates were based on the surface weather observation records for extreme 24-hour snowfalls.

There have been some major, long-term, snow research projects in which TIPM's were measured directly. Stallabrass [52, 53] measured TIPM at roof-top height in snowfall episodes over a 6-year period at Ottawa, Canada. Of some 770 samples, the maximum TIPM was about 1.7 g/m^3. The observed cumulative frequencies of occurrence for this data set gave the following percentile values of TIPM [53]:

Percentile	TIPM (g/m^3)
50	0.15
90	0.6
95	1.0
97.5	1.25
100	1.7

A curve fitted to these observed frequencies of occurrence suggests a value of about 2 g/m^3 for the maximum likely TIPM.

Stallabrass suggested that these results were typical of many regions of Canada and the United States, with the possible exception of (a) coastal regions and in the lee of the Great Lakes where more of the larger TIPM's may be found and (b) in the colder subarctic and arctic regions where fewer of the large TIPM's would be expected. He also noted that the largest TIPM's occurred at ambient temperatures between -10 and -14°C.

Another multiyear snow characterization project has been the 5-year series of SNOW (Scenario Normalization for Operations in Winter) field experiments led by the U.S. Army's Cold Regions Research and Engineering Laboratory (CRREL). There are a series of data reports and symposia proceedings published by CRREL. References 54 and 55 are recent samples of each. These were multiagency, cooperative projects conducted in Vermont and Michigan during the winters of 1980-81 through 1984-85. A review of the data reports and symposia proceedings reveals that the largest TIPM's observed were in the range of 0.6 to 1 g/m^3 at the sampling heights a few feet above ground level.

These results from large numbers of near-surface measurements indicate that the frequencies and maximum values of TIPM are similar to those computed from airborne measurements up to about 10,000 ft (3 km) AGL.

RECOMMENDATION

SUGGESTED CHARACTERIZATION OF SNOW AND ICE PARTICLE SIZE AND MASS CONCENTRATIONS TO 15 km (50,000 ft).

Table 8 provides a logical and natural way to characterize snow and ice particle size and mass concentrations for aviation purposes. The values listed in the table are based on the results presented here, augmented by the anvil data in [57]. The latter extend the temperature limits to -60°C and the TIPM range to 2.5 g/m^3 for anvil clouds. Table 8 categorizes the data according to the predominant cloud types to be found above or below 6 km (20,000 ft). This break point in altitude reflects the observed natural tendency for smaller ice crystals to dominate above 6 km (except for the special class of anvil clouds) and for snowflakes (aggregates if ice crystals) to form and grow larger in the relatively warmer, moister air below 6 km. This altitude division is also convenient for specifying ice/snow conditions affecting helicopters or other aircraft limited to altitudes below 20,000 ft. They can be treated separately from aircraft that are able to reach all altitudes.

This table is suggested as a possible set of criteria for the "falling and blowing snow" requirement for turbine engine ice protection in paragraph 1093 of FARs 23, 25, 27, and 29 and as a possible improvement to the provisional set of ice crystal conditions given in table 3 of the Joint Airworthiness Authority's guidance document ACJ.1419 [58].

An accepted set of design and test variables, as shown in table 8, would help modernize and harmonize the American and European airworthiness specifications for snow and ice particles in flight.

TABLE 8. PROPOSED ICE/SNOW TEST SPECIFICATIONS FOR IN-FLIGHT CONDITIONS

1. Anvil Clouds (Above 25,000 ft ASL):

	Range of Variables	Representative Values
Altitude	25,000-50,000 ft ASL	25,000-35,000 ft ASL
Temperature	-25 to -60°C	-25 to -35°C
Ice mass	up to 2.5 g/m^3	1.0 g/m^3
Max Dia.	1-10 mm	1-10 mm
Horiz Ext.	undetermined	5-20 nmi

2. Cirrus Clouds and Deep Winter Storms (Above 20,000 ft ASL):

	Range of Variables	Representative Values
Altitude	20,000 - 50,000 ft ASL	20,000-35,000 ft ASL
Temperature	-20 to -50°C	-20 to -50°C
Ice mass	0 to 0.2 g/m^3	0.05 g/m^3
Max Dia.	0-3 mm	1 mm
Horiz. Ext.	5-100 nm	20 nm (for cirrus)
Horiz. Ext.	100-500 nm	100 nm (for deep winter storms)

3. Other Snow/Ice Clouds (below 20,000 ft ASL):

	Range of Variables	Representative Values
For temperatures from 0 to -30°C		-5 to -25°C
For temperatures from 0 to -20°C:		
Ice mass	0-3 g/m^3	0.6 g/m^3 (for Horiz. Ext. < 30 nm)
Ice mass	0-1 g/m^3	0.4 g/m^3 (for Horiz. Ext. > 30 nm)
Max Dia.	1-10 mm	1-8 mm
For temperatures from -20 to -30°C:		
Ice mass	0-1 g/m^3	0.2 g/m^3 (for all Horiz. Extents)
Max Dia.	1-5 mm	1-4 mm

Note: 1. This table does not include hail or heavy rain. Recommended values for those conditions are found elsewhere. Nor does the table include graupel or other large particles which can be found in the updraft cores of thunderstorms.

2. Values for this table are submitted by R. Jeck, AAR-421 (FAA William J. Hughes Technical Center) based on analyses of 7600 nm of select ice particle measurements in a variety of cloud types over the U.S. at altitudes up to 30,000 ft ASL.

REFERENCES

1. Federal Aviation Regulations, Part 25, Appendix C, in the Code of Federal Regulations, Title 14, Aeronautics and Space, Federal Aviation Administration, Washington, DC 20591 (issued annually).

2. Houghton, H.G., Physical Meteorology, MIT Press, Massachusetts Institute of Technology, Cambridge, Massachusetts, 1985.

3. Marshall, J.S. and Palmer, W., "The Distribution of Raindrops With Size," J. Meteor., 5, 165-166 (1948).

4. Gunn, K.L.S. and Marshall, J.S., "The Distribution with Size of Aggregate Snowflakes," J. Meteor., 15, 452-461 (1958).

5. Douglas, R.H., "Hail Size Distributions, Proc. 1964 World Conf. Radio Meteorology and 11th Weather Radar Conf.," Boulder, Colorado, Amer. Meteor. Soc., 47-49 (1964).

6. Simpson, J.S. and Wiggert, V., "1968 Florida Cumulus Seeding Experiment, Numerical Model Results," Mon. Wea. Rev., 99, 87-118 (1971).

7. Lo, K.K. and Passarelli, R.E., "The Growth of Snow in Winter Storms: An Airborne Observational Study," J. Atm. Sci., 39, 697 (1982).

8. Pruppacher, H.R. and Klett, J.D., Microphysics of Clouds and Precipitation, D. Reidel Publishing Co. (1978).

9. Heymsfield, A.J., "Ice Particle Evolution in the Anvil of a Severe Thunderstorm During CCOPE," J. Atm. Sci., 43, 2463 (1986).

10. Hobbs, P.V. and Rangno, A.L., "Ice Particle Concentrations in Clouds," J. Atm. Sci., 42, 2523 (1985).

11. Heymsfield, A.J., "Precipitation Development in Stratiform Ice Clouds: A Microphysical and Dynamical Study," J. Atm. Sci., 34, 367 (1977).

12. Duroure, C., "Mecanismes de Glaciation Secondaire dans les Stratocumulus: Importance du 'Splintering' dans les Zones de Melange des Regions Convectives," J. Rech. Atmos., 16, 353-367 (1982).

13. Churchill, D.D. and Houze, R.A., "Development and Structure of Winter Monsoon Cloud Clusters on 10 December 1978," J. Atm. Sci., 41, 933-960 (1984).

14. Valdvogel, A., Klein, L., Musil, D.J., and Smith, P.L., "Characteristics of Radar-Identified Big Drop Zones in Swiss Hailstorms," J. Climate and Appl. Meteor., 26, 861-877 (1987).

15. Sekhon, R.S. and Srivastava, R.C., "Snow Size Spectra and Radar Reflectivity," J. Atm. Sci., 27, 299-307 (1970).

16. Werner, J.B., "The Development of an Advanced Anti-Icing/Deicing Capability for U.S. Army Helicopters, Vol. 1 - Design Criteria and Technology Considerations," Report No. USAAMRDL-TR-75-34A, 1975, U.S. Army Air Mobility Research and Development Laboratory, Fort Eustis, Virginia, 23604.

17. Knollenberg, R.G., "Techniques for Probing Cloud Microstructure, in Clouds, Their Formation, Optical Properties, and Effects," P.V. Hobbs and A. Deepak, editors, Academic Press (1981).

18. Jeck, R.K., "Airborne Cloud Physics Projects From 1974 Through 1984," Bull. Amer. Meteor. Soc., 67, 1473-77 (1986).

19. Varley, D.J., "Cirrus Particle Distribution Study, Part 1," Report No. AFGL-TR-78-0192 (1978), Air Force Geophysics Laboratory, Hanscom AFB, Massachusetts 01731.

20. Varley, D.J. and Brooks, D., "Cirrus Particle Distribution Study, Part 2," Report No. AFGL-TR-78-0248 (1978), Air Force Geophysics Laboratory, Hanscom AFB, Massachusetts 01731.

21. Varley, D.J. and Barnes, A., "Cirrus Particle Distribution Study, Part 4," Report No. AFGL-TR-79-0134 (1979), Air Force Geophysics Laboratory, Hanscom AFB, Massachusetts 01731.

22. Cohen, I.D., "Cirrus Particle Distribution Study, Part 5," Report No. AFGL- TR-79-0155 (1979), Air Force Geophysics Laboratory, Hanscom AFB, Massachusetts 01731.

23. Cohen, I.D. and Barnes, A., "Cirrus Particle Distribution Study," Part 6, Report No. AFGL-TR-80-0261 (1980), Air Force Geophysics Laboratory, Hanscom AFB, Massachusetts 01731.

24. Varley, D.J., Cohen, I.D., and Barnes, A.A., "Cirrus Particle Distribution Study, Part 7," Report No. AFGL-TR-80-0324 (1980), Air Force Geophysics Laboratory, Hanscom AFB, Massachusetts 01731.

25. Cohen, I.D., "Cirrus Particle Distribution Study, Part 8," Report No. AFGL- TR-81-0316 (1981), Air Force Geophysics Laboratory, Hanscom AFB, Massachusetts 01731.

26. Varley, D.J., “Microphysical Properties of a Large Scale Cloud System, 1-3 March 1978,” Report No. AFGL-TR-80-0002 (1980), Air Force Geophysics Laboratory, Hanscom AFB, Massachusetts 01731.

27. Cohen, I.D., “Development of a Large Scale Cloud System, 23-27 March 1978,” Report No. AFGL-TR-81-0127 (1981), Air Force Geophysics Laboratory, Hanscom AFB, Massachusetts 01731.

28. Rauber, R.M., “Microphysical Processes in Two Stably Stratified Orographic Cloud Systems, Atmospheric Science Paper,” No. 337 (1981), Colorado State Univ., Fort Collins, Colorado 80523.

29. Cunning, J.B., “The Oklahoma-Kansas Preliminary Regional Experiment for STORM-Central,” Bull. Amer. Meteor. Soc., 67, 1478 (1986).

30. Anthes, R.A., “The National STORM Program (Scientific and Technical Bases and Major Objectives),” unnumbered UCAR report prepared for NOAA (1983), University Corporation for Atmospheric Research, P.O. Box 3000, Boulder, Colorado 80307.

31. Heymsfield, A.J., private communication.

32. Reynolds, D.W. and Dennis, A.S., “A Review of the Sierra Cooperative Pilot Project,” Bull. Amer. Meteor. Soc., 67, 513 (1986).

33. Glossary of Meteorology, American Meteorological Society, Boston, Massachusetts, 1970.

34. Hacker, P.T. and Dorsch, R.G., “A Summary of Meteorological Conditions Associated With Aircraft Icing and a Proposed Method of Selecting Design Criterions for Ice-Protection Equipment,” NACA TN 2569, 1951. National Aeronautics and Space Administration, Washington, DC.

35. Bowden, D.T., Gensemer, A.E., and Skeen, C.A., “Engineering Summary of Airframe Icing Technical Data,” Technical Report ADS-4, 1963, Federal Aviation Administration, Washington, DC.

36. Locatelli, J.D. and Hobbs, P.V., “Fall Speeds and Masses of Solid Precipitation Particles,” J. Geophys. Res., 79, 2185-2197 (1974).

37. Starr, D.O. and Cox, S.K., “Cirrus Clouds. Part I: A Cirrus Cloud Model,” J. Atm. Sci., 42, 2663 (1985).

38. Gordon, G.L. and Marwitz, J.D., “Hydrometeor Evolution in Rainbands Over the California Valley,” J. Atm. Sci., 43, 1087-1100 (1986).

39. Heymsfield, A.J. and Knollenberg, R.G., "Properties of Cirrus Generating Cells," J. Atm. Sci., 29, 1358-1366 (1972).

40. Kosarev, A.L., Nevzorov, A.N., and Shugaev, F.V., "On the Microstructure and Ice Water Content of High Clouds, Proceedings of the 9th International Cloud Physics Conference," p. 73-76, Tallinn, USSR (1984).

41. Heymsfield, A.J. and Platt, C.M.R., "A Parameterization of the Particle Size Spectrum of Ice Clouds in Terms of the Ambient Temperature and the Ice Water Content," J. Atm. Sci., 41, 846-855 (1984).

42. Griffith, K.T., Cox, S.K., and Knollenberg, R.G., "Infrared Radiative Properties of Tropical Cirrus Clouds Inferred from Aircraft Measurements," J. Atm. Sci., 37, 1077-87 (1980).

43. Stickel, P.G., "Observation of Ice Aggregation at Temperatures Near -50°C," preprints of the AMS Conference on Cloud Physics, Chicago, Illinois (1982), p. 226-229.

44. Booker, D.R. and Stickel, P.G., "High Altitude Cirrus Cloud Observations," preprints of the AMS Conference on Cloud Physics, Chicago, Illinois (1982), p. 215-217.

45. Heymsfield, A.J., "Ice Particles Observed in a Cirriform Cloud at -83°C and Implications for Polar Stratospheric Clouds," J. Atm. Sci., 43, 851-855 (1986).

46. Knollenberg, R.G., Dascher, A.J., and Huffman, D., "Measurements of the Aerosol and Ice Crystal Populations in Tropical Stratospheric Cumulonimbus Anvils," Geophys. Resch. Letters, 9, 613-616 (1982).

47. Heymsfield, A.J. and Palmer, A.G., "Relationships for Deriving Thunderstorm Anvil Ice Mass for CCOPE Storm Water Budget Estimates," J. Climate and Appl. Meteor., 25, 691-702 (1986).

48. Leary, C.A. and Houze, R.A., "Melting and Evaporation of Hydrometeors in Precipitation from the Anvil Clouds of Deep Tropical Convection," J. Atm. Sci., 36, 669-679 (1979).

49. Churchill, D.D. and Houze, R.A., "Mesoscale Updraft Magnitude and Cloud-Ice Content Deduced from the Ice Budget of the Stratiform Region of a Tropical Cloud Cluster," J. Atm. Sci., 41, 1717-1725 (1984).

50. Houze, R.A., "Structure and Dynamics of a Tropical Squall-Line System, Monthly Weather Review," 105, 1540-1567 (1977).

51. Houze, R.A., Geotis, S.G., Marks, F.D., and West, A.K., "Winter Monsoon Convection in the Vicinity of North Borneo, Part I, Structure and Time Variation of the Clouds and Precipitation," Monthly Weather Review, 109, 1595-1614 (1981).

52. Stallabrass, J.R., “The Airborne Concentration of Falling Snow,” DME/NAE Quarterly Bulletin, Vol. 3 (1976), National Research Council of Canada, Ottawa, Canada K1A 0R6.

53. Stallabrass, J.R., “Snow Concentration Measurements and Correlation With Visibility,” AGARD Conference Proceedings No. 236 (Icing Testing for Aircraft Engines), London (1978).

54. Jordan, R. (ed.), “SNOW-TWO Data Report,” Vol. 1, Special Report 84-20 (June 1984), U.S. Army CRREL, Hanover, NH 03755-1290.

55. “SNOW Symposium VI,” Vol. 1, Special Report 87-12 (July 1987), U.S. Army CRREL, Hanover, NH 03755-1290.

56. Rutledge, S.A., Houze, R.A., Heymsfield, A.J., and Biggerstaff, M.I., “Dual-Doppler and Airborne Microphysical Observations in the Stratiform Region of the 10-11 June MCS over Kansas during PRE-STORM,” preprints from the 10th International Cloud Physics Conference, p. 702-704, Bad Homburg, FRG (1988).

57. Lawson, R.P., Angus, L.J., and Heymsfield, A.J., “Cloud Particle Measurements in Thunderstorm Anvils and Possible Weather Threat to Aviation,” Paper No. AIAA 96-0400, 34th AIAA Aerospace Sciences Meeting, January 15-18, 1996, Reno, Nevada. (American Institute of Aeronautics and Astronautics, 1801 Alexander Bell Drive, Suite 500, Reston, Virginia 20191-4344.

58. Joint Aviation Requirements (JAR), JAA Secretariat, Aviation House, Gatwick Airport, West Sussex RH6 0YR, United Kingdom.

GLOSSARY

Agglomerate	A clump or random accumulation of particles that has grown by collision with other particles.
Aggregate	(see agglomerate).
Conglomerate	(see agglomerate).
Crystal	A single ice particle which has grown by vapor diffusion and condensation only and has a symmetrical shape (e.g., needle, hexagonal plate, stellar).
Crystal habit	The shape classification (needle, plate, dendrite, etc.)
Data miles	The number of nautical miles over which usable flight data have been obtained.
Database	Refers to the computerized compilation of ice particle data described in this report.
Deposition	The growth of ice particles by the condensation of water vapor from the ambient humidity of the surrounding air or which has diffused to the ice particles from nearby evaporating, supercooled cloud droplets.
Encounter	An averaging interval consisting of one or more events added sequentially until a cloud-free distance of one nautical mile or more is reached.
Event	A variable flight time or distance interval over which the measured quantities are averaged during a given cloud penetration. The interval duration is selected according to the rules in table A-3 in appendix A.
Glaciated	Composed entirely of ice particles.
Graupel	An ice particle rimed to the extent that the features of the primary ice particle are only faintly or no longer visible. Such particles have a white, opaque, and fluffy appearance due to the presence of a large number of capillaries or air spaces in the ice structure.
Ice crystal	A crystal or particle that is smaller than 0.3 mm in maximum dimension (as contrasted with larger snow particles).
Ice particle	The general term for any piece or mass of icy substance observable as an individual, suspended, or freely falling entity, regardless of size, shape, or number of components.

Riming	Supercooled droplets colliding with and freezing on an ice particle.
Snow	A crystal or particle that is larger than 0.3 mm.
Snow flake	Usually an aggregate of crystals or particles; sometimes a single crystal.
Snow pellet	(see graupel).
Soft hail	(see graupel).
Supercooled	The condition of remaining liquid at temperatures below the freezing point.

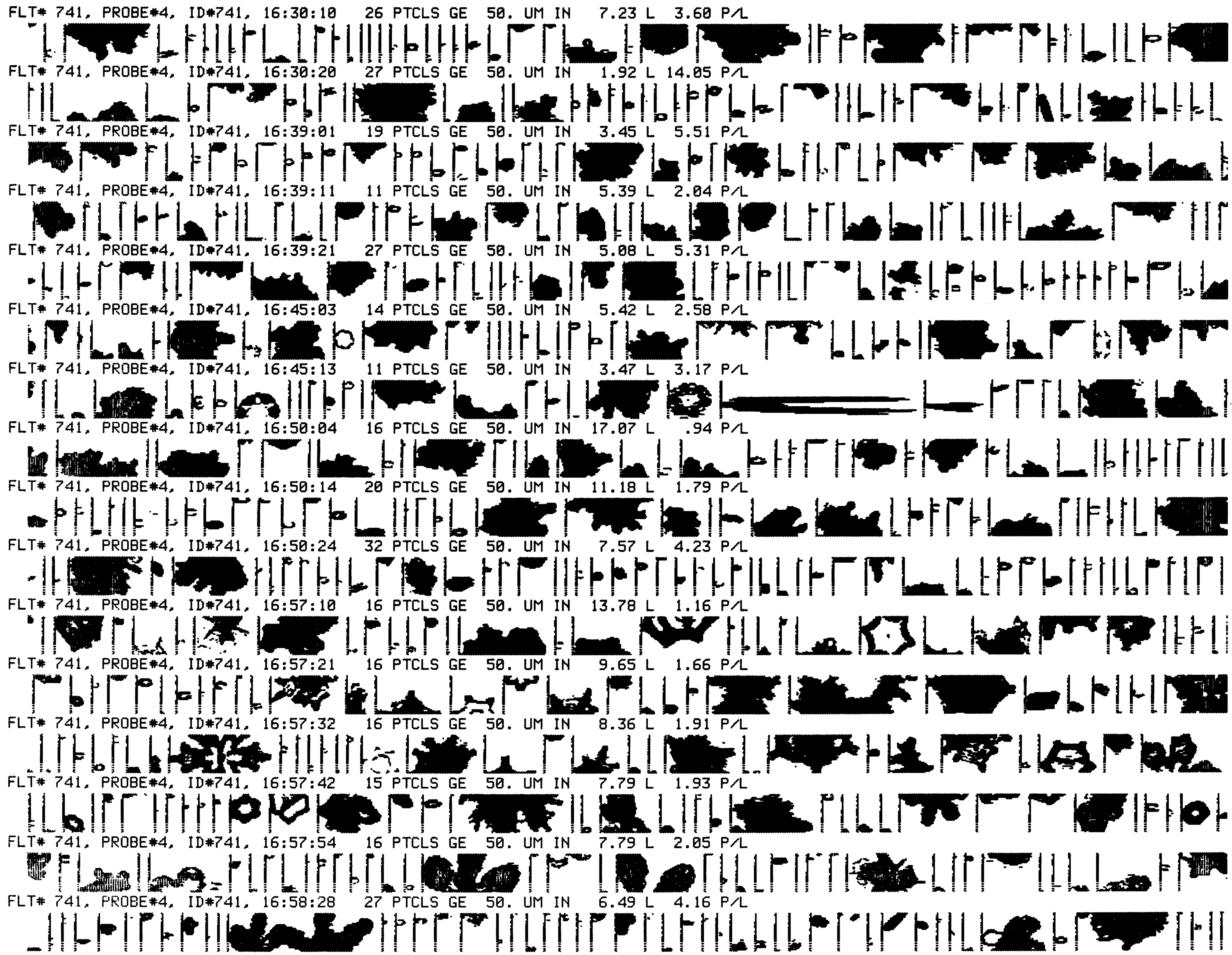

FIGURE 1. EXAMPLE OF ICE PARTICLE SHADOWGRAMS AVAILABLE FROM PMS 2D-C OR 2D-P IMAGING SIZE SPECTROMETERS

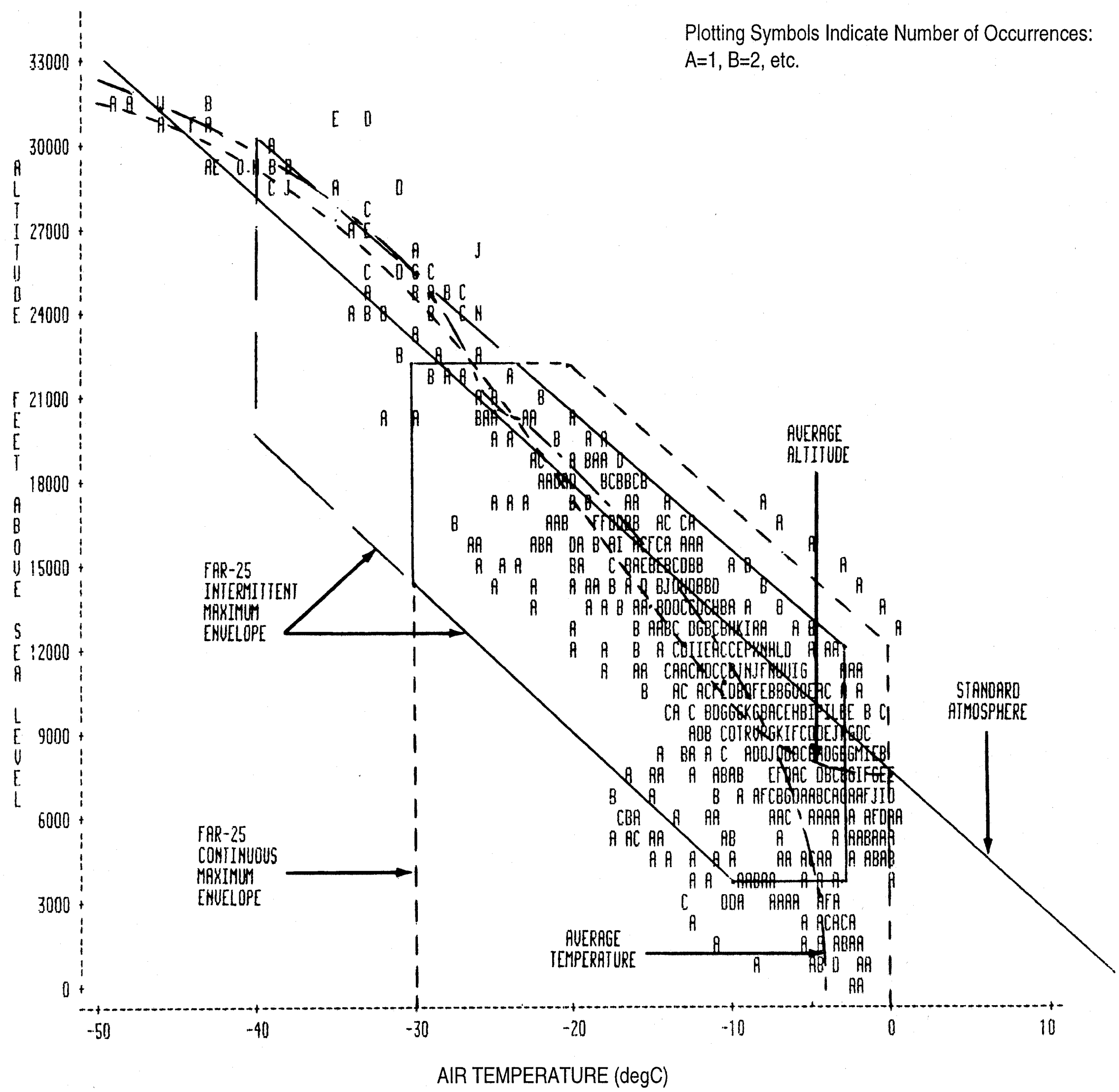

FIGURE 2. RECORDED IN-CLOUD TEMPERATURES VERSUS ALTITUDE (ASL) FOR ALL TYPES OF ICE PARTICLE CLOUDS

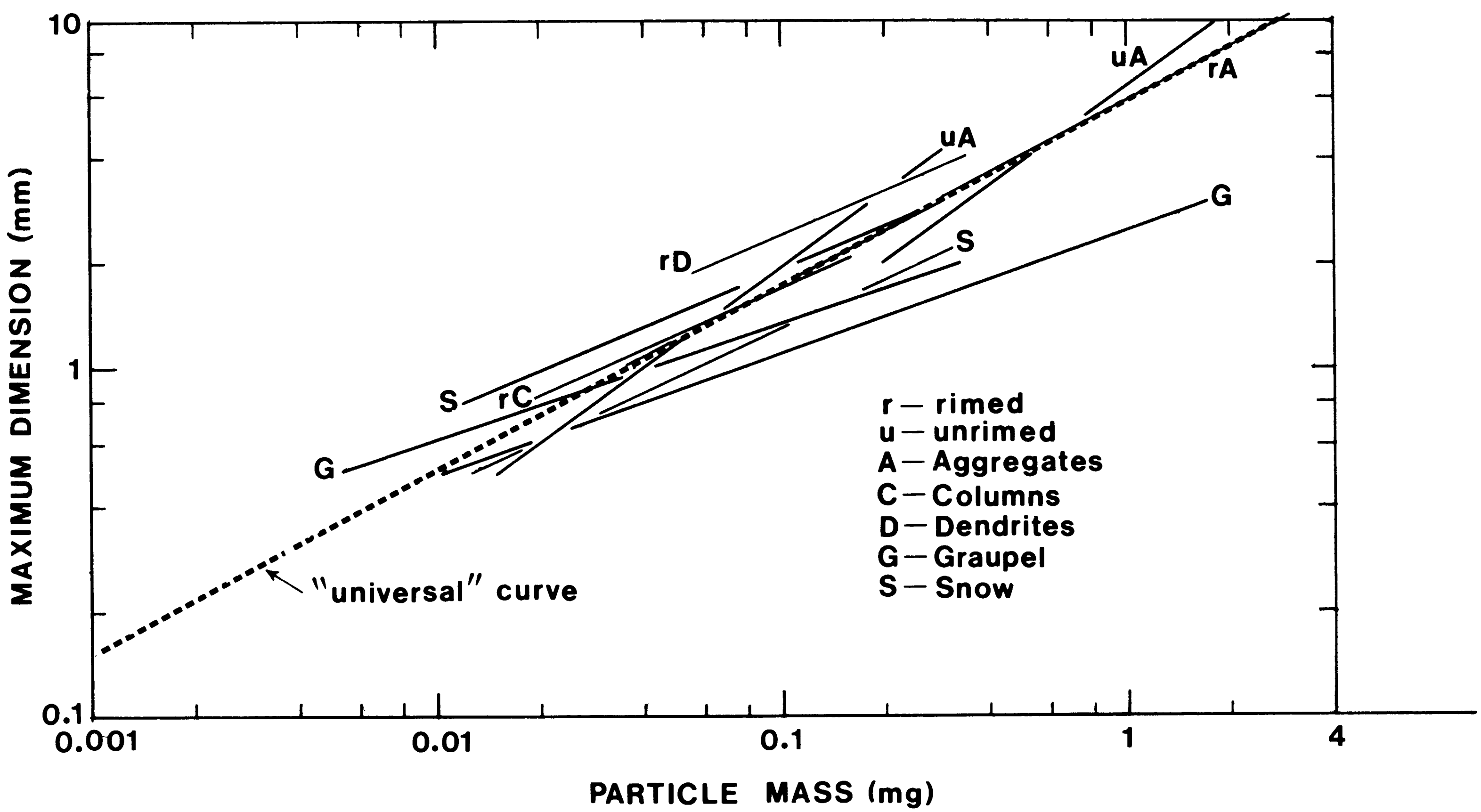

FIGURE 3. MASS VERSUS SIZE RELATIONSHIPS FOR DIFFERENT ICE PARTICLE TYPES

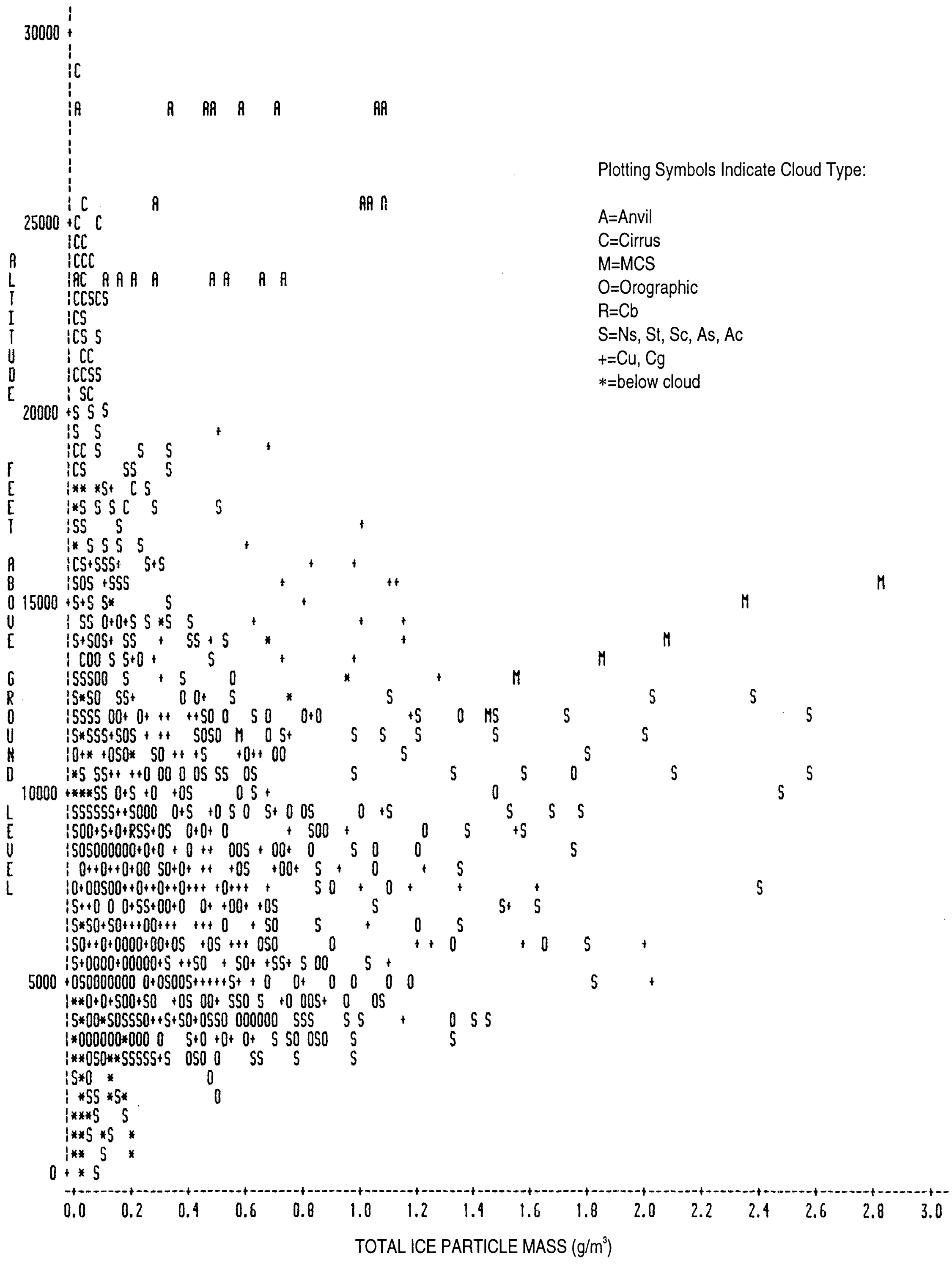

FIGURE 4a. COMPUTED, EVENT-AVERAGED, TOTAL ICE PARTICLE MASS VERSUS ALTITUDE (AGL) FOR ALL TYPES OF ICE PARTICLE CLOUDS

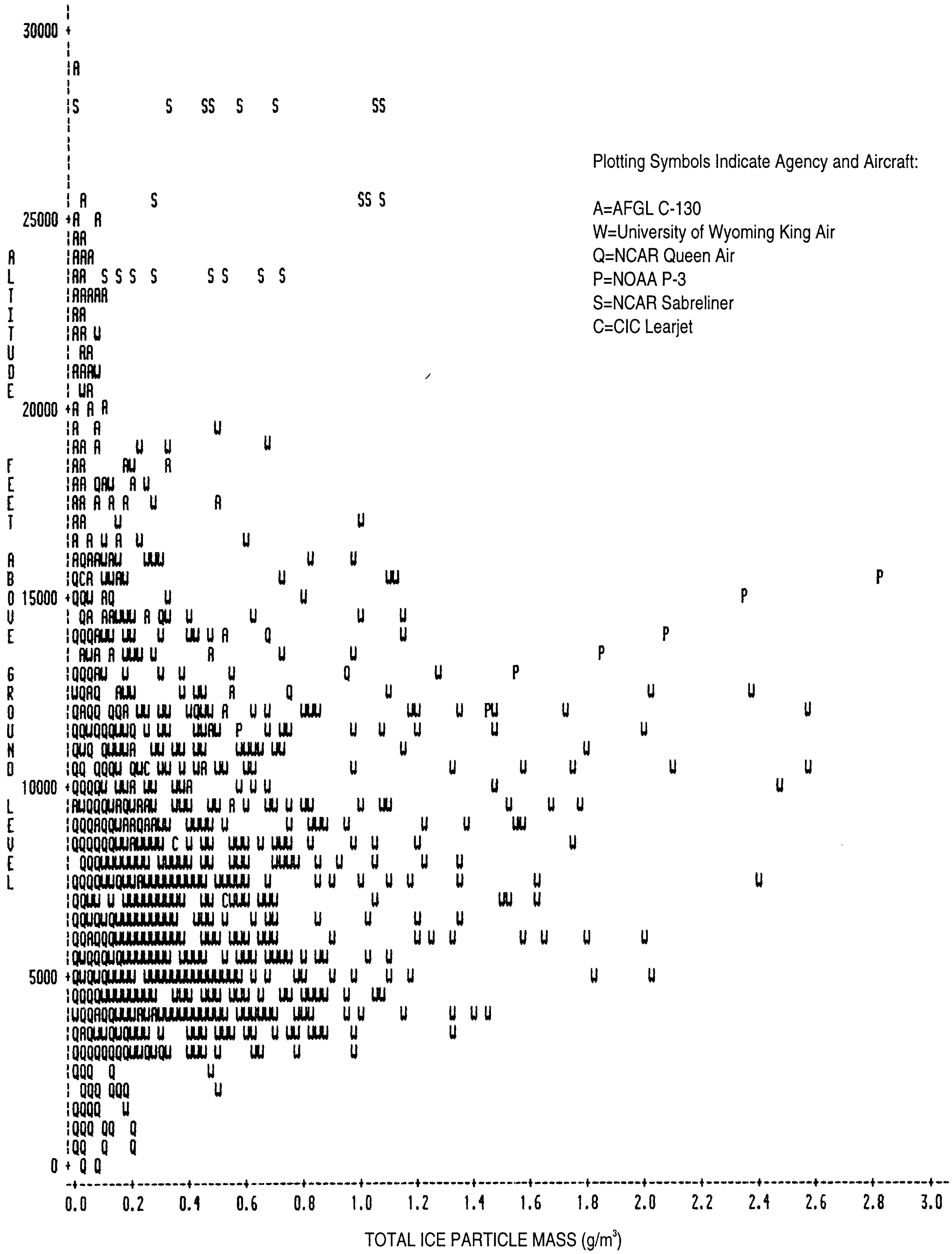

FIGURE 4b. COMPUTED, EVENT-AVERAGED, TOTAL ICE PARTICLE MASS VERSUS ALTITUDE (AGL) FOR ALL TYPES OF ICE PARTICLE CLOUDS

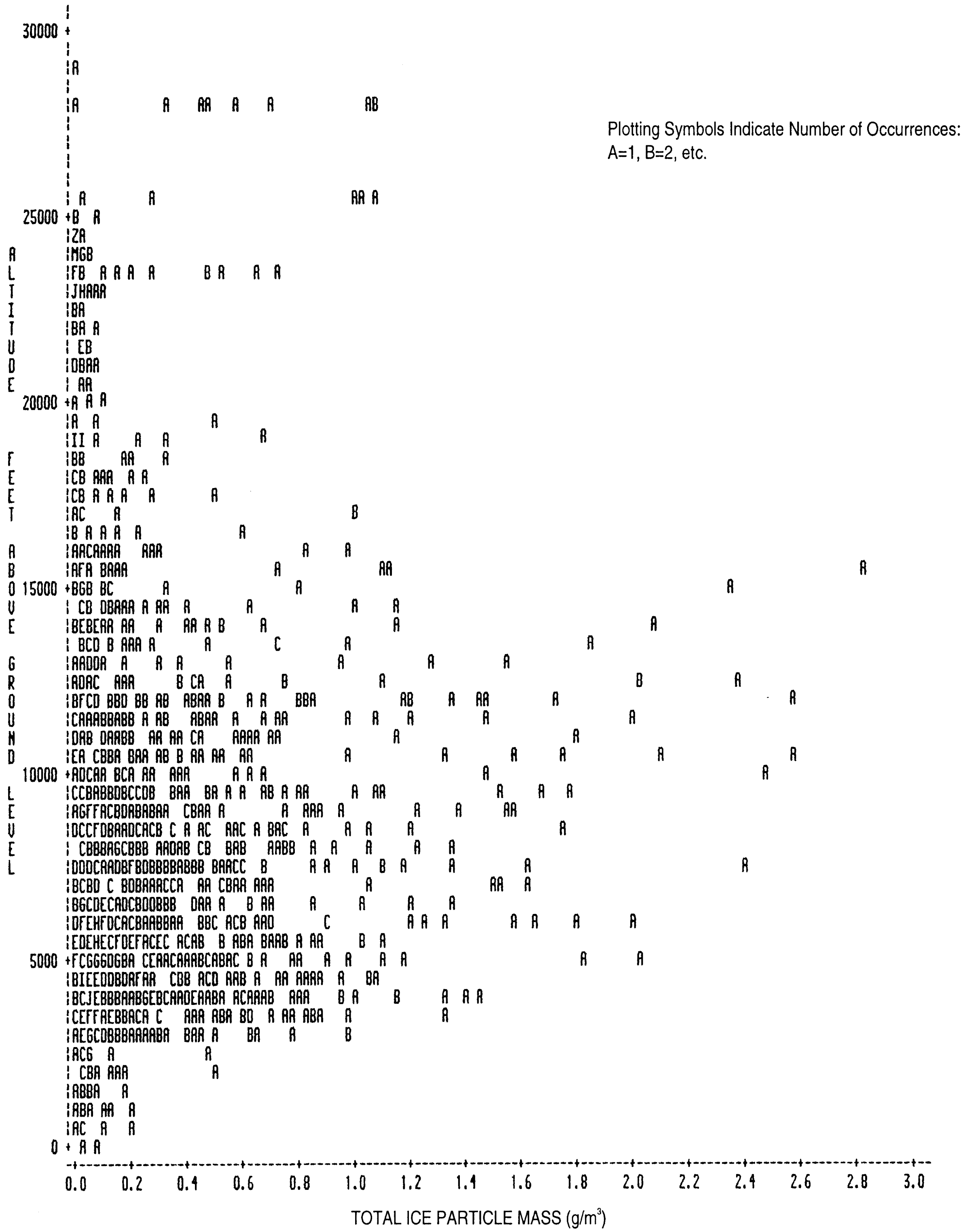

FIGURE 4c. COMPUTED, EVENT-AVERAGED, TOTAL ICE PARTICLE MASS VERSUS ALTITUDE (AGL) FOR ALL TYPES OF ICE PARTICLE CLOUDS

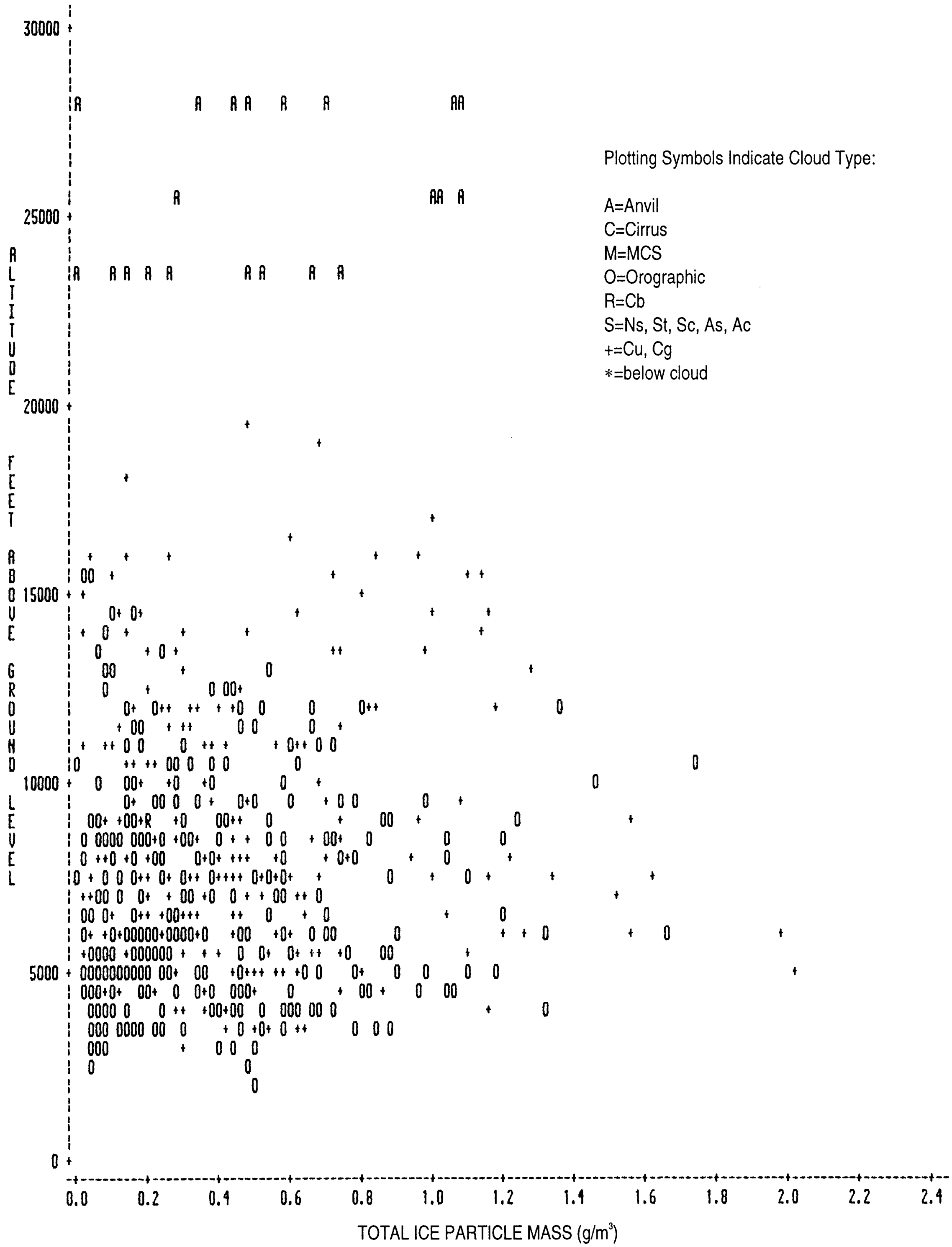

FIGURE 4d. COMPUTED, EVENT-AVERAGED, TOTAL ICE PARTICLE MASS VERSUS ALTITUDE (AGL) FOR CONVECTIVE CLOUDS (Cu, Cg, Cb, Or) ONLY

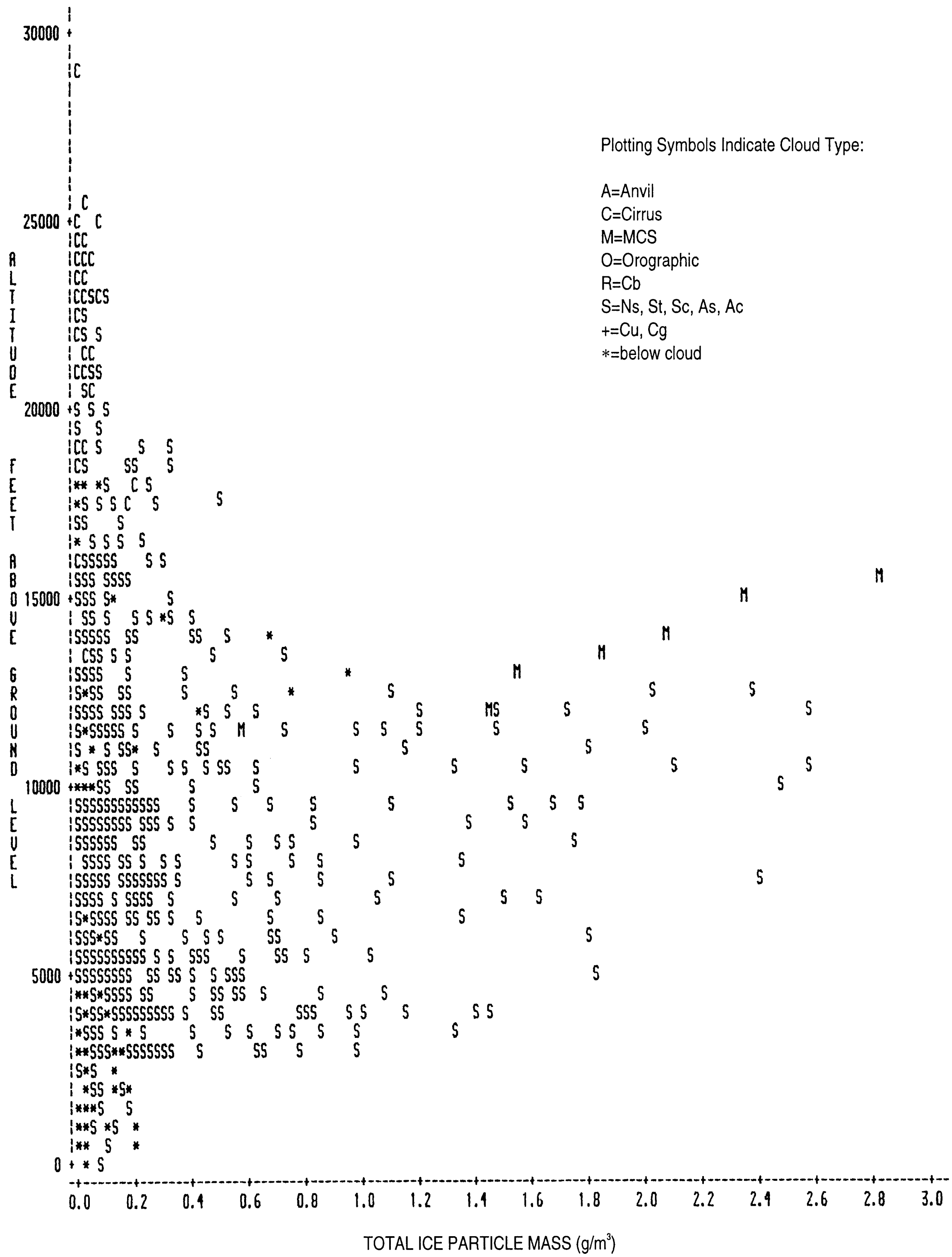

FIGURE 4e. COMPUTED, EVENT-AVERAGED, TOTAL ICE PARTICLE MASS VERSUS ALTITUDE (AGL) FOR LAYER CLOUDS (Ns, St, Sc, As, Ac, Ci, Cs) ONLY

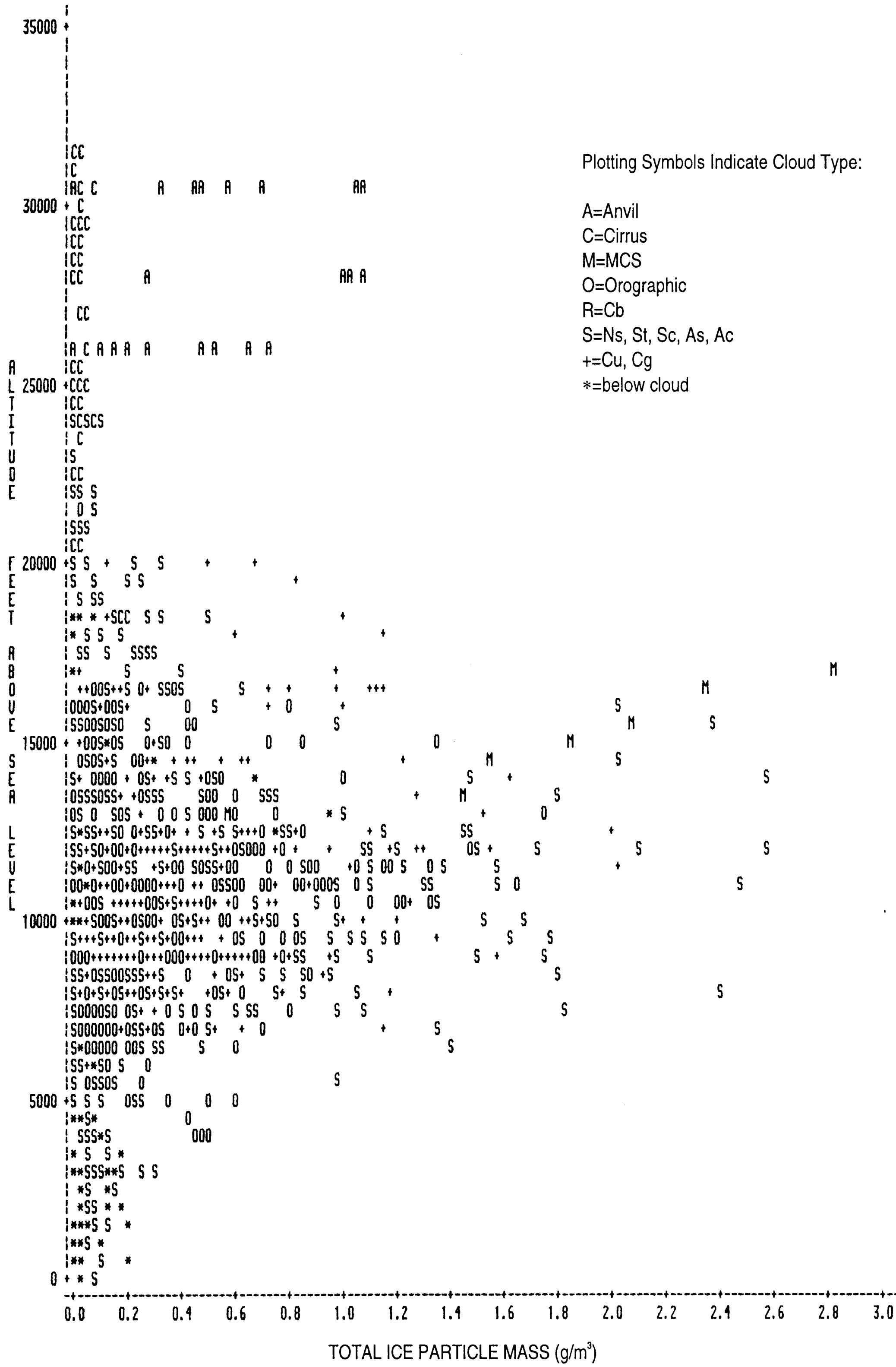

FIGURE 4f. COMPUTED, EVENT-AVERAGED, TOTAL ICE PARTICLE MASS VERSUS ALTITUDE (ASL) FOR ALL TYPES OF ICE PARTICLE CLOUDS

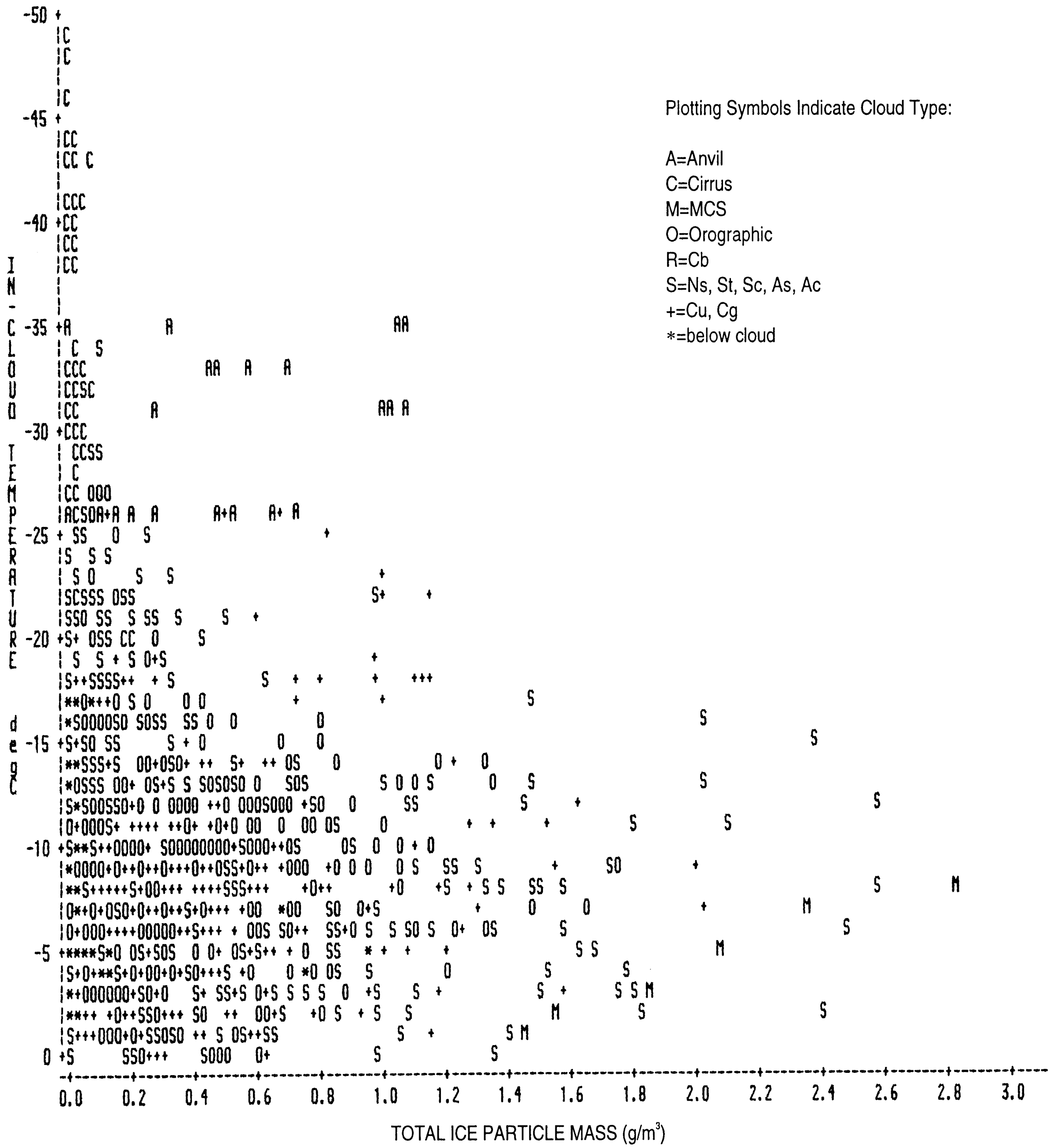

FIGURE 5a. COMPUTED, EVENT-AVERAGED, TOTAL ICE PARTICLE MASS VERSUS TEMPERTURE FOR ALL TYPES OF ICE PARTICLE CLOUDS

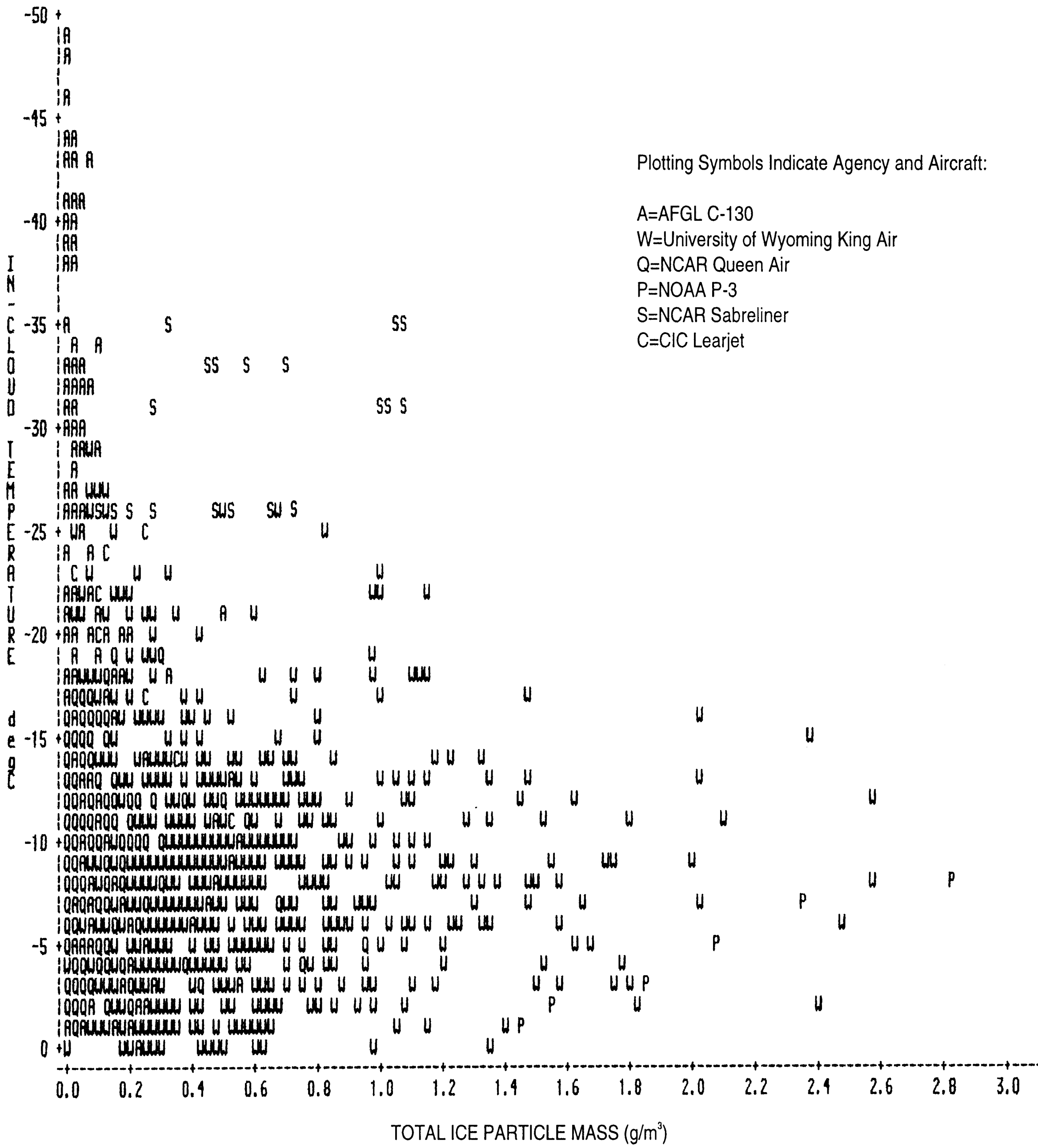

FIGURE 5b. COMPUTED, EVENT-AVERAGED, TOTAL ICE PARTICLE MASS VERSUS TEMPERTURE FOR ALL TYPES OF ICE PARTICLE CLOUDS

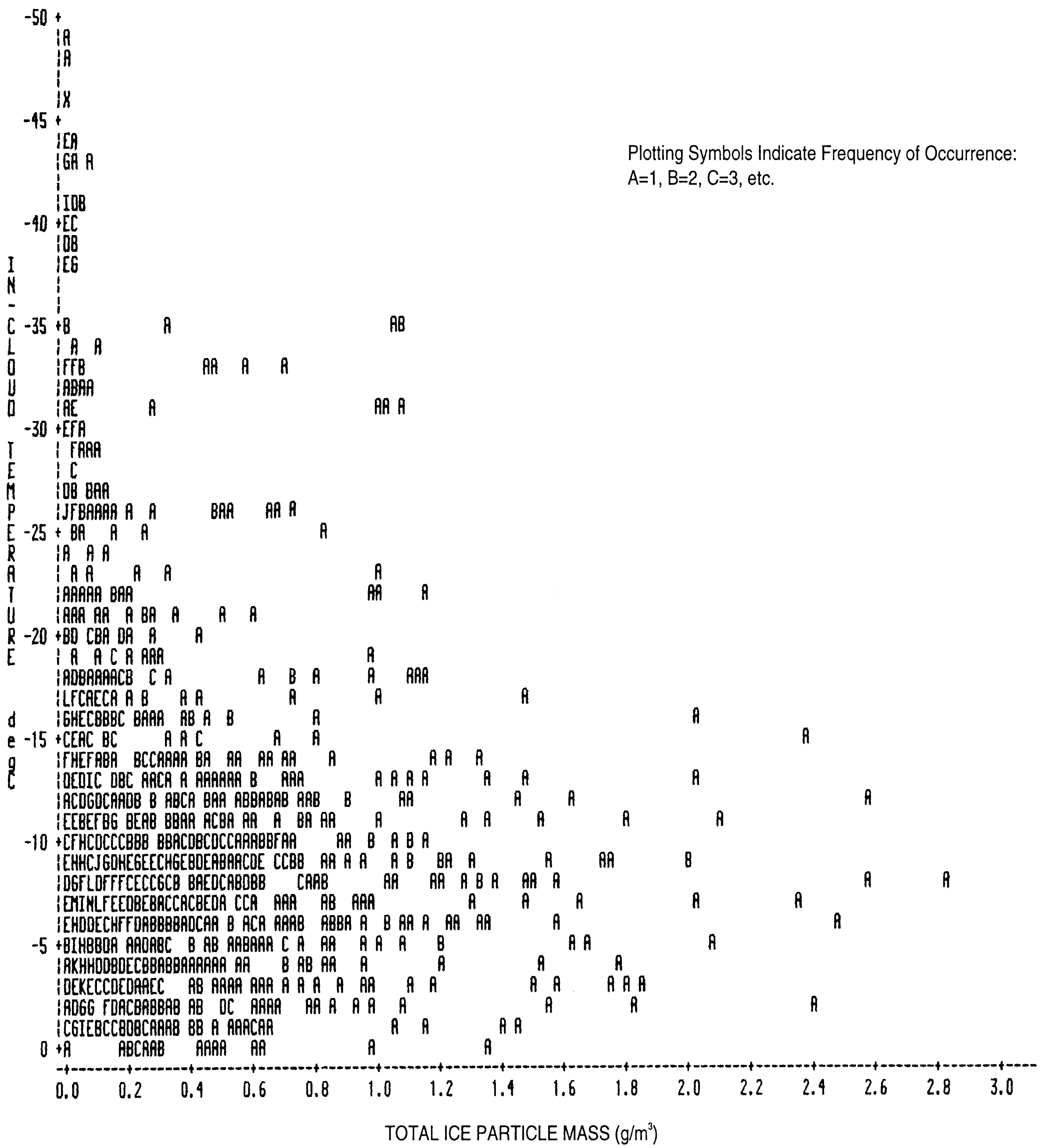

FIGURE 5c. COMPUTED, EVENT-AVERAGED, TOTAL ICE PARTICLE MASS VERSUS TEMPERTURE FOR ALL TYPES OF ICE PARTICLE CLOUDS

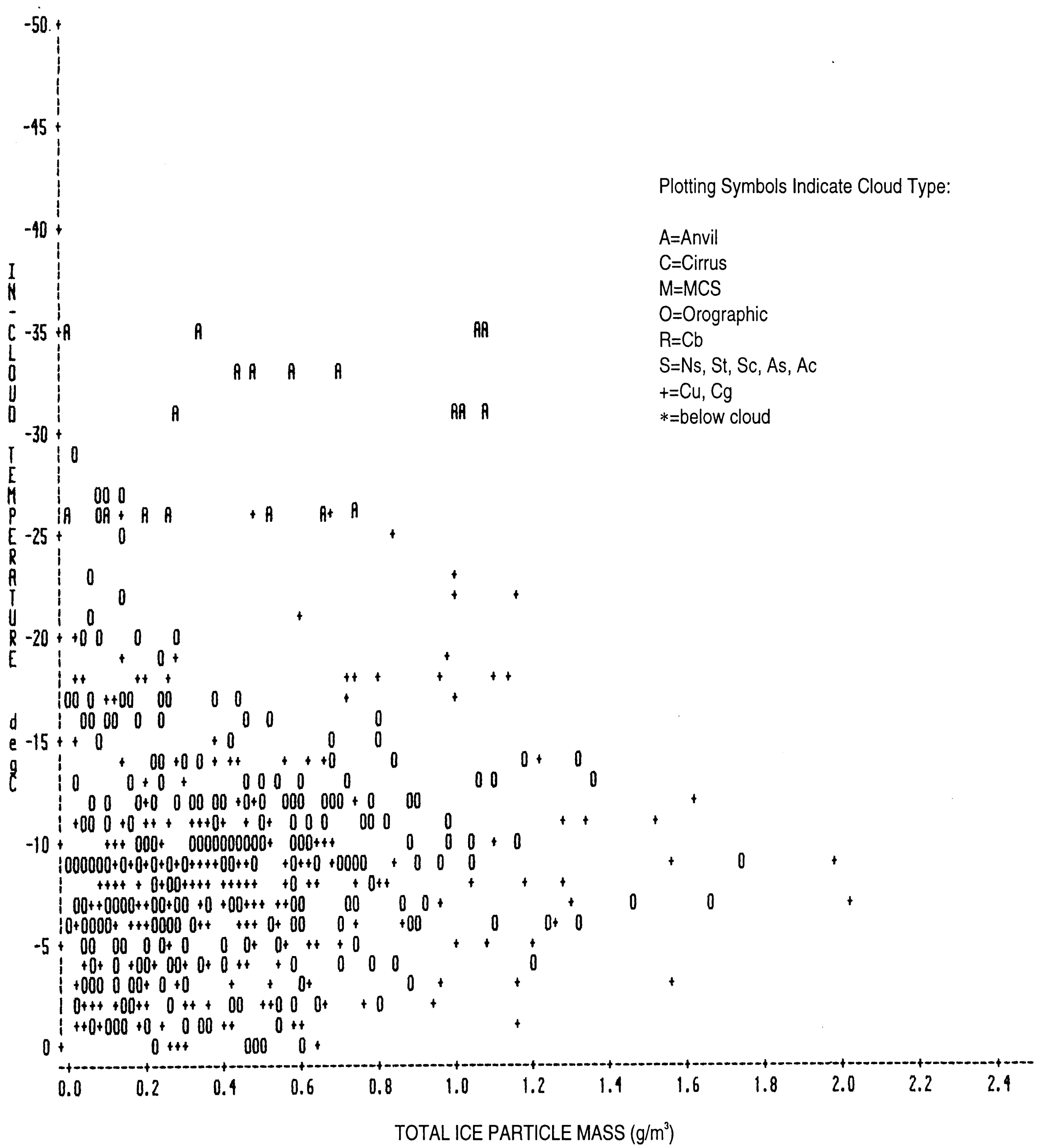

FIGURE 5d. COMPUTED, EVENT-AVERAGED, TOTAL ICE PARTICLE MASS VERSUS TEMPERTURE FOR CONVECTIVE CLOUDS (Cu, Cg, Cb, Or) ONLY

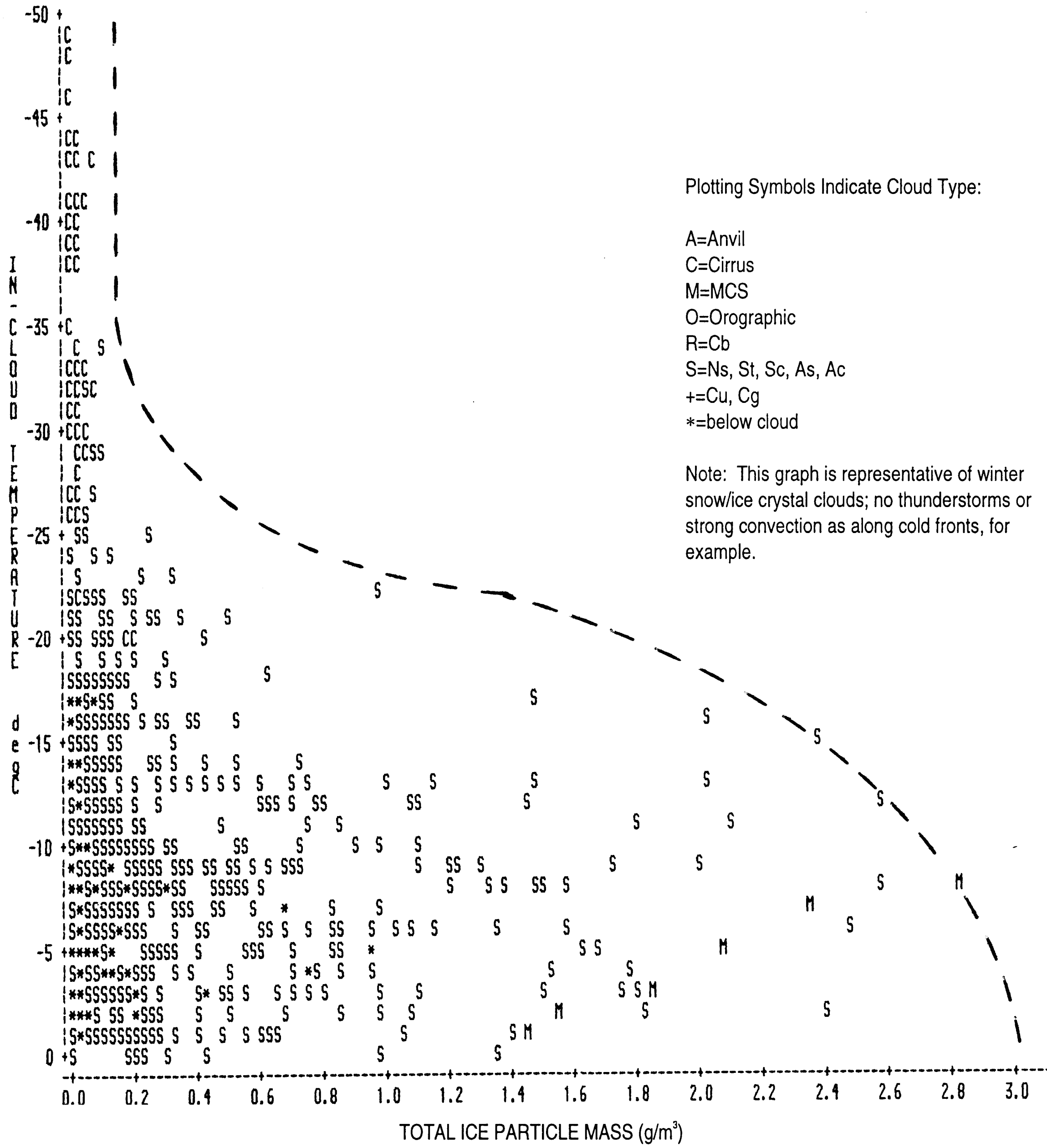

FIGURE 5e. COMPUTED, EVENT-AVERAGED, TOTAL ICE PARTICLE MASS VERSUS TEMPERTURE FOR LAYER CLOUDS (Ns, St, Sc, As, Ac, Ci, Cs) ONLY

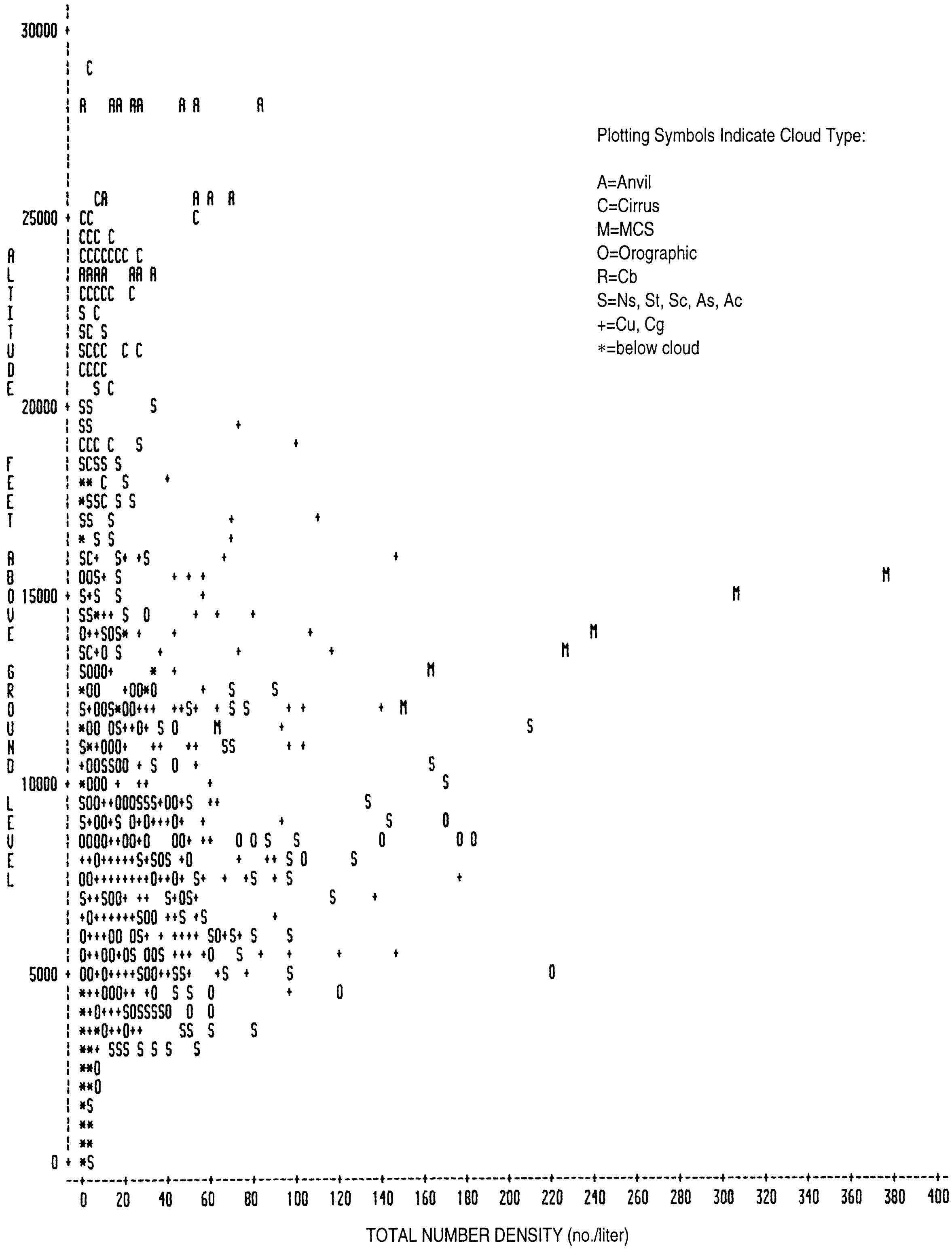

FIGURE 6a. EVENT-AVERAGED ICE PARTICLE CONCENTRATIONS (LINEAR SCALE) VERSUS ALTITUDE (AGL) FOR PARTICLES LARGER THAN 0.1 mm AND FOR ALL TYPES OF ICE PARTICLE CLOUDS

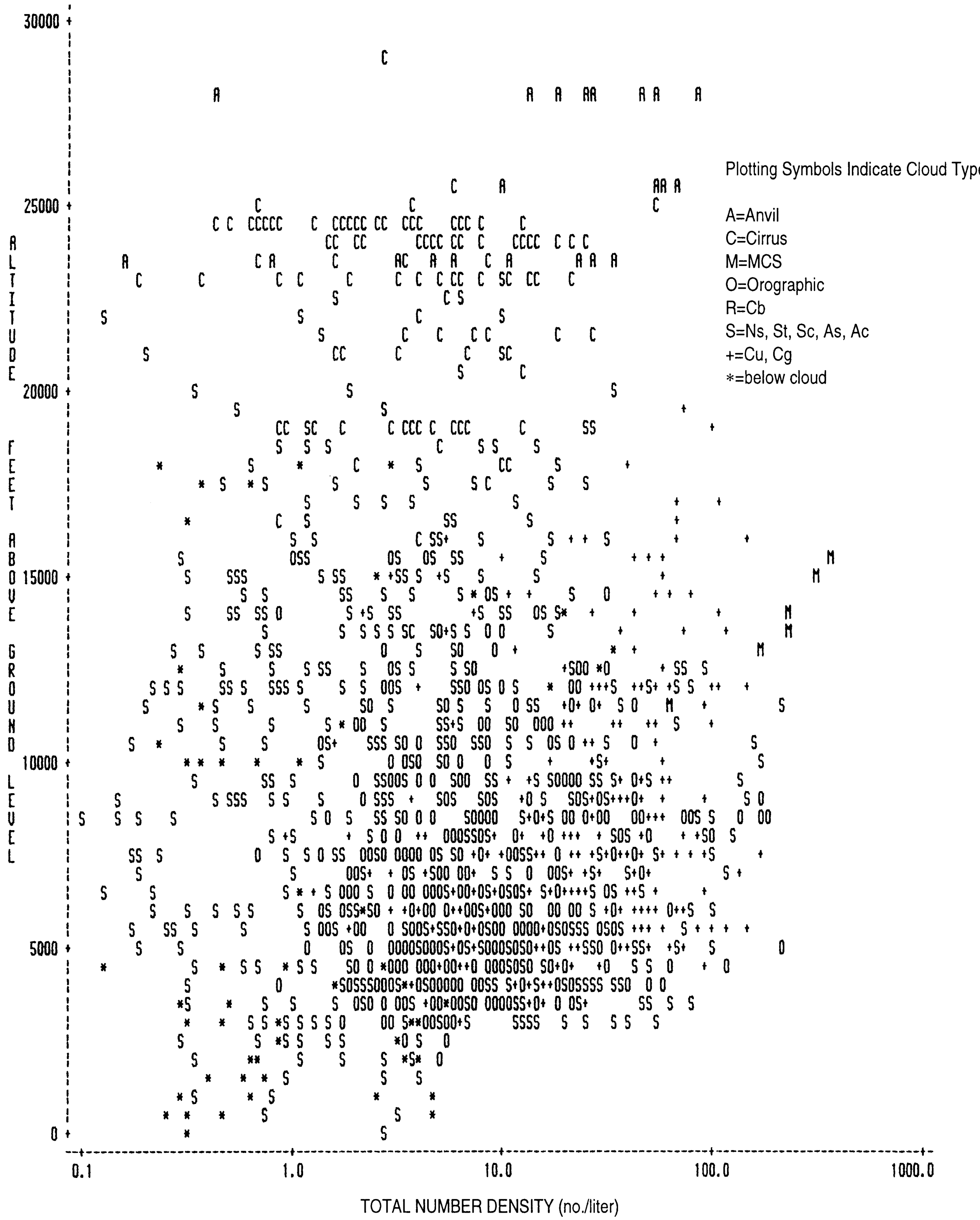

FIGURE 6b. EVENT-AVERAGED ICE PARTICLE CONCENTRATIONS (LOG SCALE) VERSUS ALTITUDE (AGL) FOR PARTICLES LARGER THAN 0.1 mm AND FOR ALL TYPES OF ICE PARTICLE CLOUDS

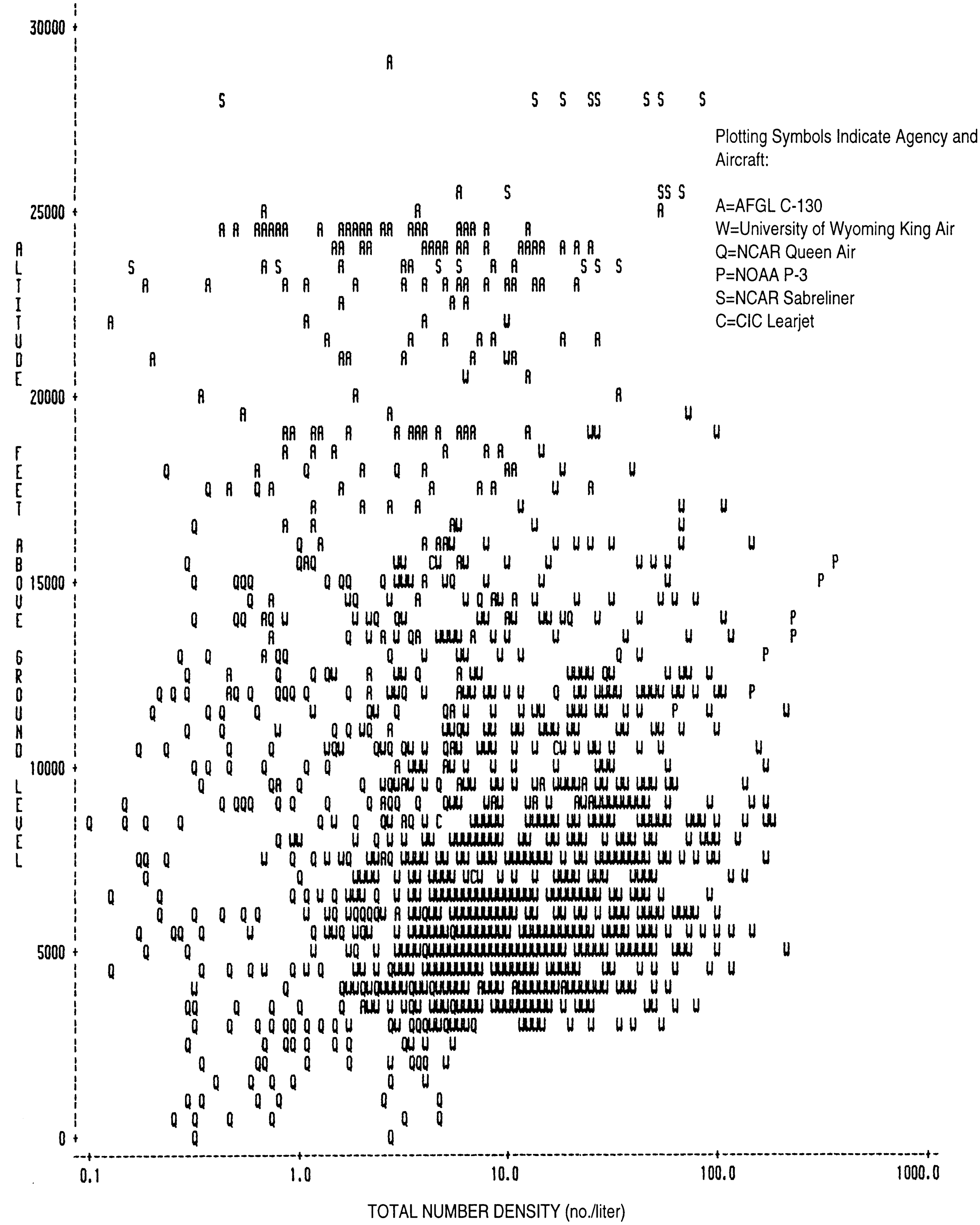

FIGURE 6c. EVENT-AVERAGED ICE PARTICLE CONCENTRATIONS (LOG SCALE) VERSUS ALTITUDE (AGL) FOR PARTICLES LARGER THAN 0.1 mm AND FOR ALL TYPES OF ICE PARTICLE CLOUDS

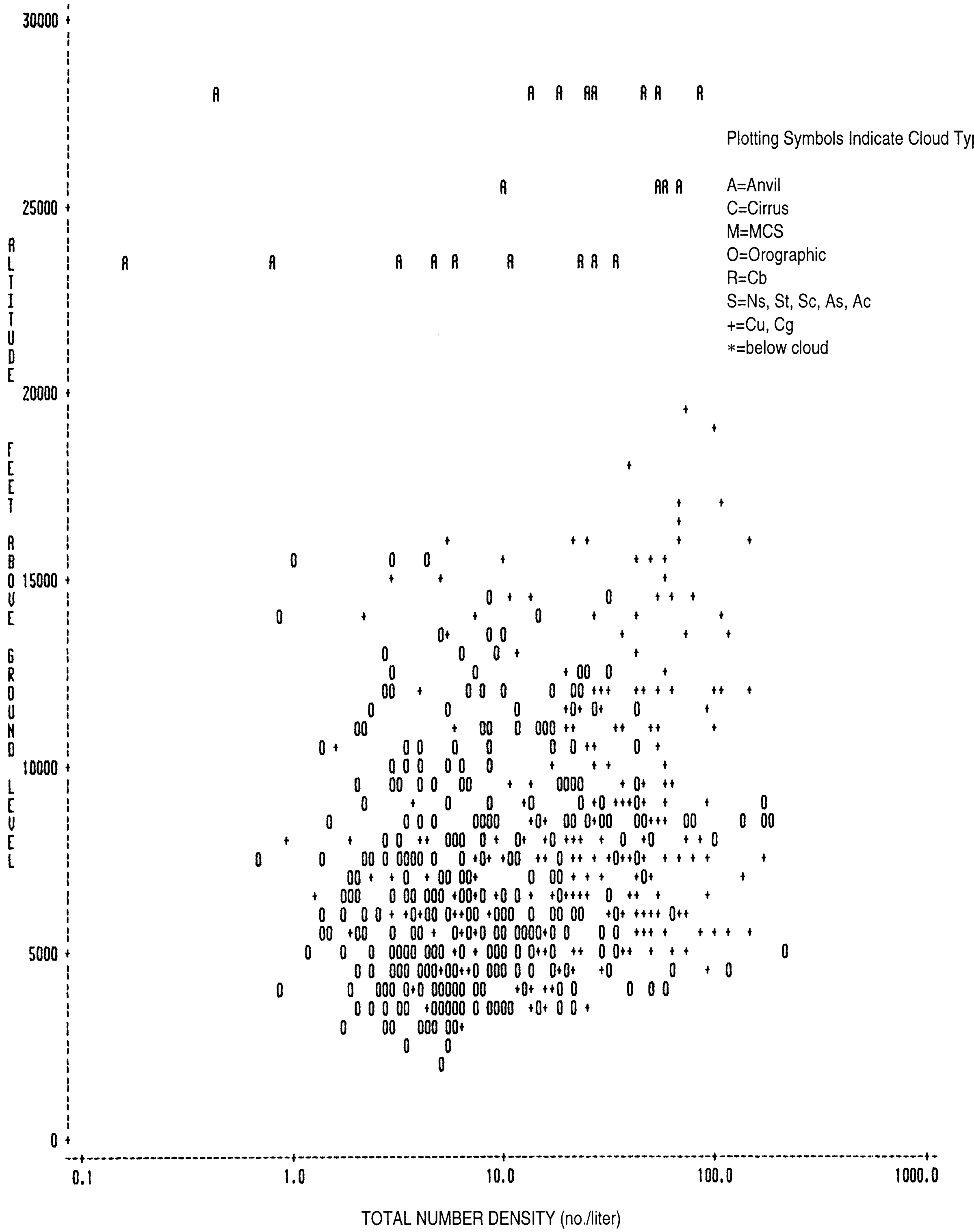

FIGURE 6d. EVENT-AVERAGED ICE PARTICLE CONCENTRATIONS (LOG SCALE) VERSUS ALTITUDE (AGL) FOR PARTICLES LARGER THAN 0.1 mm AND FOR CONVECTIVE CLOUDS (Cu, Cg, Cb, Or) ONLY

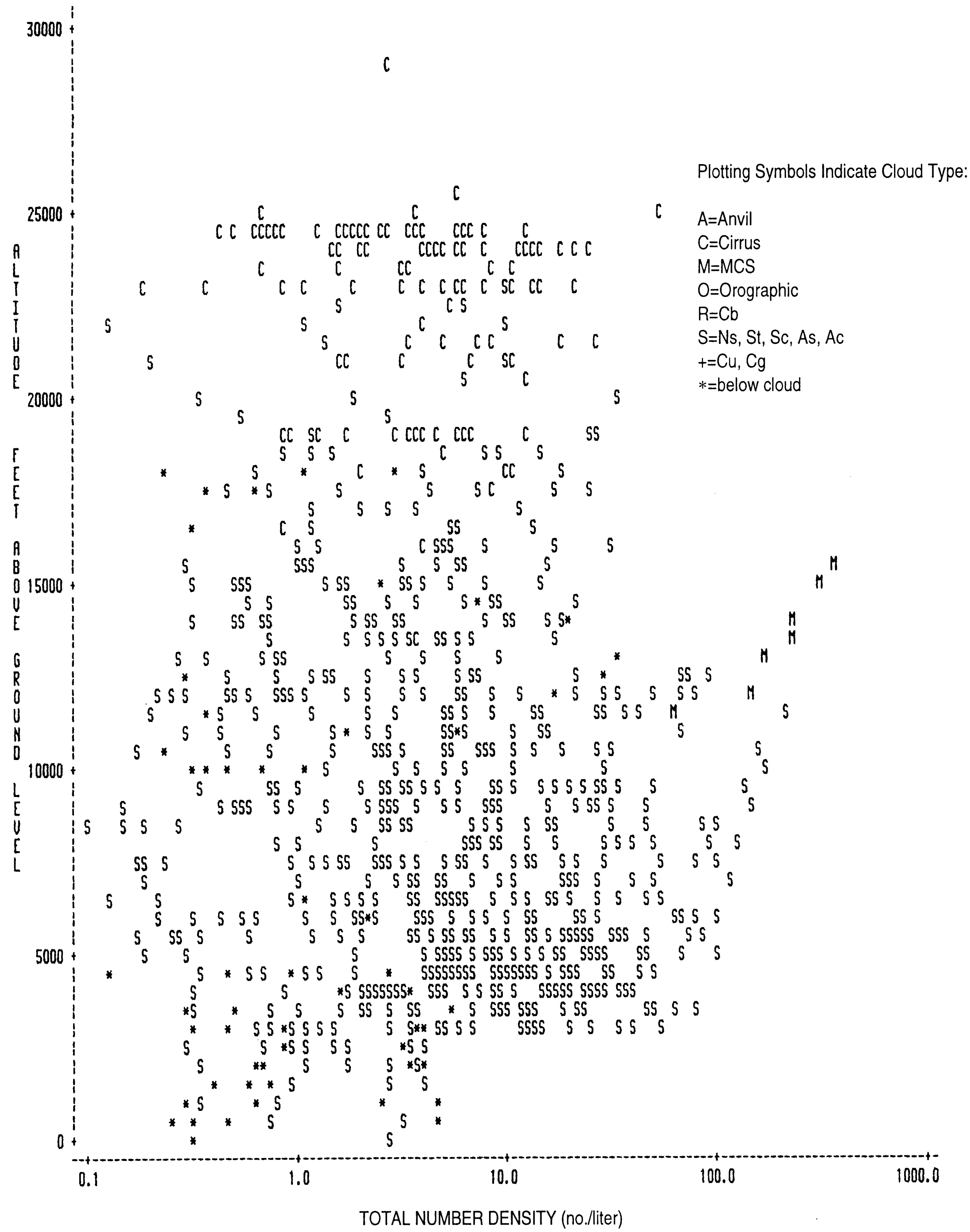

FIGURE 6e. EVENT-AVERAGED ICE PARTICLE CONCENTRATIONS (LOG SCALE) VERSUS ALTITUDE (AGL) FOR PARTICLES LARGER THAN 0.1 mm AND FOR LAYER CLOUDS (Ns, St, Sc, As, Ac, Ci, Cs) ONLY

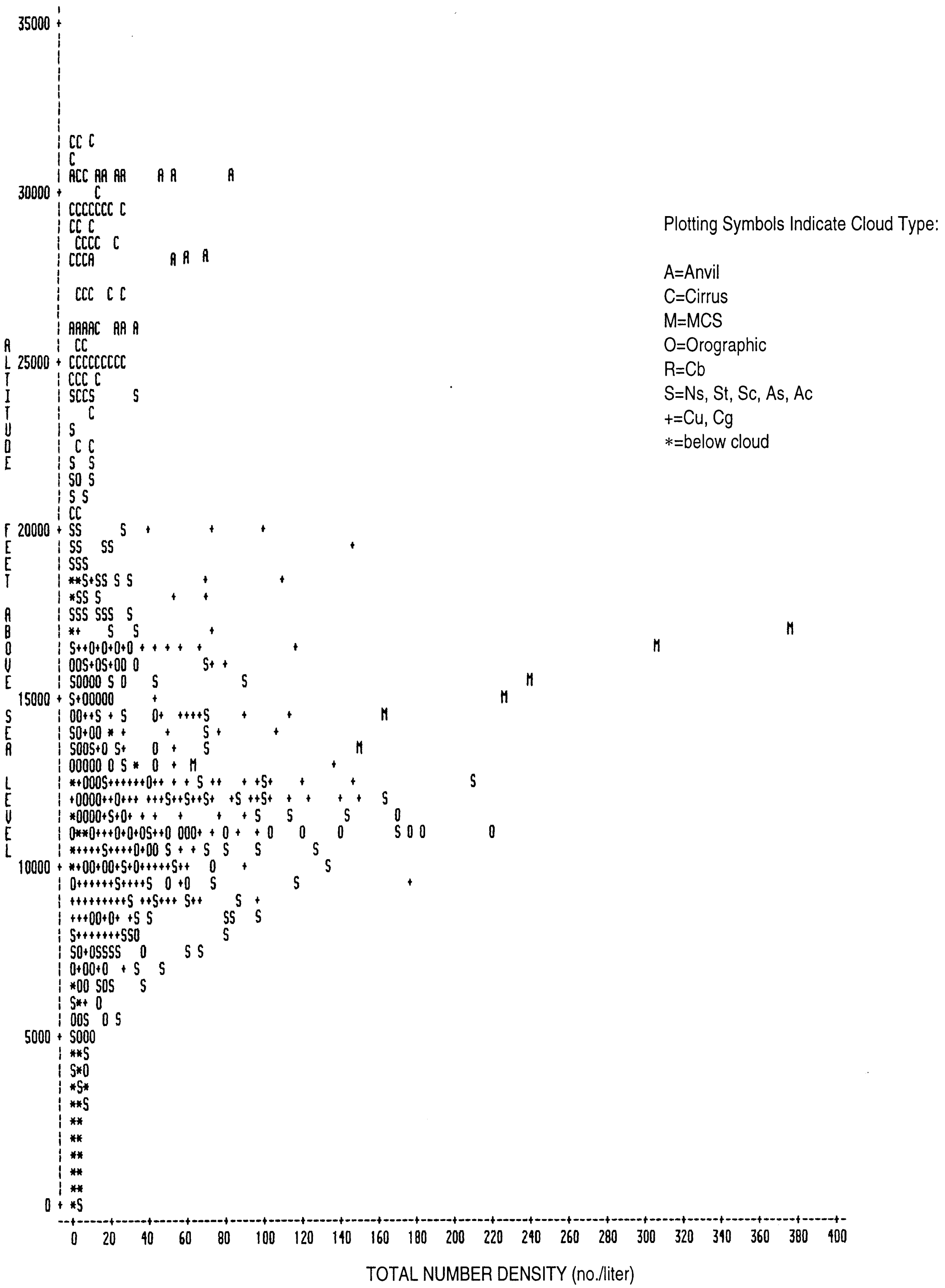

FIGURE 6f. EVENT-AVERAGED ICE PARTICLE CONCENTRATIONS (LINEAR SCALE) VERSUS ALTITUDE (ASL) FOR PARTICLES LARGER THAN 0.1 mm AND FOR ALL TYPES OF ICE PARTICLE CLOUDS

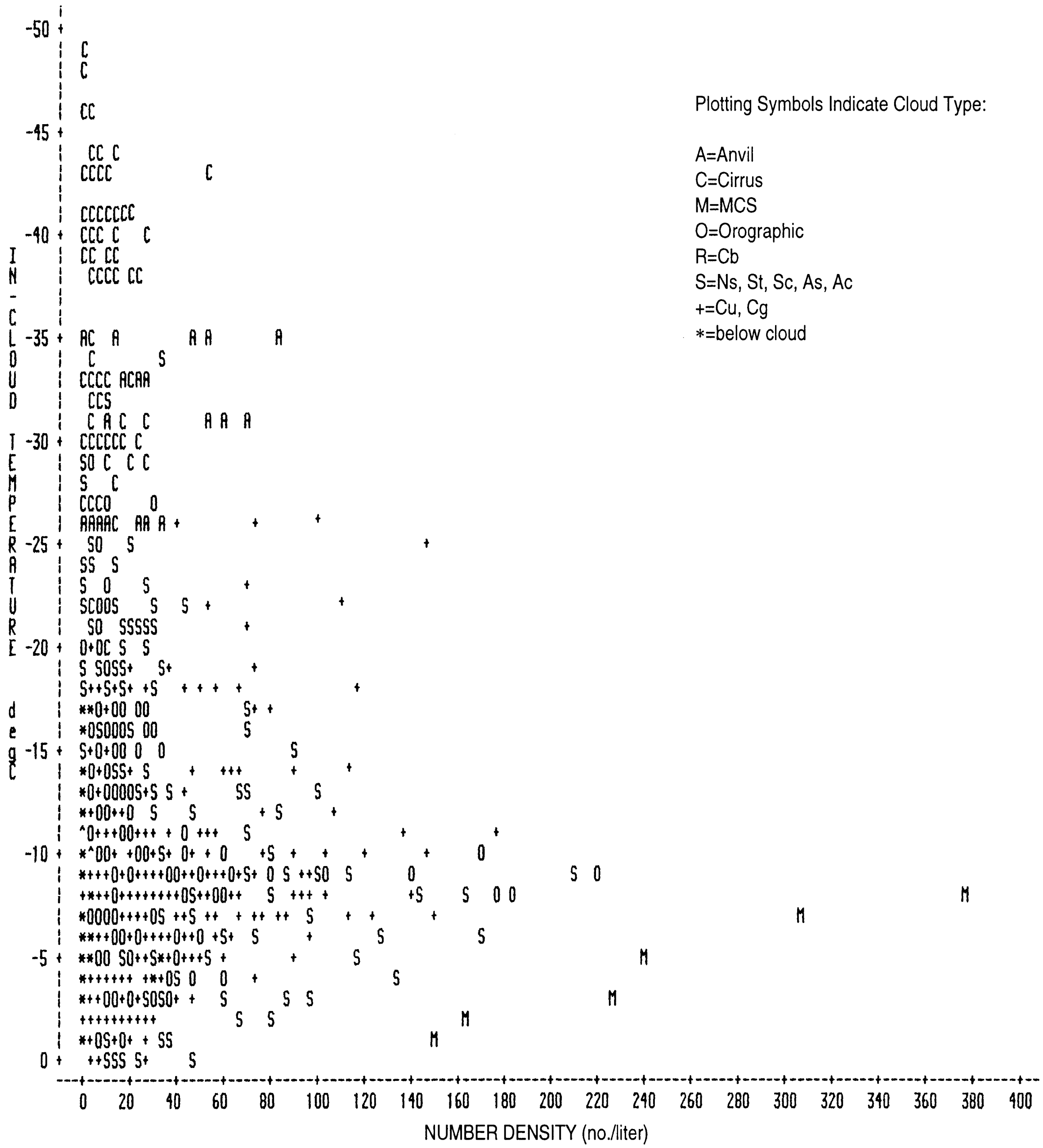

FIGURE 7a. EVENT-AVERAGED ICE PARTICLE CONCENTRATIONS (LINEAR SCALE) VERSUS TEMPERATURE FOR PARTICLES LARGER THAN 0.1 mm AND FOR ALL TYPES OF ICE PARTICLE CLOUDS

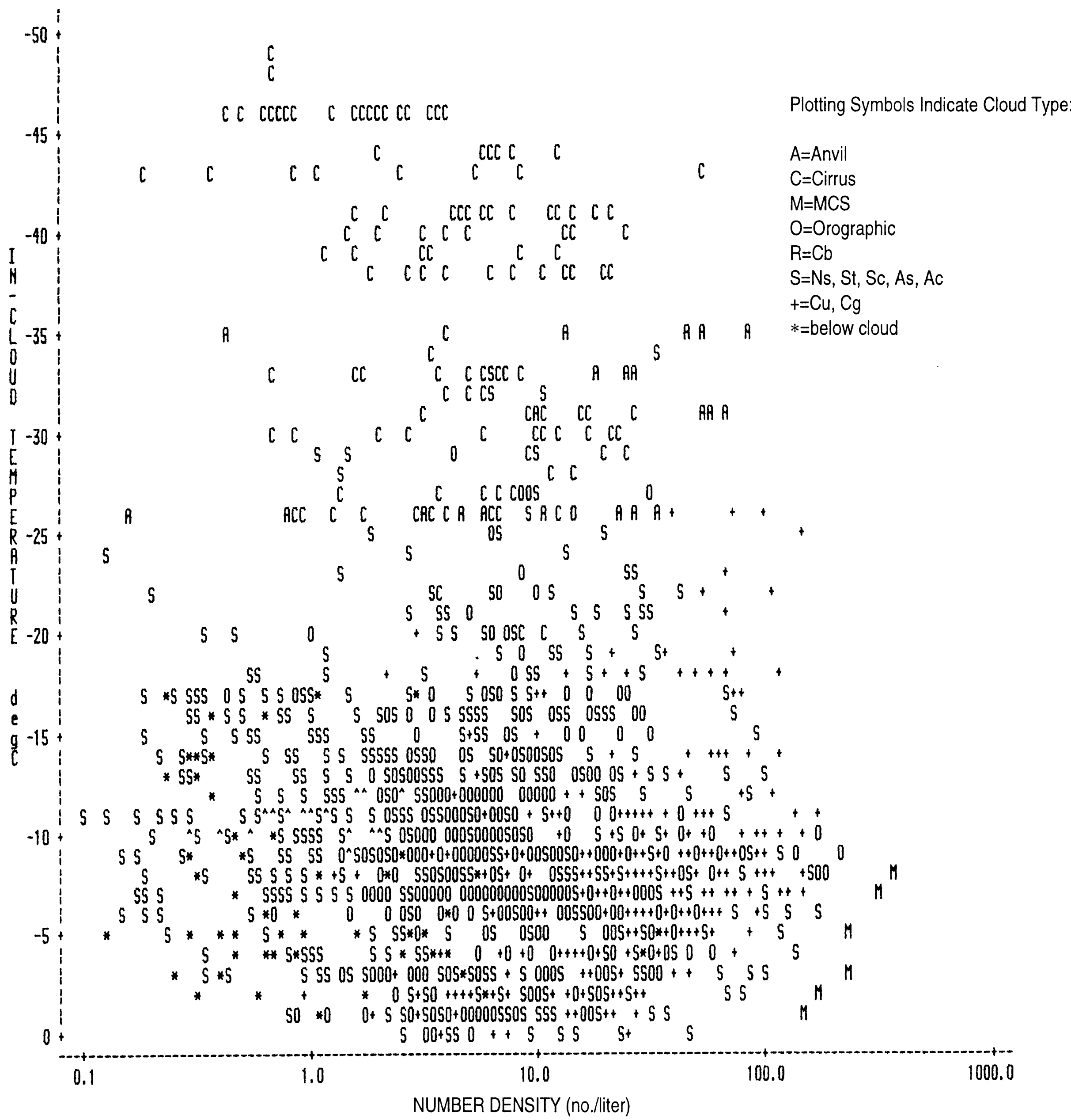

FIGURE 7b. EVENT-AVERAGED ICE PARTICLE CONCENTRATIONS (LOG SCALE) VERSUS TEMPERATURE FOR PARTICLES LARGER THAN 0.1 mm AND FOR ALL TYPES OF ICE PARTICLE CLOUDS

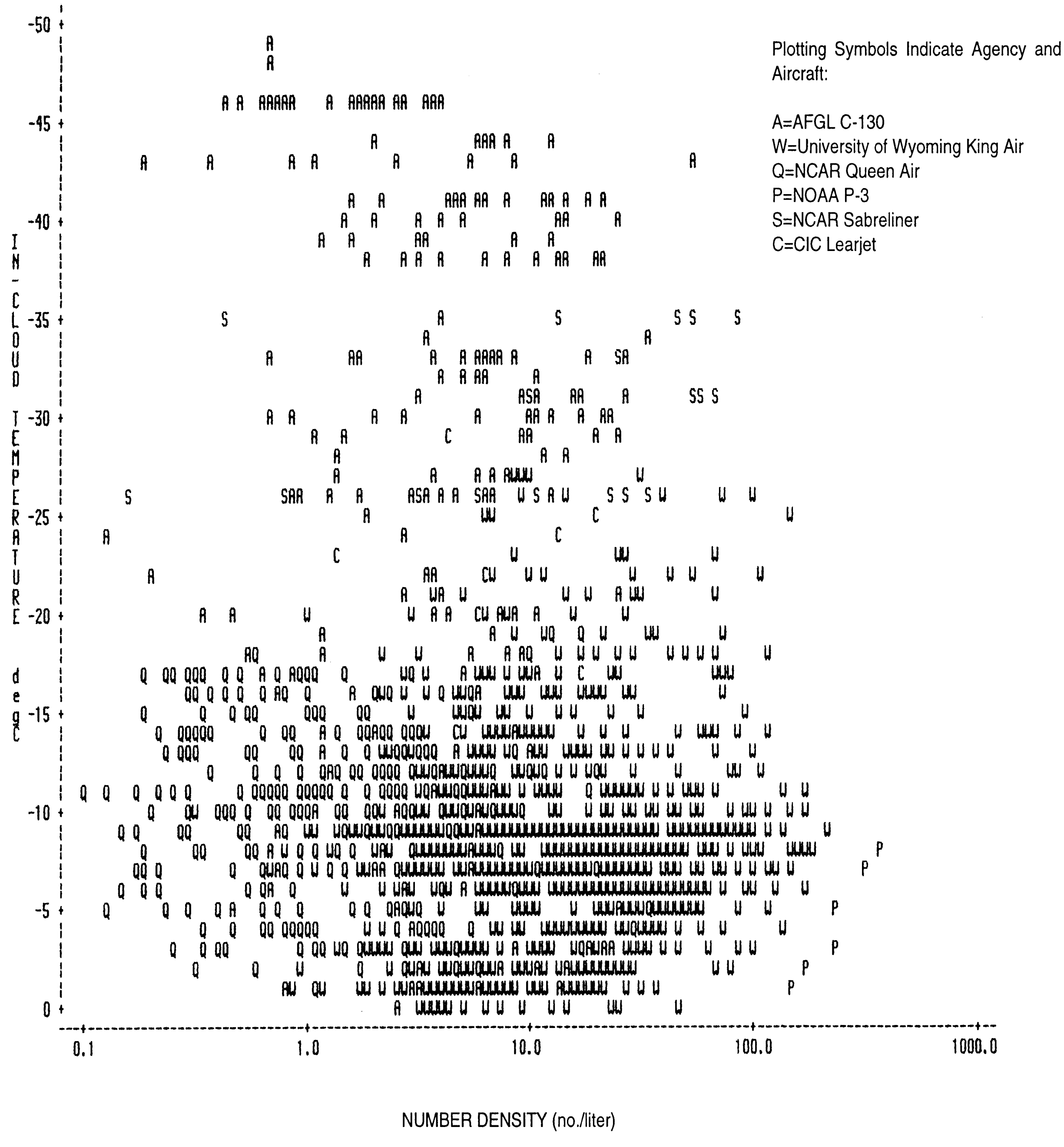

FIGURE 7c. EVENT-AVERAGED ICE PARTICLE CONCENTRATIONS (LOG SCALE) VERSUS TEMPERATURE FOR PARTICLES LARGER THAN 0.1 mm AND FOR ALL TYPES OF ICE PARTICLE CLOUDS

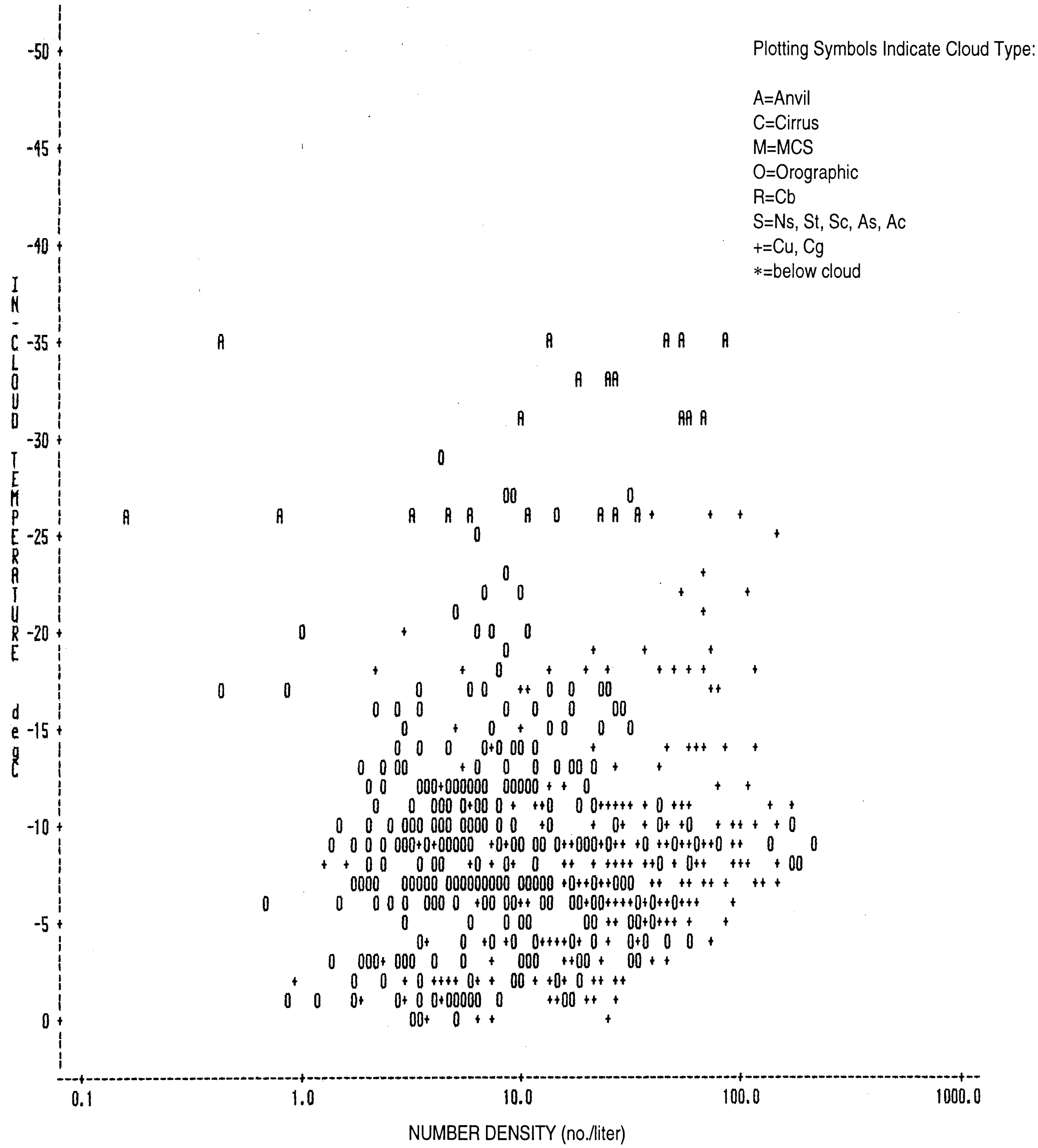

FIGURE 7d. EVENT-AVERAGED ICE PARTICLE CONCENTRATIONS (LOG SCALE) VERSUS TEMPERATURE FOR PARTICLES LARGER THAN 0.1 mm AND FOR CONVECTIVE CLOUDS (Cu, Cg, Cb, Or) ONLY

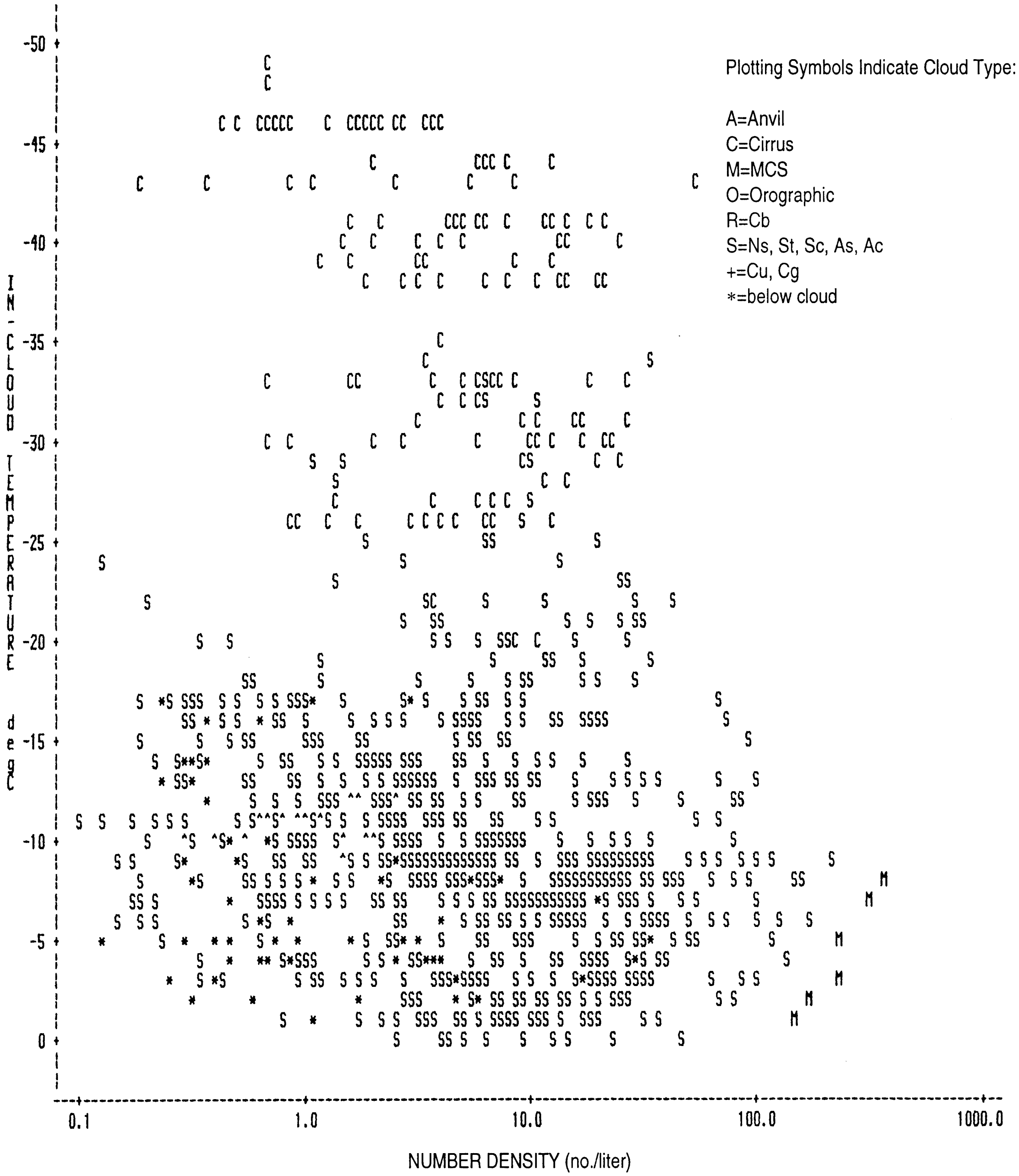

FIGURE 7e. EVENT-AVERAGED ICE PARTICLE CONCENTRATIONS (LOG SCALE) VERSUS TEMPERATURE FOR PARTICLES LARGER THAN 0.1 mm AND FOR LAYER CLOUDS (Ns, St, Sc, As, Ac, Ci, Cs) ONLY

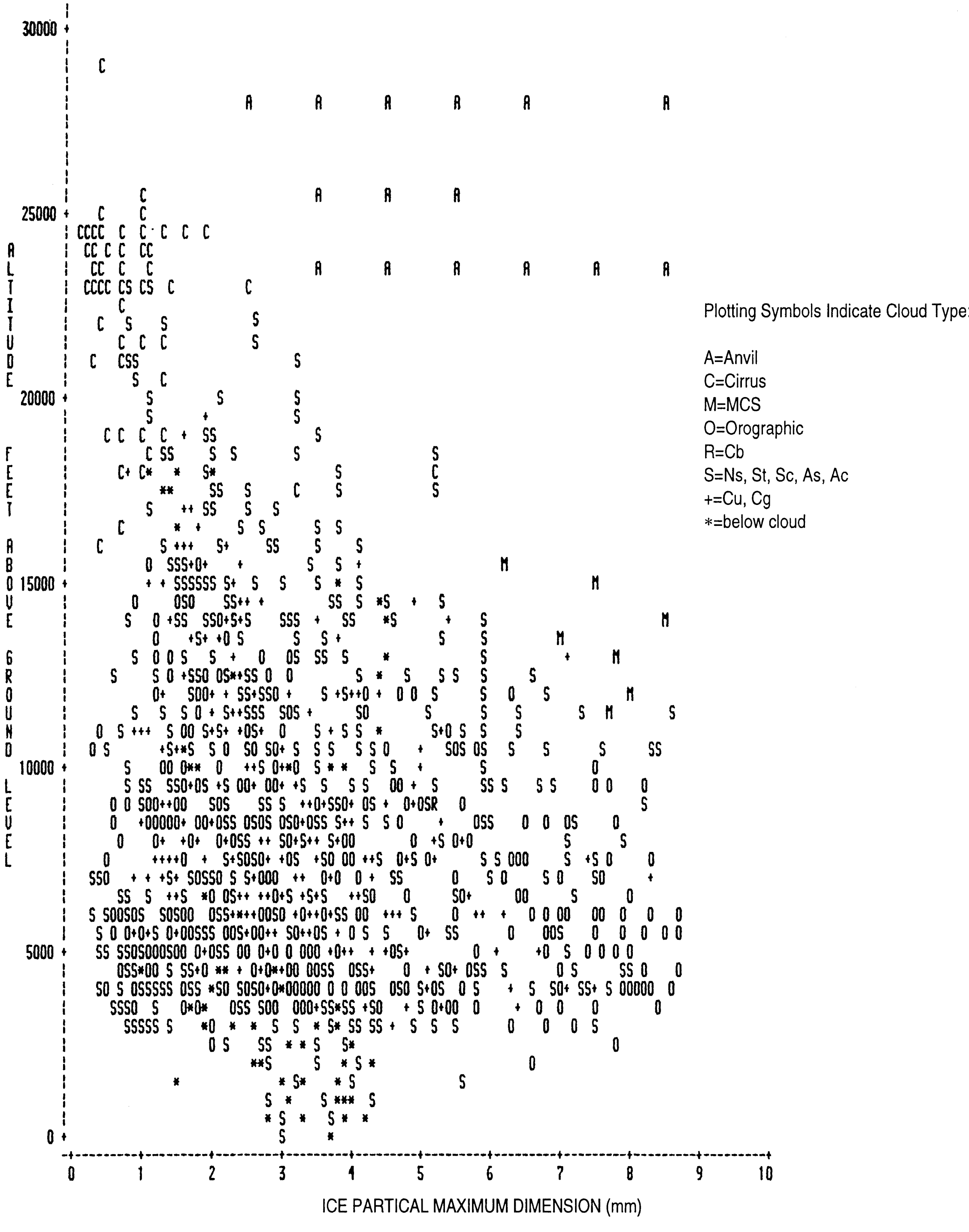

FIGURE 8a. EVENT-AVERAGED ICE PARTICLE MAXIMUM DIMENSION VERSUS ALTITUDE (AGL) FOR PARTICLES LARGER THAN 0.1 mm AND FOR ALL TYPES OF ICE PARTICLE CLOUDS

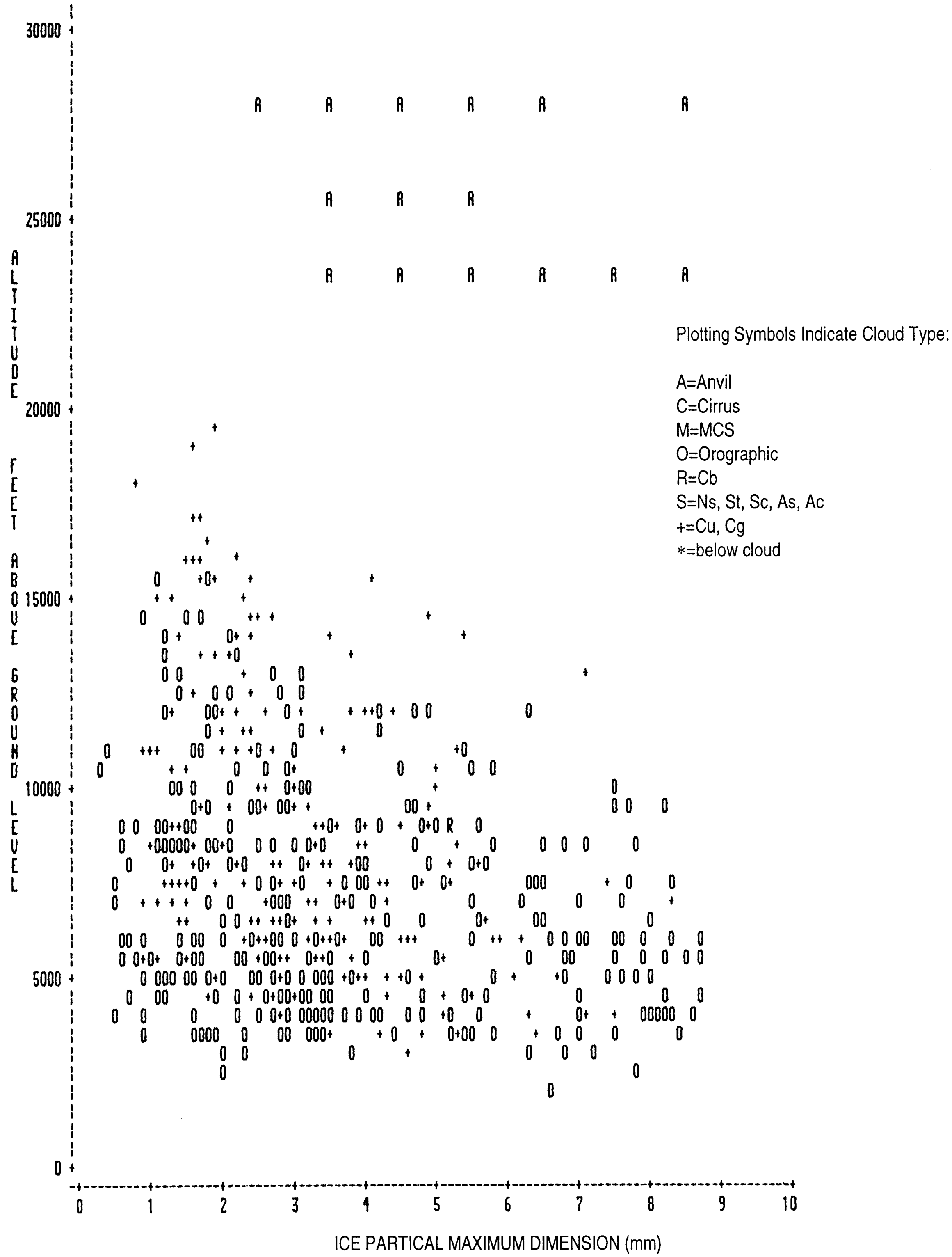

FIGURE 8b. EVENT-AVERAGED ICE PARTICLE MAXIMUM DIMENSION VERSUS ALTITUDE (AGL) FOR PARTICLES LARGER THAN 0.1 mm AND FOR CONVECTIVE CLOUDS (Cu, Cg, Cb, Or) ONLY

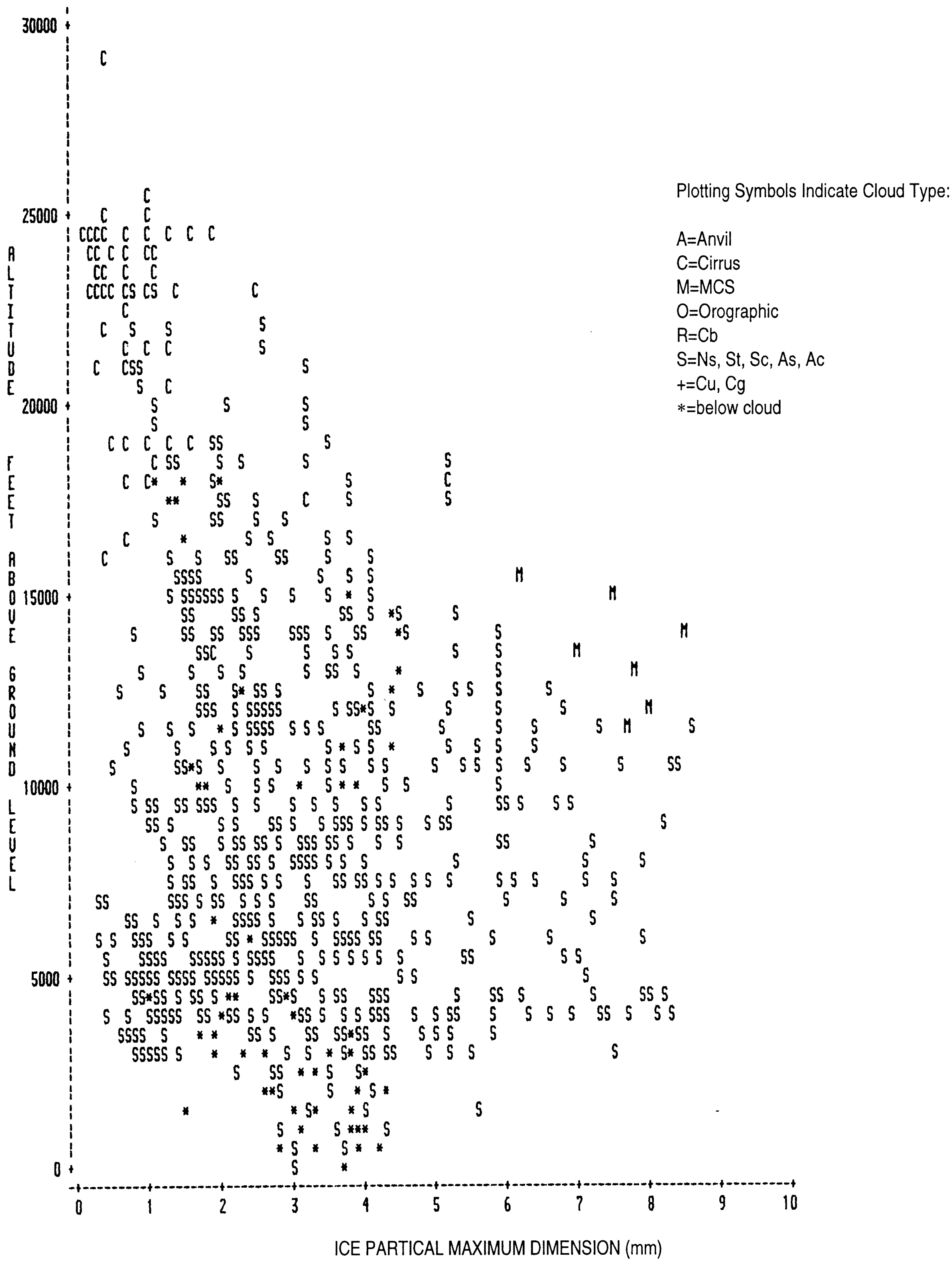

FIGURE 8c. EVENT-AVERAGED ICE PARTICLE MAXIMUM DIMENSION VERSUS ALTITUDE (AGL) FOR PARTICLES LARGER THAN 0.1 mm AND FOR LAYER CLOUDS (Ns, St, Sc, As, Ac, Ci, Cs) ONLY

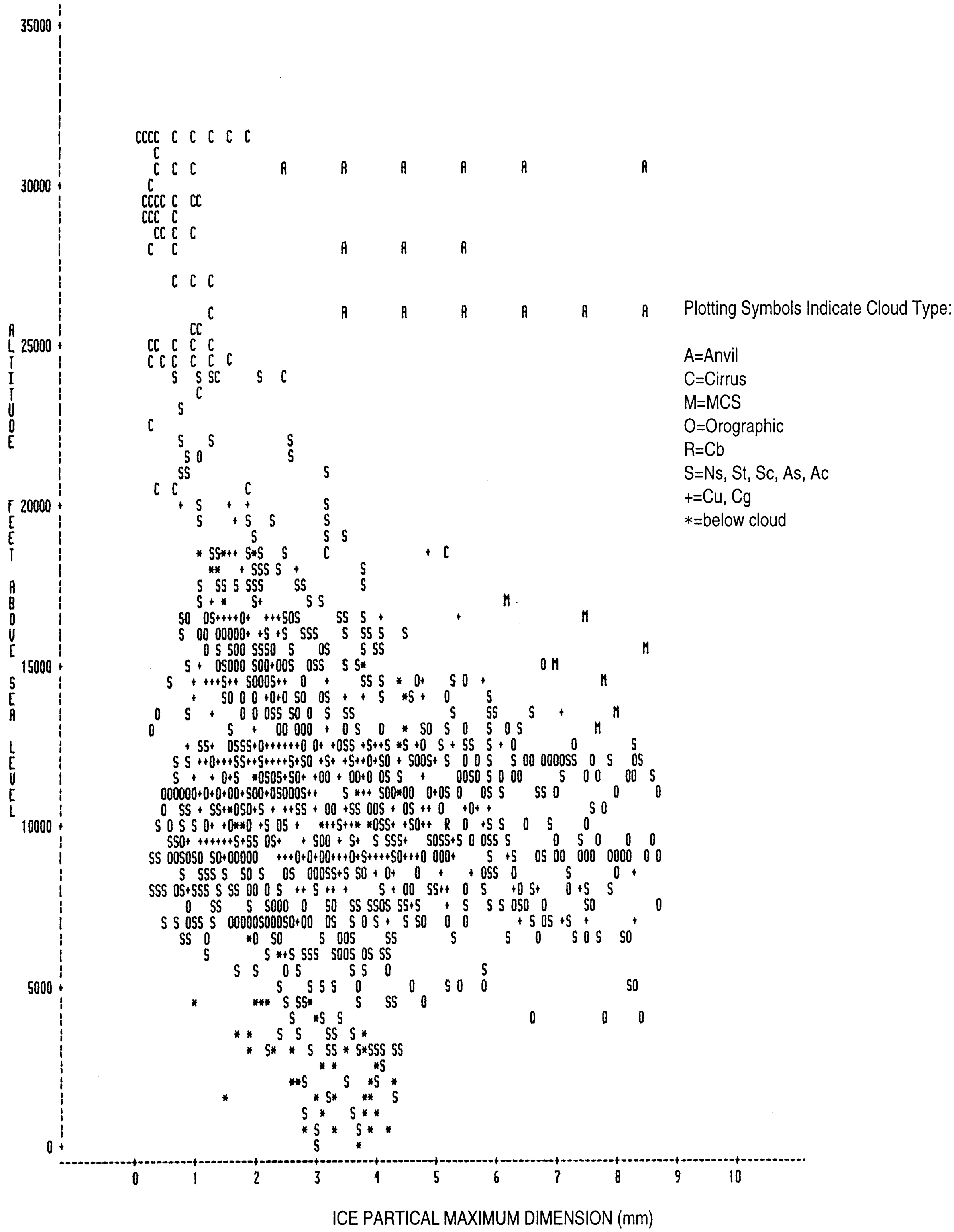

FIGURE 8d. EVENT-AVERAGED ICE PARTICLE MAXIMUM DIMENSION VERSUS ALTITUDE (ASL) FOR PARTICLES LARGER THAN 0.1 mm AND FOR ALL TYPES OF ICE PARTICLE CLOUDS

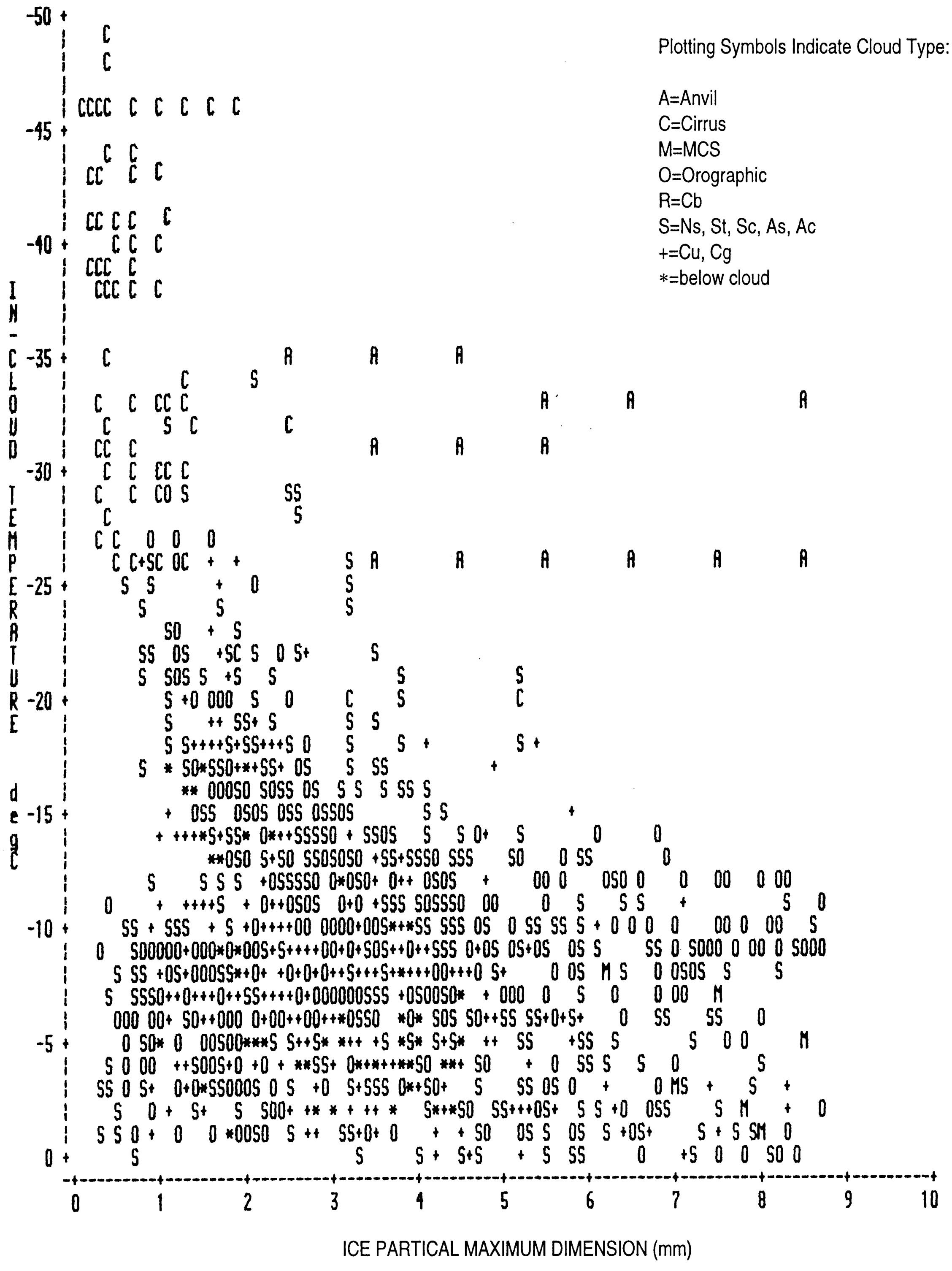

FIGURE 9a. EVENT-AVERAGED ICE PARTICLE MAXIMUM DIMENSION VERSUS TEMPERATURE FOR PARTICLES LARGER THAN 0.1 mm AND FOR ALL TYPES OF ICE PARTICLE CLOUDS

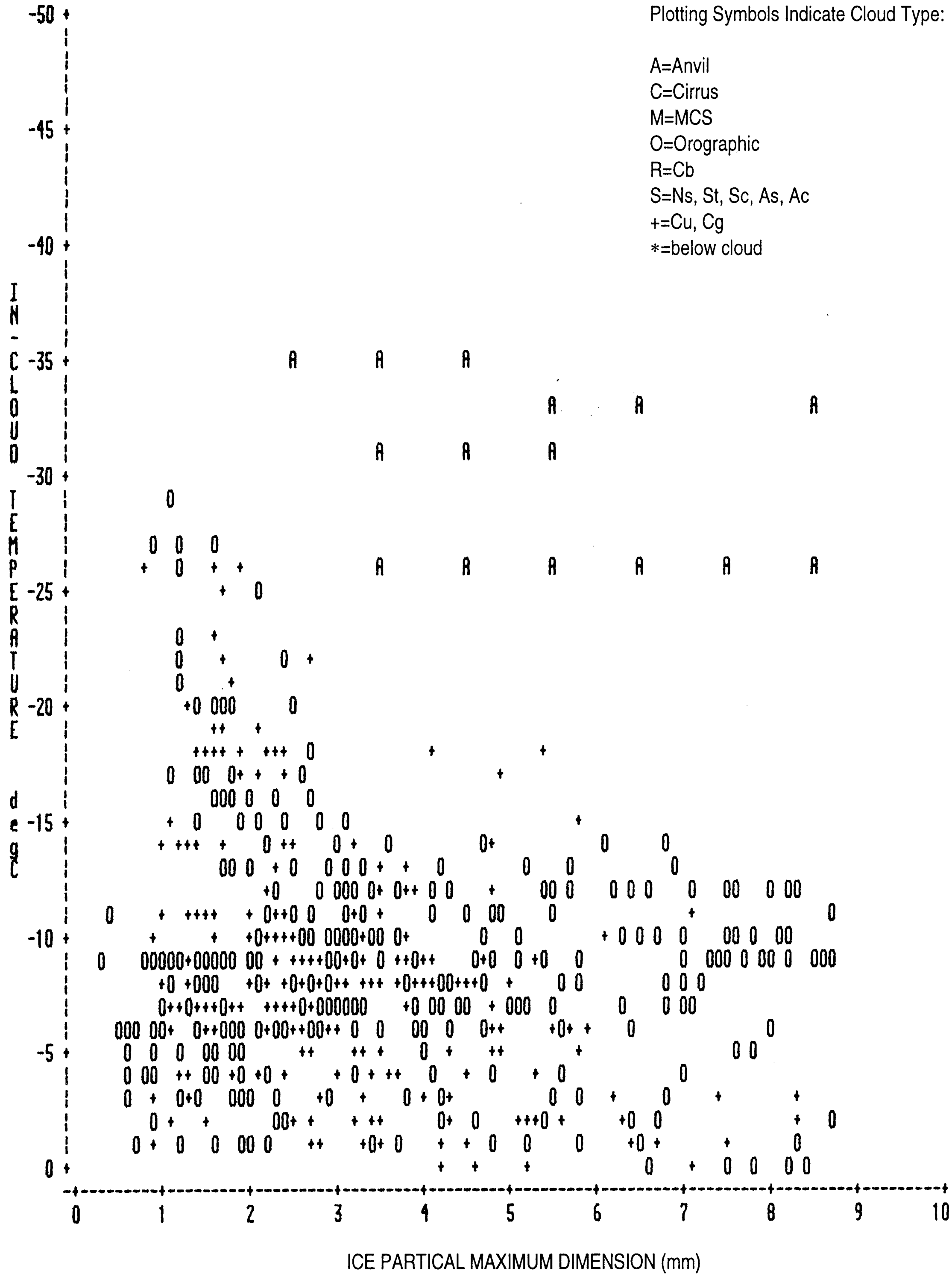

FIGURE 9b. EVENT-AVERAGED ICE PARTICLE MAXIMUM DIMENSION VERSUS TEMPERATURE FOR PARTICLES LARGER THAN 0.1 mm AND FOR CONVECTIVE CLOUDS (Cu, Cg, Cb, Or) ONLY

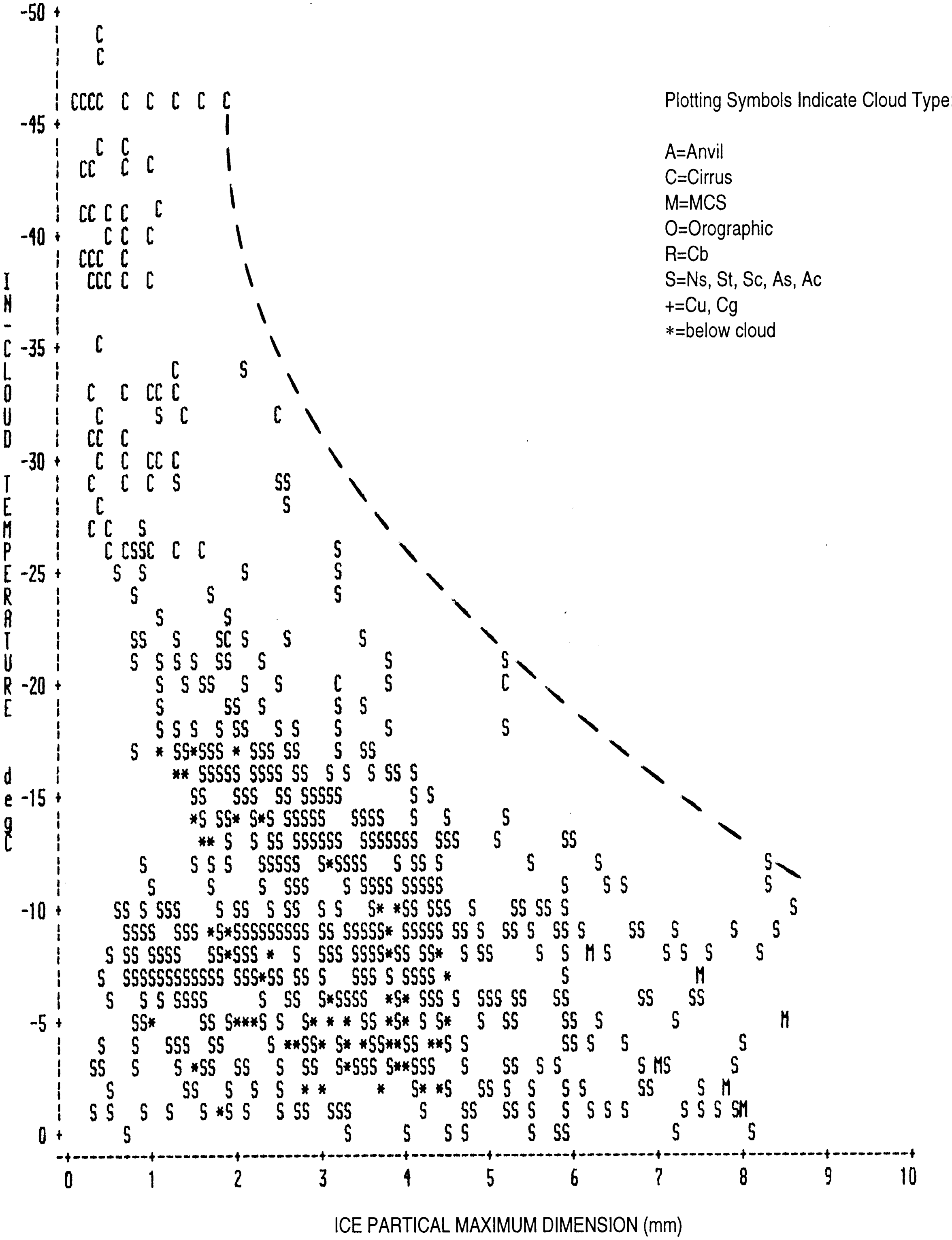

FIGURE 9c. EVENT-AVERAGED ICE PARTICLE MAXIMUM DIMENSION VERSUS TEMPERATURE FOR PARTICLES LARGER THAN 0.1 mm AND FOR LAYER CLOUDS (Ns, St, Sc, As, Ac, Ci, Cs) ONLY

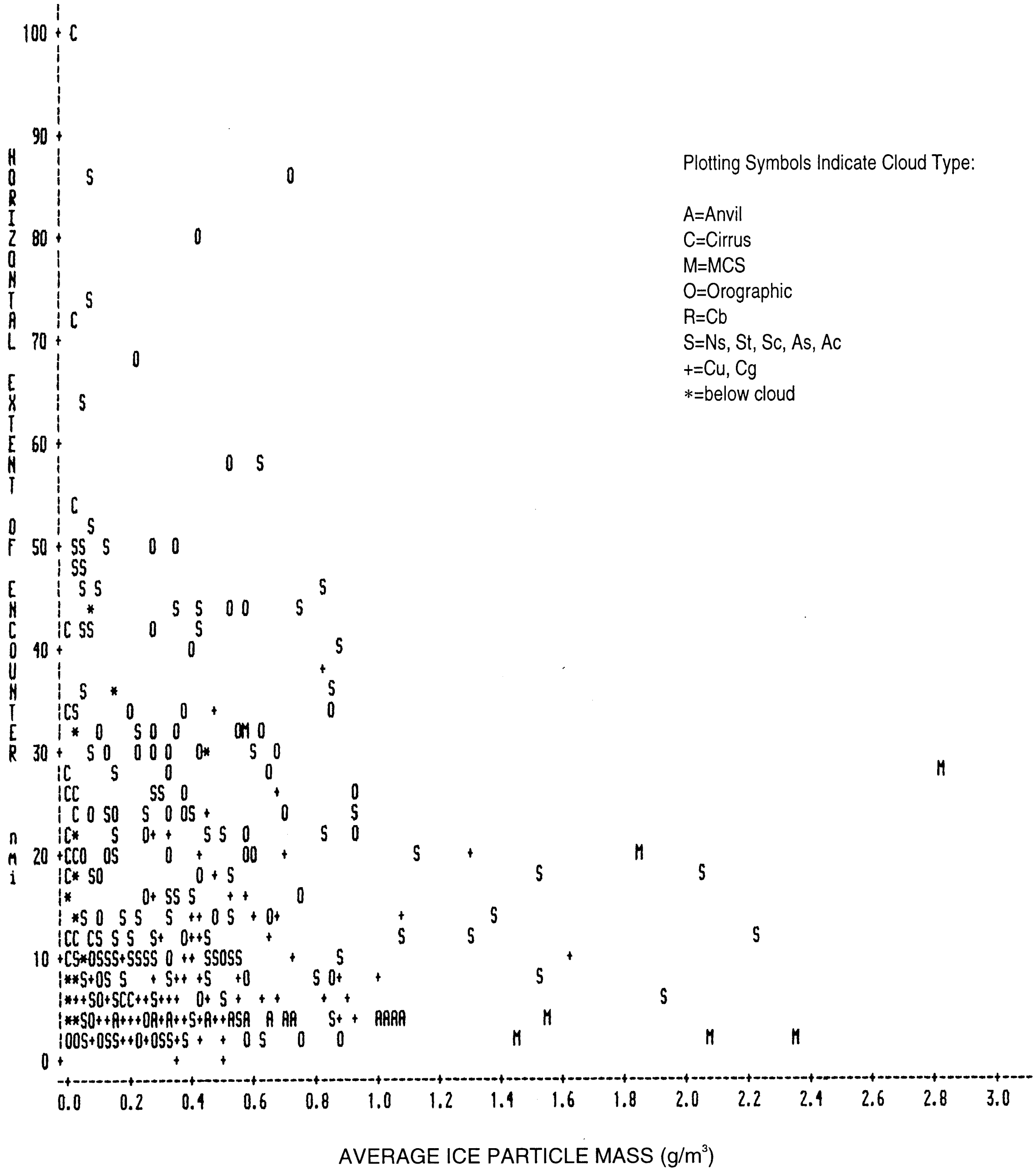

FIGURE 10a. ENCOUNTER-AVERAGED, TOTAL ICE PARTICLE MASS VERSUS HORIZONTAL EXTENT OF ENCOUNTERS (FOR ENCOUNTERS WITH BREAKS LESS THAN 1 nm LONG) AND FOR ALL TYPES OF ICE PARTICLE CLOUDS

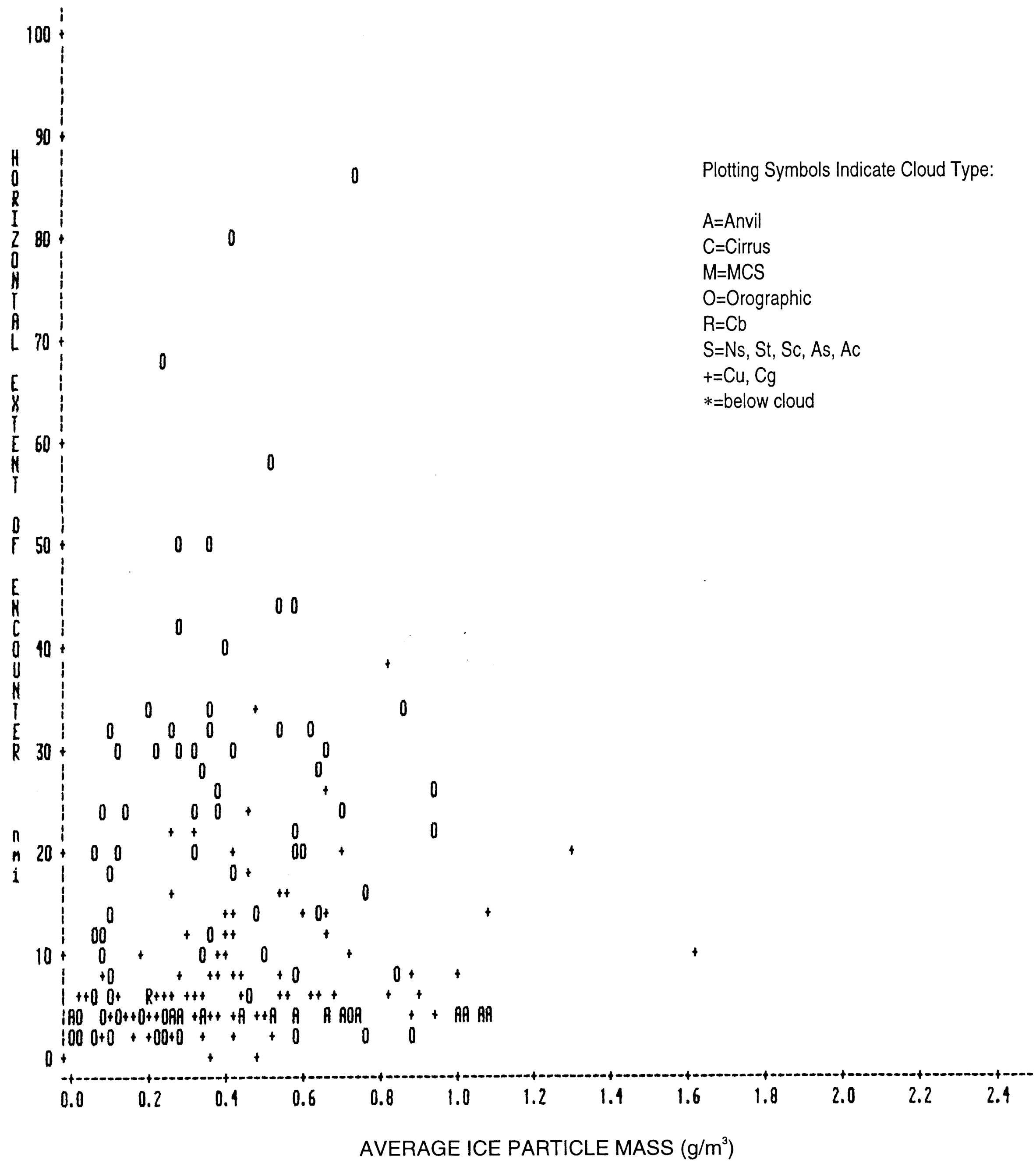

FIGURE 10b. ENCOUNTER-AVERAGED, TOTAL ICE PARTICLE MASS VERSUS HORIZONTAL EXTENT OF ENCOUNTERS (FOR ENCOUNTERS WITH BREAKS LESS THAN 1 nm LONG) AND FOR CONVECTIVE CLOUDS (Cu, Cg, Cb, Or) ONLY

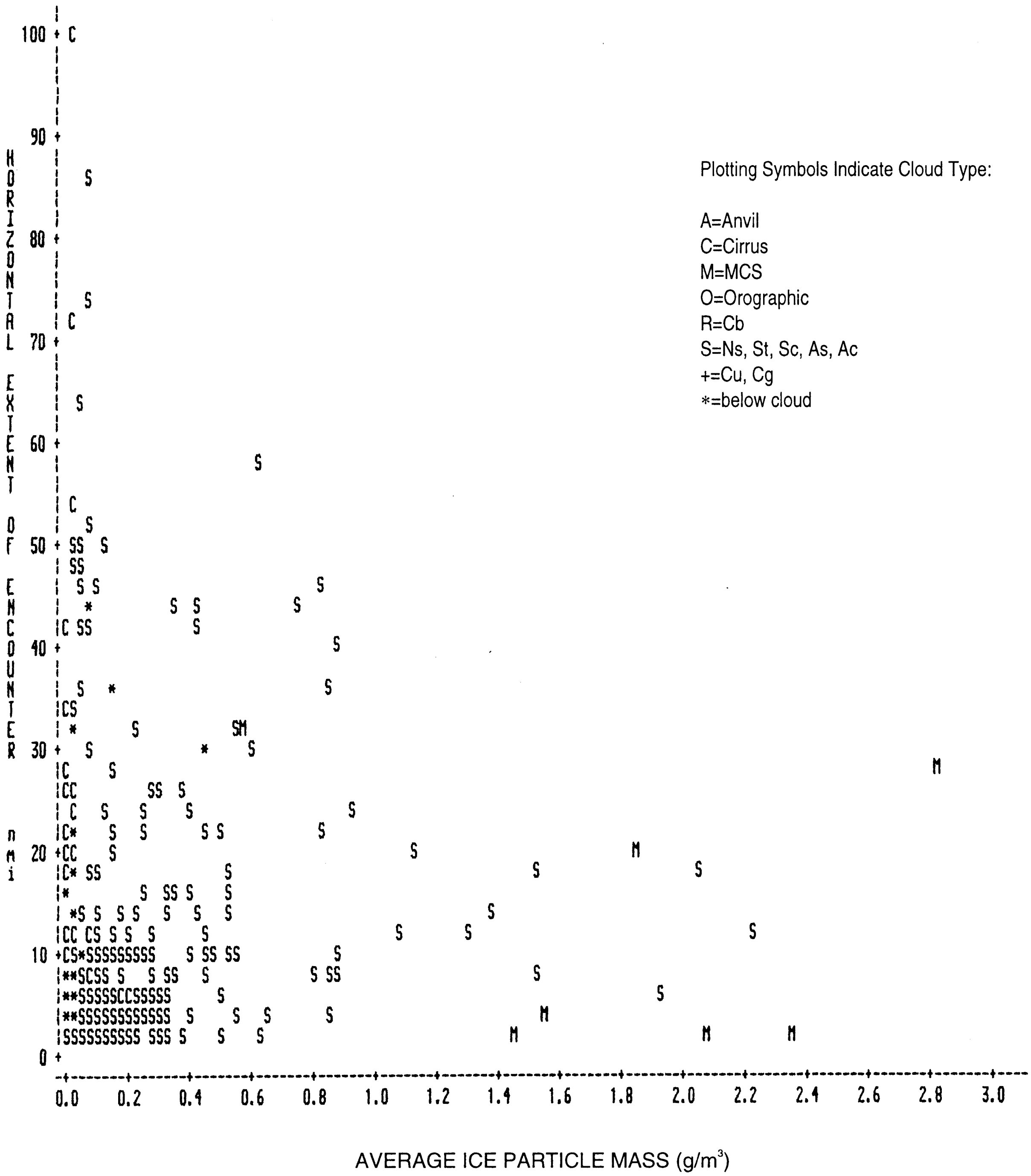

FIGURE 10c. ENCOUNTER-AVERAGED, TOTAL ICE PARTICLE MASS VERSUS HORIZONTAL EXTENT OF ENCOUNTERS (FOR ENCOUNTERS WITH BREAKS LESS THAN 1 nm LONG) AND FOR LAYER CLOUDS (Ns, St, Sc, As, Ac, Ci, Cs) ONLY

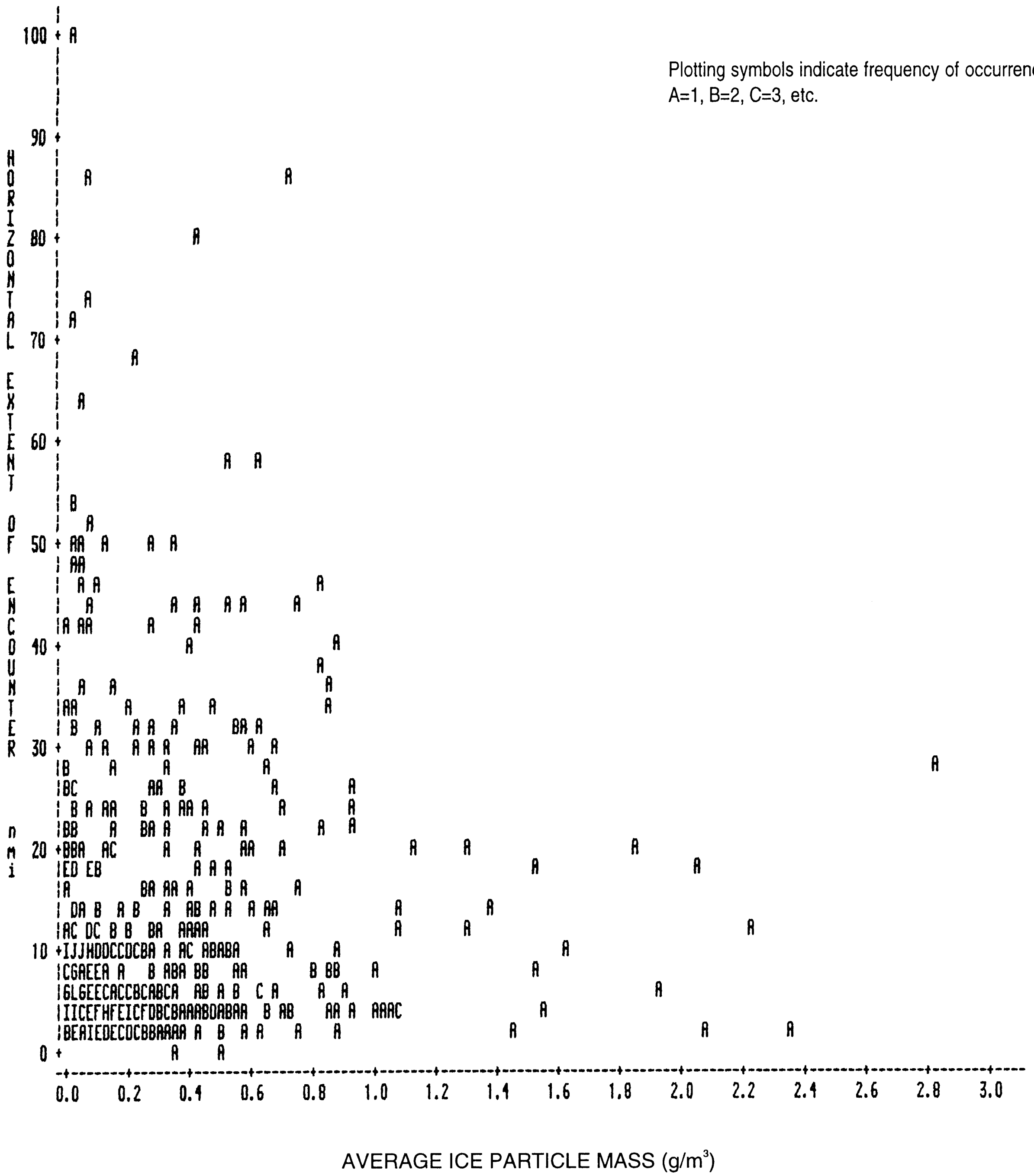

FIGURE 10d. ENCOUNTER-AVERAGED, TOTAL ICE PARTICLE MASS VERSUS HORIZONTAL EXTENT OF ENCOUNTERS (FOR ENCOUNTERS WITH BREAKS LESS THAN 1 nm LONG) AND FOR ALL TYPES OF ICE PARTICLE CLOUDS

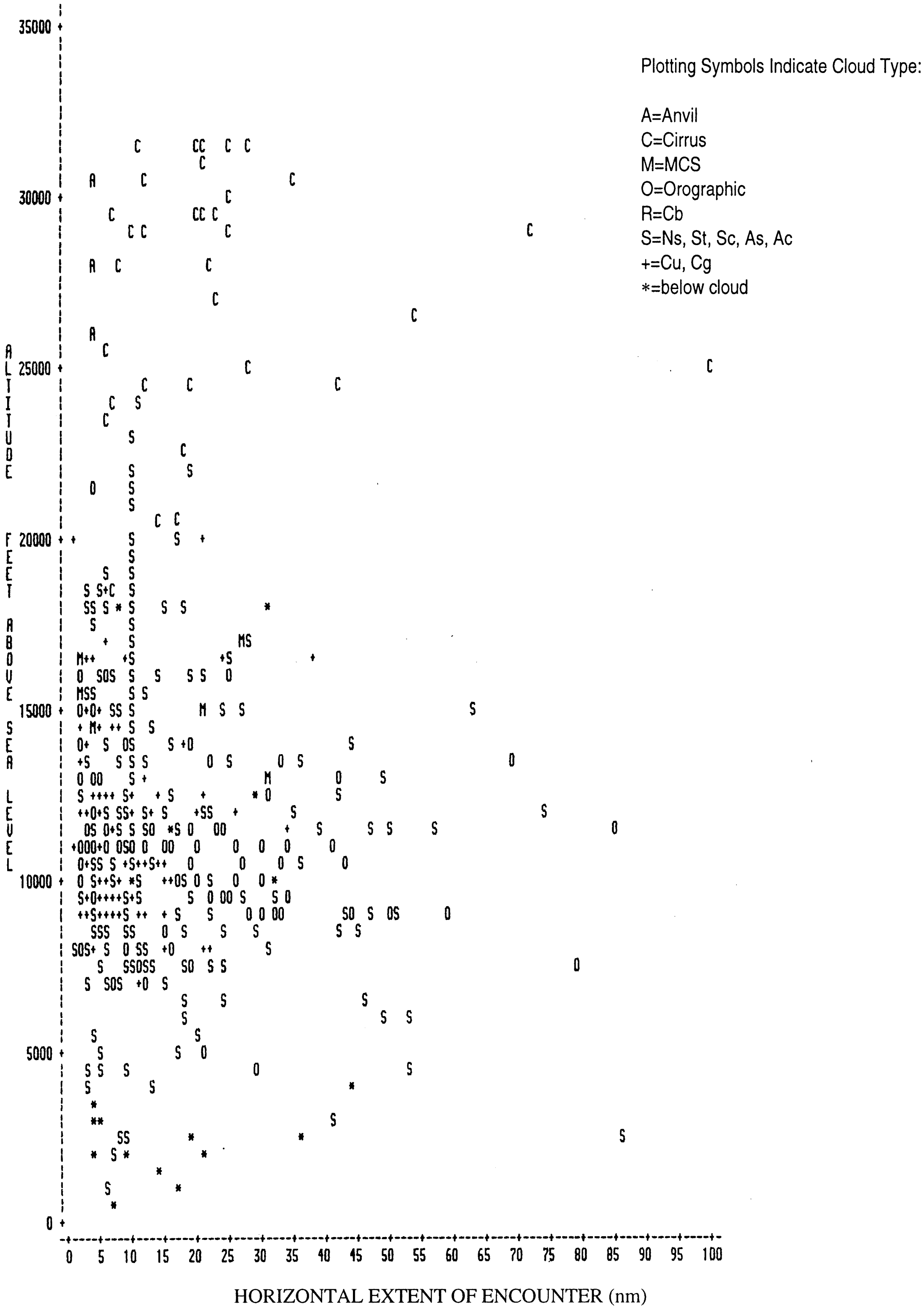

FIGURE 11a. HORIZONTAL EXTENT OF ENCOUNTERS VERSUS ALTITUDE (ASL) (FOR ENCOUNTERS WITH BREAKS LESS THAN 1 nm LONG) AND FOR ALL TYPES OF ICE PARTICLE CLOUDS

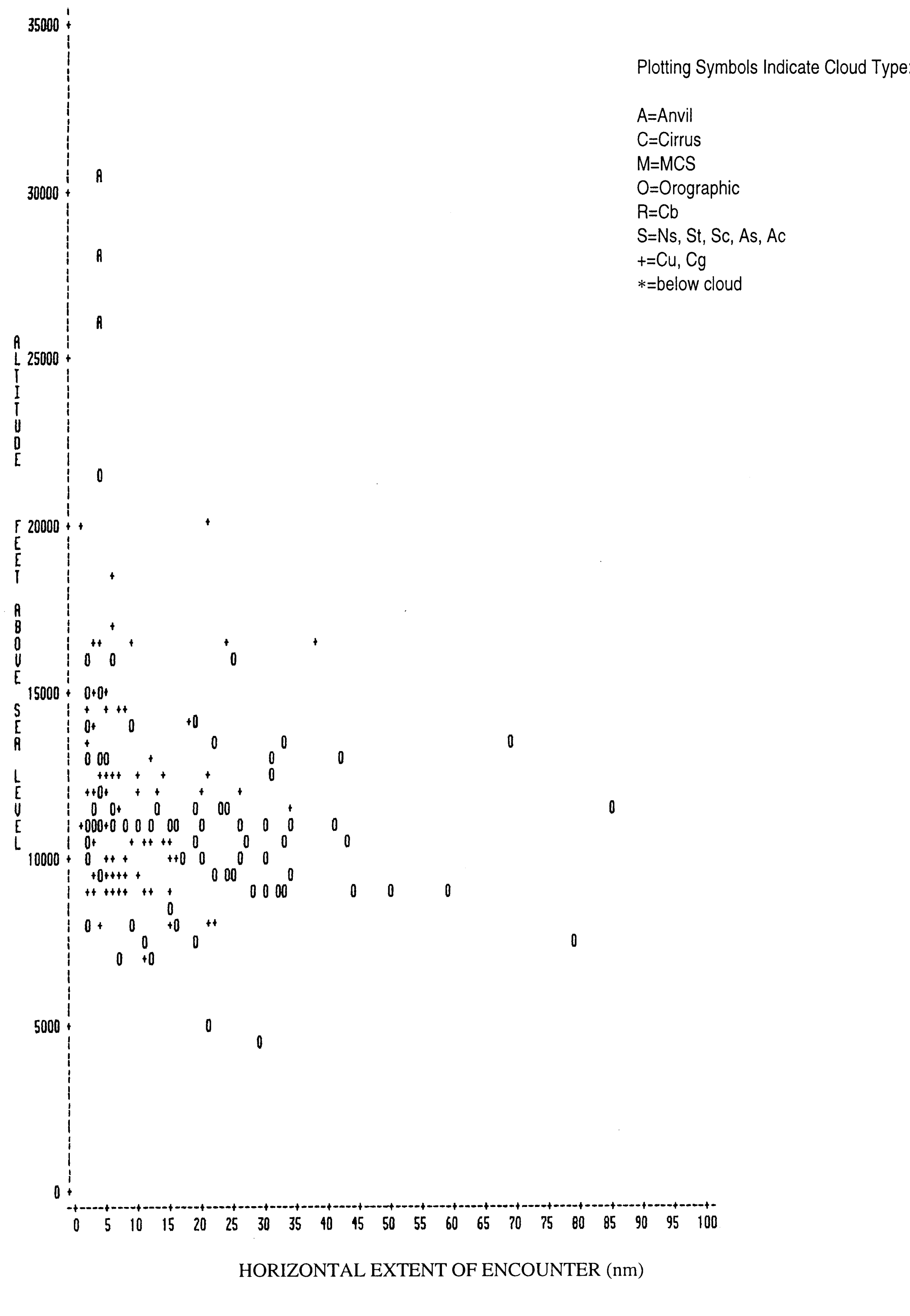

FIGURE 11b. HORIZONTAL EXTENT OF ENCOUNTERS VERSUS ALTITUDE (ASL) (FOR ENCOUNTERS WITH BREAKS LESS THAN 1 nm LONG) AND FOR CONVECTIVE CLOUDS (Cu, Cg, Cb, Or) ONLY

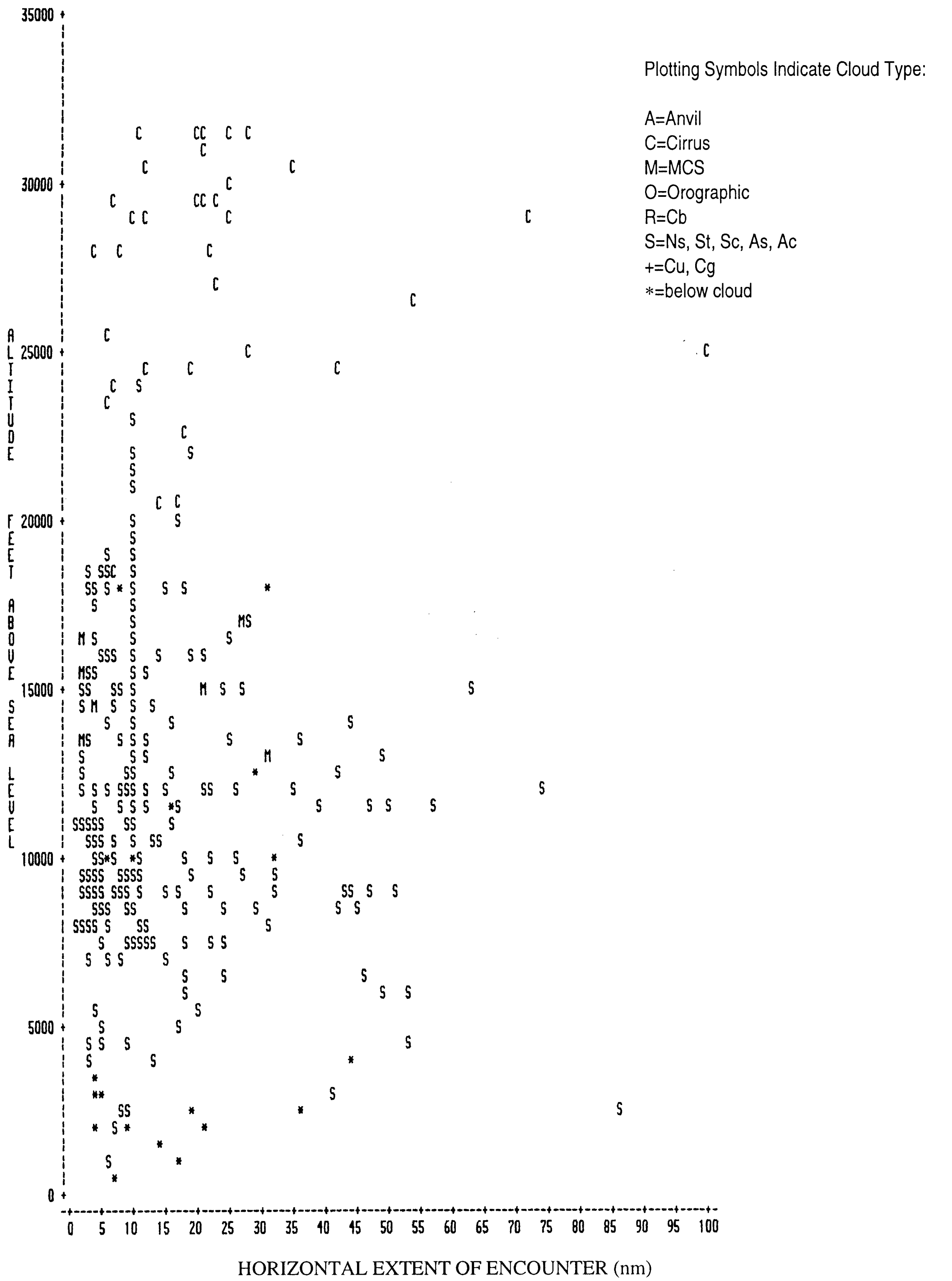

FIGURE 11c. HORIZONTAL EXTENT OF ENCOUNTERS VERSUS ALTITUDE (ASL) (FOR ENCOUNTERS WITH BREAKS LESS THAN 1 nm LONG) AND FOR LAYER CLOUDS (Ns, St, Sc, As, Ac, Ci, Cs) ONLY

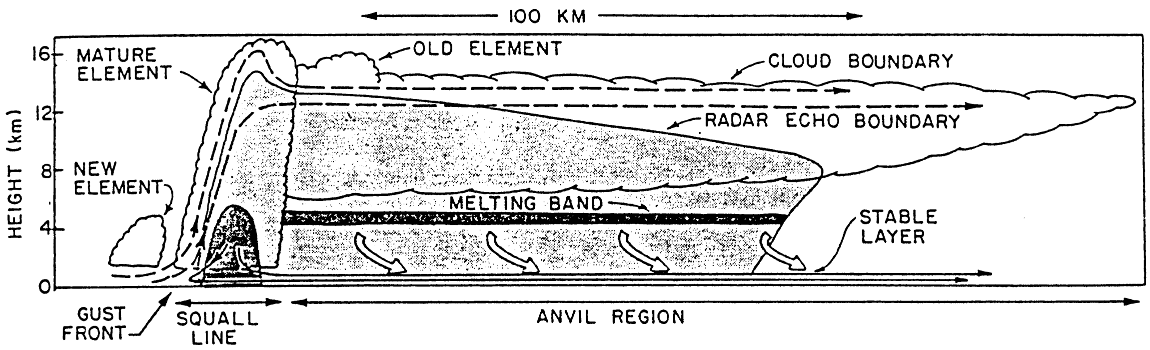

(a)

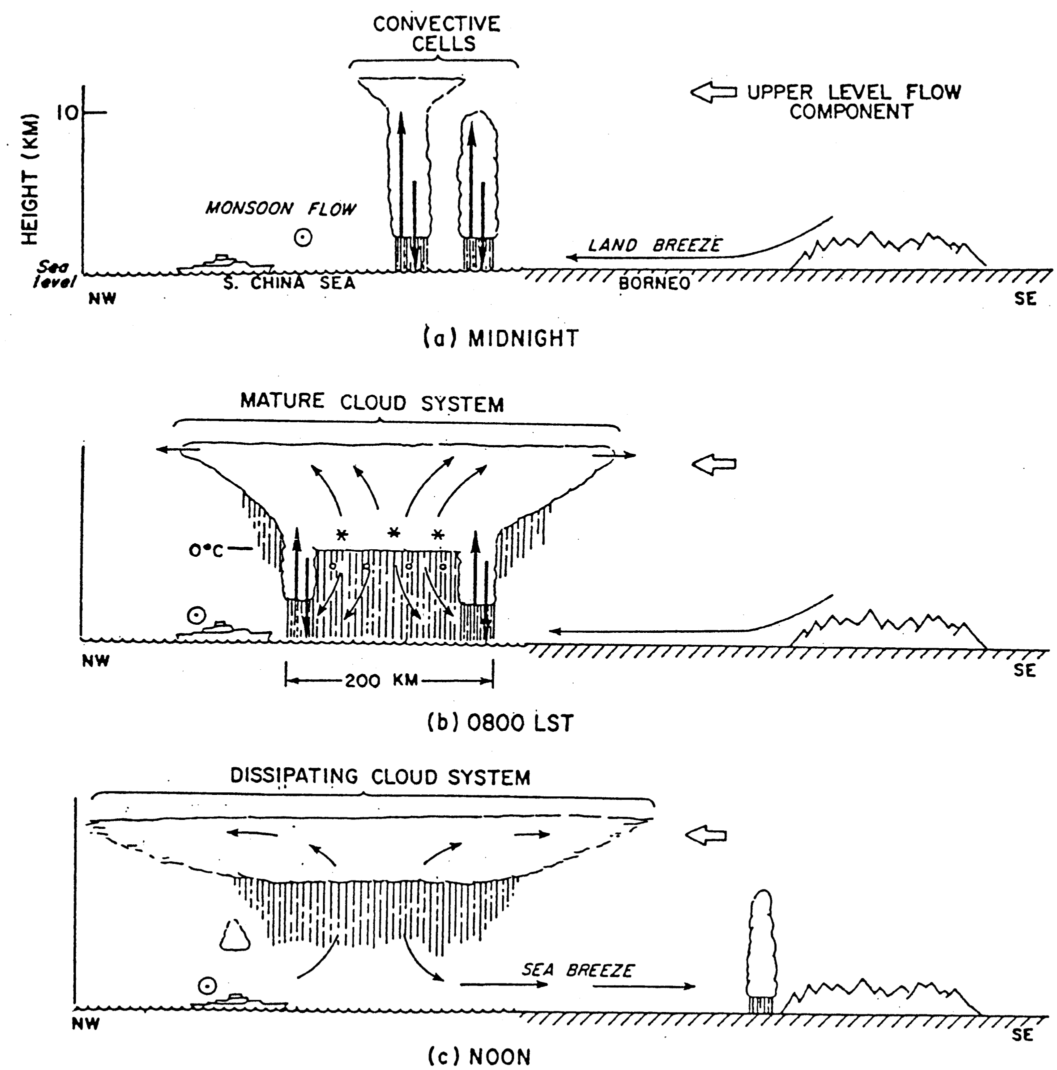

(b)

FIGURE 12. TYPICAL FORMS OF ANVIL CLOUDS IN TROPICAL CONVECTION
(a) Schematic cross section through a squall-line system [50], (b) Schematic development of a nonsquall cloud cluster anvil [51]

APPENDIX A—EXPLANATION OF THE VARIABLES USED IN THE DATABASE

DATA MANAGEMENT PHILOSOPHY

The data originally obtained from various sources (digital tapes, tabular reports, and journal articles) have been computerized in a condensed, standardized format according to the following scheme.

AVERAGING INTERVALS.

Modern, electronic, and electro-optical cloud physics probes and sensors provide digitized measurements typically once per second or more during flight in clouds. A reel of data tape may therefore contain 3600 or more individual readouts from each sensor per hour of flight. Naturally these large numbers of samples have to be reduced in some way to obtain a manageable set of data to work with. The data that are available from technical reports or journal articles have already been condensed to averages over some arbitrary time or distance intervals. For the high-resolution data available directly from the digital tapes, the following averaging scheme has been devised.

Each variable (LWC, air temperature, droplet number density, etc.) is averaged over continuous, uniform portions of clouds as indicated in table A-3. These averaging intervals are termed events. If the aircraft is still in continuous clouds at the end of one event, then a new averaging interval (event) is immediately begun and continued until the next significant change in cloud properties occurs. Otherwise, the next event is not begun until the aircraft enters another continuous, uniform section of cloud.

This averaging scheme has a number of advantages:

- Inflexible, fixed intervals such as 1-minute averages, or averages over entire cloud passes are avoided. (These are undesirable if they wash out useful detail otherwise available with modern, high-resolution measurements.)

- The events can be short enough to resolve any significant changes in cloud characteristics along the flight path—i.e., the natural variability in clouds can be preserved and documented.

- Intervals of uniform, constant conditions within clouds can be preserved whole so their durations and characteristics can be documented without the ambiguity that would occur if the average included voids or adjacent parcels having significantly different or variable properties.

- The averages can resolve extremes of particle mass concentrations or other variables without dilution.

- The averages can preserve altitude dependent changes in cloud properties observed during ascents or descents through clouds.

- The scheme can accommodate broken or scattered cloud conditions as well as widespread continuous clouds.

- Not only are data available on the extents of individual, uniform, cloud intervals, but the overall horizontal extent of continuous or semicontinuous icing conditions is available simply by summing the extents of consecutive events.

DATA MILES AS A MEASURE OF FREQUENCY OF OCCURRENCE.

During the early phases of this project, it became clear that usage of number of cases or number of events, as is conventionally done to represent the frequency of occurrence of any of the variables, was unsatisfactory. The deficiency was twofold. Firstly, momentary icing events would incorrectly carry just as much statistical weight as long-lasting events. Thus, there was no way to emphasize the statistical importance of an extended encounter with an extreme value of particle mass, for example, compared to a relatively insignificant, brief encounter. Secondly, the reader would have no information as to whether a given number of events represented 5 miles or 500 miles of in-flight measurements.

Data miles were therefore chosen as the most informative measure of frequency of occurrence. The term is defined as the distance flown (in nautical miles) during an individual icing event. This convention automatically weights each icing event (or measurement of particle mass, for example) by its duration or extent. The other principal advantage is that the reader can easily judge the statistical significance of a data set by the number of data miles it represents.

DATA FORMAT.

Table A-1 lists all of the variables that have been selected to describe the events.

The entire database of event-averaged variables is available on digital magnetic tape. The data are coded in ASCII for simplicity of use. A sample printout of all the variables associated with a few representative events is given in table A-4.

TABLE A-1. DESCRIPTION OF THE PRINCIPAL VARIABLES

MISSION IDENTIFIERS		
Variable	Type	Explanation or Example
PROJECT	Char	CCOPE, SCPP, NEWS, COSE, etc., (see table 1 in text).
DATE	Num	MMDDYY that the flight took place
AGENCY	Char	U. WYOMING (King Air), NRL (P-3), etc., where the type of aircraft is given in parentheses.
LOCATION	Char	Name of the nearest city or airport, including its 3-letter code, such as DEN, SFO, STL, etc.
SURFELEV	Num	The elevation of the local surface in feet above sea level. Special missing data indicators are M, U, E, V, for mountainous, unknown, estimated, and variable values (consult ELEVNOTE for additional information).
ELEVNOTE	Char	For example, an entry of "5000-8500" indicates that the surface elevation ranges between 5000 and 8500 ft in the nearby downwind vicinity of the measurements.
ALT_CONV	Char	ASL, PA, or AGL indicate that all the height or altitude data are in terms of height above sea level, pressure altitude, or height above ground level, respectively.
CLOUD INFORMATION		
Variable	Type	Explanation or Example
CLOUDGRP	Char	A letter, A, B, C, etc., denoting a group of similar type clouds being sampled.
CLOUDNUM	Num	A number, 1, 2, 3, etc., denoting which cloud in CLOUDGRP contributed to the data for the present observation.
CLD_PASS	Char	A number, 1, 2, 3, etc., indicating which pass the current observation represents through the cloud identified by CLOUDGRP and CLOUDNUM.
CLOUDTYP	Char	Conventional cloud type abbreviations such as Cu, Sc, (see table A-2).
CLD_DIST	Char	Descriptive words, such as broken, scattered, etc., to indicate the prevailing cloud distribution.
CLDSTATE	Char	Coded notation indicating the state of the cloud particles sampled by the aircraft. For example: W = all water droplets, I = all ice particles, etc., (see table A-2).
PRECIP	Char	Conventional notation indicating the type and intensity of precipitation, if any, observed at flight level from the aircraft (a/c) or on the ground (gnd) below the cloud under study. For example: S- = light snow, G+ = heavy graupel, etc., (see table A-2).
XTALTYPE	Char	Predominant particle type(s) or crystal habit(s), if known. For example: Br = bullet rosettes, Pl = plates, etc.

TABLE A-1. DESCRIPTION OF THE PRINCIPAL VARIABLES (Continued)

CLOUD INFORMATION (continued)		
Variable	Type	Explanation or Example
CLDBASHT	Num	Numerical values such as 3650, 12000, etc., giving cloud base height in feet according to the convention defined by ALT_CONV for the flight in question. Special missing data indicators are U, V, and E for unknown, variable, or estimated values (consult CLDBHNOT for additional information).
CLDBHNOT	Char	Additional information on the cloud base height. For example, the entry CLDBHNOT=11000 (along with CLDBASHT=E) indicates that the cloud base is estimated to be at 11,000 feet.
CLDTOPHT	Num	Numerical values giving cloud top height in feet at the time of the observation. (Other usage is the same as for CLDBASHT above.)
CLDTHNOT	Char	(Same usage as for CLDBHNOT above.)
CLDBAS_T	Num	Numerical values giving cloud base temperature in degrees Celsius. Special symbols for missing data are U, V, and E as above.
CLDBTNOT	Char	Additional information on cloud base temperature when CLDBAS_T = E or V.
CLDTOP_T	Num	Numerical values giving cloud top temperature in degrees Celsius. Special symbols for missing data are U, V, and E as above.
CLDTTNOT	Char	Additional information on cloud top temperature when CLDTOP_T = E or V.
WEATHER FACTORS		
Variable	Type	Explanation or Example
AIRMASS	Char	Conventional air mass abbreviations such as: mT = maritime tropical, McP = modified continental polar, etc.
WEATHER	Char	A coded description of the weather conditions associated with the clouds under study. A list of the code symbols are given in table A-2. For example, “Lc 200nm W & Ws Pr(S-)” means “a low pressure center 200 nautical miles to the west and widespread precipitation (light snow).”
MEASUREMENT-RELATED VARIABLES		
Variable	Type	Explanation or Example
ST_TIME	Char	The time, HH:MM:SS, at the beginning of the sample.
TIMECONV	Char	Time zone code applicable to ST_TIME. For example, GMT = Greewich Mean Time, MDT = Mountain Daylight Time (USA), PST = Pacific Standard Time (USA).
PROBE_ID	Char	Identifies which PMS probes (1D-C, 2D-C 1D-P or 2D-P) were in use during the flight.

TABLE A-1.   DESCRIPTION OF THE PRINCIPAL VARIABLES (Continued)

MEASUREMENT-RELATED VARIABLES (continued)		
Variable	Type	Explanation or Example
DIACUTOF	Char	The largest particle size (mm) measurable by the available PMS probes.
MAXDIAM	Num	The average value of the largest particle size (mm) detected by the available PMS probe(s).
DURATION	Num	A number indicating the time duration (in seconds) of the cloud sample.
DISTANCE	Num	A number indicating the distance (in nautical miles) traveled by the aircraft during the sample.
EVENTDEF	Char	A letter code, A, B, C, etc., to indicate why the sample was terminated. The code is given in table A-3.
MANEUVER	Char	A description (level, slant, spiral) of the aircraft flight path during the sample.
AVERAGED VARIABLES		
Variable	Type	Explanation or Example
TAS	Num	Average True Airspeed (knots) during the sample.
ALT	Num	Average altitude (feet) during the sample, according to the convention defined by ALT_CONV.
TEMP	Num	Average outside (true) air temperature (°C) during the sample.
JWLWC	Num	Average value of the liquid water content (g/m) indicated by a hot-wire type of LWC meter. (Usually the LWC meter is a Johnson-Williams model, but occasionally a CSIRO-King type is used.).
FLWC	Num	Average value of the LWC (g/m) computed from the droplet size distribution indicated by the PMS, ASSP, or FSSP probe.
CONC	Num	Average value of the droplet number density (no./cm) indicated by the FSSP or ASSP.
CONC_1D-C	Num	Average value of the particle number density (no./liter) indicated by the PMS 1D-C (200X) probe.
CONC_2D-C	Num	Average value of the particle number density (no./liter) indicated by the PMS 2D-C probe.
CONC_1D-P	Num	Average value of the particle number density (no./liter) indicated by the PMS 1D-P (200Y) probe.
CONC_2D-P	Num	Average value of the particle number density (no./liter) indicated by the PMS 2D-P probe.
C50_100	Num	Average value of the particle number density (no./l) in the 50-100 μm range of the PMS probe(s).
C100_300	Num	Average value of the particle number density (no./l) in the 100-300 μm range of the PMS probe(s).

TABLE A-1. DESCRIPTION OF THE PRINCIPAL VARIABLES (Continued)

AVERAGED VARIABLES (continued)		
Variable	Type	Explanation or Example
C300_1K	Num	Average value of the particle number density (no./l) in the 300-1000 μm range of the PMS probe(s).
C1_3 mm	Num	Average value of the particle number density (no./l) in the 1-3 mm range of the PMS probe(s).
C3_6 mm	Num	Average value of the particle number density (no./l) in the 3-6 mm range of the PMS probe(s).
C6_10 mm	Num	Average value of the particle number density (no./l) in the 6-10 mm range of the PMS probe(s).
M50_100	Num	Computed mass (g/m^3) of particles in the 50-100 μm range of the PMS probe(s).
M100_300	Num	Computed mass (g/m^3) of particles in the 100-300 μm range of the PMS probe(s).
M300_1K	Num	Computed mass (g/m^3) of particles in the 300-1000 μm range of the PMS probe(s).
M1_3 mm	Num	Computed mass (g/m^3) of particles in the 1-3 mm range of the PMS probe(s).
M3_6 mm	Num	Computed mass (g/m^3) of particles in the 3-6 mm range of the PMS probe(s).
M6_10 mm	Num	Computed mass (g/m^3) of particles in the 6-10 mm range of the PMS probe(s).
MASS1CT	Num	Computed mass (g/m^3) of particles in the entire range of the PMS 1D-C probe.
MASS2CT	Num	Computed mass (g/m^3) of particles in the entire range of the PMS 2D-C probe.
MASS1PT	Num	Computed mass (g/m^3) of particles in the entire range of the PMS 1D-P probe.
MASS2PT	Num	Computed mass (g/m^3) of particles in the entire range of the PMS 2D-P probe.

TABLE A-2. DESCRIPTION OF SECONDARY VARIABLES

WEATHER CODE SYMBOLS

Al = Along
Ao = Ahead of
Am = Airmass
B = Bands
Bt = Between
C = Convergence
Cd = Cold
Cf = Cold front
Cl = Cloud(s)
Cu = Cut(off)
Cv = Convection
Cx = Complex
Cy = Cyclone, cyclonic flow
D = Dense
Dy = Dry
d = due to
E = East
Em = Embedded
Ey = Easterly
F = Following
Fl = Flight level
Fm = Fast moving
Fr = Front, Frontal
Fw = Fair weather
g = generally
Hc = High pressure center
Hp = High pressure region
Ht = Heating
I = Inversion
Js = Jetstream
L = Layer
Lc = Low-pressure center
Le = Lake effect
Li = Line(s)
Ll = Low level
Lp =Low-pressure region
M = Moderate, medium
MCS=Mesoscale Convective System
Ml = Mid level
Ms = Moist
Mu = Multiple
N = North
Ny = Northerly
nm = nautical miles
O = Over
Oc = Occluded
Of = Occluded front
Or = Orographic
Ot = Outside of
Ovc= Overcast
Pa = Passage, passing
Pg = Pressure gradient
Po = Possibly, possible
Pr = Precipitation
R = Ridge
Ra = Rain
Rb = Rainband
S = South
Sa = Stable air
Sb = Stable, stability
Sc = Scattered
Sf = Stationary front
Sh = Short
Sm = Slow moving
Sn = Snow
Sq = Squall
Sr = Strong, deep
St = Stationary
Su = Surface
Sv = Severe
Sw = Shower(s)
Sy = Southerly
s = some
T = Thin
Tb = Turbulence
Tn = Tornado
Tr = Trough
Ts = Thunderstorm
Ua = Unstable air
Ud = Updraft
Uf = Upslope flow
Up = Upper, upper level, upper part
u = usually
W = West
w = with
Wf = Warm front
Wi = Wind(s)
Wk = Weak
Wm = Warm
Ws = Widespread
Wv = Wave
Wx = Weather
Wy = Westerly
Z = Zone
* = Estimated value follows
? = Amount or type uncertain

TABLE A-2. DESCRIPTION OF SECONDARY VARIABLES (Continued)

PRECIPITATION CODE SYMBOLS	AGENCY CODES (for use as ploting symbols) Agency	One-Letter Code
A = Hail	AFGL (C-130)	A
E = Sleet	CIC (Learjet)	C
L = Drizzle	NCAR (Sabreliner)	S
R = Rain	NCAR (Queen Air)	Q
S = Snow	NOAA (P-3)	P
SP = Snow pellets	U. Wyoming (King Air)	W
ZL = Freezing drizzle		
ZR = Freezing rain		
+ = heavy		
- = light		
w = showers		

CLOUD NAMES	
Layer Clouds	Convective Clouds
Ac = Altocumulus	Cb = Cumulonimbus
As = Altostratus	Cg = Cumulus congestus
Ln = Lenticular	Cu = Cumulus
Ns = Nimbostratus	TCu= Towering cumulus
Sc = Stratocumulus	
St = Stratus	

TABLE A-3. RULES FOR DEFINING UNIFORM CLOUD INTERVALS

One or two of the code letters listed below are assigned to the variable EVENTDEF to indicate why the sample averaging interval was terminated. That is, all the measured variables are averaged over the flight path in the cloud until:

A - Aircraft exits main cloud,
B - Outside air temperature (TEMP) changes by ± 1.5°C,
C - Outside air temperature (TEMP) rises above 0°C,
D - Major change in particle size distribution,
E - Aircraft changes altitude (ALT) by ± 500 feet (± 150 meters),
H - Averaging interval arbitrarily terminated,
J - Aircraft encounters momentary break in cloud.

TABLE A-4. SAMPLE PRINTOUT OF DATABASE

OBS	AIRMASS	TIMECONV	DIACUTOF	CLOUDTYP	AGENCY	WEATHER	DATE	CLOUDNUM	CLDBASHT	CLDBAS_T
1	cP	GMT	4.7mm	Ci	USAF/AFGL(C-130)	Ws Cl d Sf S & Hc N	20579	1	E	E
2	cP	GMT	4.7mm	Cs	USAF/AFGL(C-130)	Ws Cl d Sf S & Hc N	20579	1	E	E
3	cP	GMT	4.7mm	Cs	USAF/AFGL(C-130)	Ws Cl d Sf S & Hc N	20579	1	U	U
4	cP	GMT	4.7mm	Cs	USAF/AFGL(C-130)	Ws Cl d Sf S & Hc N	20579	1	U	U
5	cP	GMT	4.7mm	Cs	USAF/AFGL(C-130)	Ws Cl d Sf S & Hc N	20579	1	U	U
6	cP	GMT	4.7mm	Ci	USAF/AFGL(C-130)	Ws Cl d Sf S & Hc N	20579	1	E	-38.0
7	cP	EST	4.5mm	below As	NCAR(QueenAir)	Lp & M Lc NE, Ws Cl & S- & S @ L1 & M1	122082	1	0	-2.5
8	cP	EST	4.5mm	below As	NCAR(QueenAir)	Lp & M Lc NE, Ws Cl & S- & S @ L1 & M1	122082	1	0	-2.5
9	cP	EST	4.5mm	below As	NCAR(QueenAir)	Lp & M Lc NE, Ws Cl & S- & S @ L1 & M1	122082	1	0	-2.5
10	cP	EST	4.5mm	below As	NCAR(QueenAir)	Lp & M Lc NE, Ws Cl & S- & S @ L1 & M1	122082	1	0	-2.5
11	cP	EST	4.5mm	below As	NCAR(QueenAir)	Lp & M Lc NE, Ws Cl & S- & S @ L1 & M1	122082	1	0	-2.5
12	cP	EST	4.5mm	below As	NCAR(QueenAir)	Lp & M Lc NE, Ws Cl & S- & S @ L1 & M1	122082	1	0	-2.5
13	cP	EST	4.5mm	below As	NCAR(QueenAir)	Lp & M Lc NE, Ws Cl & S- & S @ L1 & M1	122082	1	0	-2.5
14	cP	EST	4.5mm	below As	NCAR(QueenAir)	Lp & M Lc NE, Ws Cl & S- & S @ L1 & M1	122082	1	0	-2.5
15	cP	EST	4.5mm	below As	NCAR(QueenAir)	Lp & M Lc NE, Ws Cl & S- & S @ L1 & M1	122082	1	0	-2.5
16	cP	EST	4.5mm	below As	NCAR(QueenAir)	Lp & M Lc NE, Ws Cl & S- & S @ L1 & M1	122082	1	0	-2.5
17	cP	EST	4.5mm	below As	NCAR(QueenAir)	Lp & M Lc NE, Ws Cl & S- & S @ L1 & M1	122082	1	0	-2.5
18	cP	GMT	7mm	Ns	NCAR(QueenAir)	Ws Cl & Pr(S) 100nm F Sm Cf	112679	1	9200	-10.0
19	cP	GMT	7mm	Ns	NCAR(QueenAir)	Ws Cl & Pr(S) 100nm F Sm Cf	112679	1	9200	-10.0
20	cP	GMT	7mm	Ns	NCAR(QueenAir)	Ws Cl & Pr(S) 100nm F Sm Cf	112679	1	9200	-10.0
21	cP	GMT	7mm	Ns	NCAR(QueenAir)	Ws Cl & Pr(S) 100nm F Sm Cf	112679	1	9200	-10.0
22	cP	GMT	7mm	Ns	NCAR(QueenAir)	Ws Cl & Pr(S) 100nm F Sm Cf	112679	1	9200	-10.0
23	cP	GMT	7mm	Ns	NCAR(QueenAir)	Ws Cl & Pr(S) 100nm F Sm Cf	112679	1	9200	-10.0
24	cP	GMT	7mm	Ns	NCAR(QueenAir)	Ws Cl & Pr(S) 100nm F Sm Cf	112679	1	9200	-10.0
25	c	CDT	10 mm	As	NOAA(P-3 #43)	Mesoscale Convective System (MCS)	61085	1	U	U
26	c	CDT	10 mm	As	NOAA(P-3 #43)	Mesoscale Convective System (MCS)	61085	1	U	U
27	c	CDT	10 mm	As	NOAA(P-3 #43)	Mesoscale Convective System (MCS)	61085	1	U	U
28	c	CDT	10 mm	As	NOAA(P-3 #43)	Mesoscale Convective System (MCS)	61085	1	U	U
29	c	CDT	10 mm	As	NOAA(P-3 #43)	Mesoscale Convective System (MCS)	61085	1	U	U
30	c	CDT	10 mm	As	NOAA(P-3 #43)	Mesoscale Convective System (MCS)	61085	1	U	U
31	c	CDT	10 mm	As	NOAA(P-3 #43)	Mesoscale Convective System (MCS)	61085	1	U	U

OBS	CLDTOPHT	CLDTOP_T	CLDTHNOT	CLDTTNOT	CLD_DIST	ELEVNOTE	SURFELEV	LOCATION	CLD_PASS	EVENTDEF
1	E	E	21600	-34	Thin, isolated		4100	TCC	1	H
2	E	E	22000	-33	Thin, isolated		3600	AMA	1	H
3	E	E	24600	-34	Edge of large Ci shield		1300	OKC	1	H
4	E	E	24600	-34	Edge of large Ci shield		1300	TUL	1	H
5	E	E	24600	-34	Edge of large Ci shield		1300	SGF	1	H
6	E	-39	30000	U	Thin, wispy		600	BNA	1	H
7	U	U	up to As layer		snowfall area below cloud	U	130	BED	1	E
8	U	U	up to As layer		snowfall area below cloud	U	130	BED	1	E
9	U	U	up to As layer		snowfall area below cloud	U	130	BED	1	E
10	U	U	up to As layer		snowfall area below cloud	U	130	BED	1	E
11	U	U	up to As layer		snowfall area below cloud	U	130	BED	1	D
12	U	U	up to As layer		snowfall area below cloud	U	0	GLO	1	D
13	U	U	up to As layer		snowfall area below cloud	U	0	GLO	1	D
14	U	U	up to As layer		snowfall area below cloud	Offshore GLO	0	GLO	1	D
15	U	U	up to As layer		snowfall area below cloud	Offshore GLO	0	GLO	1	A
16	U	U	up to As layer		snowfall area below cloud	Offshore GLO	0	GLO	2	H
17	U	U	up to As layer		snowfall area below cloud	Offshore GLO	0	GLO	2	E,H
18	22500	-35			Widespread, continuous	6200-10000 mtns	U	SBS	1	H
19	22500	-35			Widespread, continuous	6200-10000 mtns	U	SBS	1	H
20	22500	-35			Widespread, continuous	6200-10000 mtns	U	SBS	1	H
21	22500	-35			Widespread, continuous	6200-10000 mtns	U	HDN	1	H
22	22500	-35			Widespread, continuous	6200-10000 mtns	U	HDN	1	H
23	22500	-35			Widespread, continuous	6200-10000 mtns	U	HDN	2	H
24	22500	-35			Widespread, continuous	6200-10000 mtns	U	HDN	2	H
25	U	U	U	U	trailing St region of MCS	flat plains	1300	ICT	2	H
26	U	U	U	U	trailing St region of MCS	flat plains	1300	ICT	3	E
27	U	U	U	U	trailing St region of MCS	flat plains	1300	ICT	3	E
28	U	U	U	U	trailing St region of MCS	flat plains	1300	ICT	3	H
29	U	U	U	U	trailing St region of MCS	flat plains	1300	ICT	3	E
30	U	U	U	U	trailing St region of MCS	flat plains	1300	ICT	3	E
31	U	U	U	U	trailing St region of MCS	flat plains	1300	ICT	4	H

TABLE A-4. SAMPLE PRINTOUT OF DATABASE (Continued)

OBS	ST_TIME	TAS	ALT	TEMP	CONC_1DC	C50_100	C100_300	C300_1K	C1_3MM	C3_6MM	C6_10MM	M50_100	M100_300	M300_1K	M1_3MM
1	180600	206	20336	-32.0	6.5274	2.50	3.955	0.072	0.00000	0.000000	0.0000000	0.00069796	0.005216	0.00030	0.000000
2	183800	206	20336	-30.0	1.3424	0.56	0.740	0.098	0.00036	0.000000	0.0000000	0.00015265	0.001245	0.00090	0.000014
3	191200	218	22304	-31.0	6.8457	3.68	3.142	0.024	0.00000	0.000000	0.0000000	0.00097996	0.003356	0.00010	0.000000
4	193200	218	22304	-31.0	19.6720	8.80	10.762	0.110	0.00000	0.000000	0.0000000	0.00241878	0.012149	0.00044	0.000000
5	201400	225	24600	-33.0	1.5768	0.92	0.656	0.001	0.00000	0.000000	0.0000000	0.00024779	0.000588	0.00000	0.000000
6	210400	256	29520	-38.0	3.5329	0.86	2.561	0.112	0.00000	0.000000	0.0000000	0.00023193	0.004926	0.00045	0.000000
7	130730	116	944	-3.6	.	.	.	1.939	0.48870	0.058080	.	.	.	0.02131	0.049898
8	130840	130	2102	-3.7	.	.	.	2.755	0.65497	0.064503	.	.	.	0.03203	0.065845
9	130952	131	3023	-3.8	.	.	.	2.910	0.80869	0.036697	.	.	.	0.03768	0.075006
10	131104	137	3930	-4.4	.	.	.	2.815	0.65514	0.010790	.	.	.	0.04130	0.054118
11	131302	148	4293	-4.7	.	.	.	1.360	0.23391	0.000000	.	.	.	0.02204	0.015007
12	131354	152	4345	-4.9	.	.	.	0.347	0.10314	0.005115	.	.	.	0.00418	0.009043
13	131610	145	4290	-5.1	.	.	.	2.076	0.63387	0.007723	.	.	.	0.02704	0.050899
14	132216	144	4300	-5.2	.	.	.	0.821	0.12736	0.001033	.	.	.	0.01267	0.009665
15	132458	144	4307	-5.4	.	.	.	0.125	0.00126	0.000000	.	.	.	0.00169	0.000081
16	134158	150	6398	-8.2	.	.	.	0.958	0.10764	0.000140	.	.	.	0.01534	0.007268
17	134756	134	6096	-7.6	.	.	.	1.531	0.59268	0.001689	.	.	.	0.02215	0.042204
18	203500	150	14432	-19.0	.	2.48	7.100	4.750	1.04200	0.000000	.	0.00050813	0.012219	0.06513	0.073058
19	203900	150	13448	-19.0	.	2.30	6.500	9.980	0.75900	0.014000	.	0.00050211	0.011391	0.22290	0.058135
20	204400	150	13448	-18.0	.	2.00	4.880	4.150	0.68000	0.000000	.	0.00044483	0.008176	0.05257	0.058323
21	205600	150	10824	-13.0	.	1.54	4.320	2.740	1.34300	0.000000	.	0.00028536	0.007650	0.04087	0.104448
22	205800	150	9512	-11.0	.	0.87	2.510	1.360	0.81000	0.000000	.	0.00019445	0.004156	0.01714	0.125404
23	210300	150	7872	-4.0	.	1.08	2.680	1.190	1.04000	0.465000	.	0.00020856	0.004603	0.01341	0.166289
24	210800	150	9184	-10.0	.	2.30	5.900	1.890	1.39300	0.067000	.	0.00045487	0.009334	0.02432	0.127845
25	223000	250	13000	0.5	.	.	43.398	16.637	1.60677	0.283277	0.0194554	.	0.060649	0.18178	0.153186
26	223800	250	13500	-0.5	.	.	94.140	51.308	3.65235	0.688940	0.0306525	.	0.136193	0.55560	0.358344
27	223900	250	14500	-2.0	.	.	102.707	57.295	4.33513	0.616457	0.0248772	.	0.149168	0.64831	0.405247
28	224030	250	15000	-3.0	.	.	145.410	74.698	5.13214	0.620755	0.0093661	.	0.205904	0.83988	0.486528
29	224800	250	15500	-5.0	.	.	153.460	78.230	5.84605	0.833465	0.0149760	.	0.220472	0.83840	0.565838
30	224900	250	16500	-7.0	.	.	202.835	95.798	6.47810	0.816500	0.0085750	.	0.295286	1.01468	0.628458
31	225000	250	17000	-8.0	.	.	234.428	134.763	8.11222	0.563145	0.0034454	.	0.337350	1.49007	0.738298

OBS	M3_6MM	M6_10MM	MAXDIAM	MASS1CT	MASS1PT	CONC_1DP	PROJECT	CLOBHNOT	CLOBTNOT	PROBE_ID	CLOUDGRP	ALT_CONV
1	0.000000	0.0000000	0.4	0.0062034	0.000301	0.03912	AFGL Cirrus:78	20600	-31	PMS 1DC & 1DP	A	ASL
2	0.000000	0.0000000	0.7	0.0015662	0.000914	0.09796	AFGL Cirrus:78	20400	-27	PMS 1DC & 1DP	B	ASL
3	0.000000	0.0000000	0.3	0.0044328	0.000001	0.00013	AFGL Cirrus:78	U	U	PMS 1DC & 1DP	C	ASL
4	0.000000	0.0000000	0.3	0.0150107	0.000001	0.00010	AFGL Cirrus:78	U	U	PMS 1DC & 1DP	C	ASL
5	0.000000	0.0000000	0.3	0.0008384	0.000000	0.00001	AFGL Cirrus:78	U	U	PMS 1DC & 1DP	C	ASL
6	0.000000	0.0000000	0.4	0.0056089	0.000397	0.05169	AFGL Cirrus:78	29500	U	PMS 1DC & 1DP	D	ASL
7	0.021815	.	3.8	.	0.093022	2.48557	NEWS:1982-83	down to surface	U	PMS 1DP	A	ASL
8	0.025550	.	3.9	.	0.123423	3.47470	NEWS:1982-83	down to surface	U	PMS 1DP	A	ASL
9	0.012937	.	3.5	.	0.125623	3.75523	NEWS:1982-83	down to surface	U	PMS 1DP	A	ASL
10	0.003957	.	3.0	.	0.099378	3.48114	NEWS:1982-83	down to surface	U	PMS 1DP	A	ASL
11	0.000000	.	2.0	.	0.037049	1.59372	NEWS:1982-83	down to surface	U	PMS 1DP	A	ASL
12	0.001866	.	2.2	.	0.015085	0.45501	NEWS:1982-83	down to surface	U	PMS 1DP	A	ASL
13	0.002699	.	2.9	.	0.080636	2.71795	NEWS:1982-83	down to surface	U	PMS 1DP	A	ASL
14	0.000369	.	2.1	.	0.022702	0.94904	NEWS:1982-83	down to surface	U	PMS 1DP	A	ASL
15	0.000000	.	1.0	.	0.001770	0.12635	NEWS:1982-83	down to surface	U	PMS 1DP	A	ASL
16	0.000042	.	1.9	.	0.022650	1.06571	NEWS:1982-83	down to surface	U	PMS 1DP	A	ASL
17	0.000654	.	2.4	.	0.065006	2.12546	NEWS:1982-83	down to surface	U	PMS 1DP	A	ASL
18	0.000000	.	2.3	.	.	.	COSE-II:1979			PMS 2DC	A	ASL
19	0.005598	.	3.5	.	.	.	COSE-II:1979			PMS 2DC	A	ASL
20	0.000000	.	1.8	.	.	.	COSE-II:1979			PMS 2DC	A	ASL
21	0.000000	.	2.8	.	.	.	COSE-II:1979			PMS 2DC	A	ASL
22	0.000000	.	2.8	.	.	.	COSE-II:1979			PMS 2DC	A	ASL
23	0.189616	.	4.5	.	.	.	COSE-II:1979			PMS 2DC	A	ASL
24	0.036582	.	4.5	.	.	.	COSE-II:1979			PMS 2DC	A	ASL
25	0.154839	0.0295650	7.7	.	.	.	OKPRESTORM:1985	U	U	PMS 2DC & 2DP	A	ASL
26	0.367645	0.0430999	8.0	.	.	.	OKPRESTORM:1985	U	U	PMS 2DC & 2DP	A	ASL
27	0.319078	0.0360926	7.8	.	.	.	OKPRESTORM:1985	U	U	PMS 2DC & 2DP	A	ASL
28	0.310018	0.0130211	7.0	.	.	.	OKPRESTORM:1985	U	U	PMS 2DC & 2DP	A	ASL
29	0.419331	0.0218703	8.5	.	.	.	OKPRESTORM:1985	U	U	PMS 2DC & 2DP	A	ASL
30	0.407300	0.0125213	7.5	.	.	.	OKPRESTORM:1985	U	U	PMS 2DC & 2DP	A	ASL
31	0.266576	0.0045337	6.2	.	.	.	OKPRESTORM:1985	U	U	PMS 2DC & 2DP	A	ASL

TABLE A-4. SAMPLE PRINTOUT OF DATABASE (Continued)

OBS	MANEUVER	PRECIP	CLDSTATE	XTALTYPE	DURATION	FROST_PT	DISTANCE	FLWC	JWLWC	CONC	END_TIME	CONC_2DC	MASS2CT	MASS2PT	CONC_2DP
1	Level		I	Br	300	-34	17.2	.	.	.	.	.	.	.	.
2	Level		I	Br	300	-29	17.2	.	.	.	.	.	.	.	.
3	Level		I	Br	300	-31	18.2	.	.	.	.	.	.	.	.
4	Level		I	Br	300	-31	18.2	.	.	.	.	.	.	.	.
5	Level		I	Br	300	-32	18.8	.	.	.	.	.	.	.	.
6	Level		I	Br	300	-37	21.3	.	.	.	.	.	.	.	.
7	Slant	S	I	U	70	.	2.3	0.01	0.01	2	130838	.	.	.	.
8	Slant	S	I	U	72	.	2.6	0.00	-0.03	1	130950	.	.	.	.
9	Slant	S	I	U	72	.	2.6	0.01	-0.04	1	131102	.	.	.	.
10	Slant	S	I	U	118	.	4.5	0.01	-0.02	1	131300	.	.	.	.
11	Level	S-	I	U	52	.	2.1	0.00	0.02	0	131352	.	.	.	.
12	Level	U	I	U	136	.	5.7	0.00	0.02	0	131608	.	.	.	.
13	Level	S-	I	U	366	.	14.7	0.01	0.03	1	132214	.	.	.	.
14	Slant	U	I	U	162	.	6.5	0.00	0.02	0	132456	.	.	.	.
15	Spiral	0	I	U	72	.	2.9	0.00	0.02	1	132608	.	.	.	.
16	Spiral	U	I	U	358	.	14.9	0.00	0.01	1	134754	.	.	.	.
17	Spiral	U	I	U	92	.	3.4	0.01	0.02	1	134926	.	.	.	.
18	Slant	S+ @sfc	I	uP	60	-21	2.5	.	.	.	.	15.372	0.15091	.	.
19	Slant	S+ @sfc	I	uP	60	-19	2.5	.	.	.	.	19.553	0.29853	.	.
20	Level	S @sfc	I	I	60	-21	2.5	.	.	.	.	11.710	0.11952	.	.
21	Slant	S- @sfc	I	uD	60	-15	2.5	.	.	.	.	9.943	0.15325	.	.
22	Slant	S- @sfc	I	I	60	-13	2.5	.	.	.	.	5.550	0.14690	.	.
23	Spiral	S- @sfc	I	sU+A	60	-6	2.5	.	.	.	.	6.455	0.37413	.	.
24	Spiral	S- @sfc	I	sU+A	60	-10	2.5	.	.	.	.	11.550	0.19853	.	.
25	Level	U	M(I+W)	Pl+A	450	.	31.3	.	.	.	33730	60.034	0.24243	0.33759	1.90950
26	Slant	U	I	Pl+A	30	.	2.1	.	.	.	33830	145.448	0.69179	0.76909	4.37194
27	Slant	U	I	Pl+A	60	.	4.2	.	.	.	34000	160.001	0.79748	0.76042	4.97647
28	Level	U	I	Pl+A	300	.	20.8	.	.	.	34530	220.108	1.04578	0.80957	5.76226
29	Spiral	U	I	Pl+A	30	.	2.1	.	.	.	34830	231.690	1.05887	1.00704	6.69449
30	Spiral	U	I	Pl+A	30	.	2.1	.	.	.	34930	298.633	1.30997	1.04828	7.30317
31	Level	U	I	Pl+A	390	.	27.1	.	.	.	35630	369.191	1.82742	1.00941	8.67881